A GEOMAGNETIC INDUCTION STUDY IN THE NORTH EAST OF TASMANIA

by

NAZHAR BUYUNG

Submitted in partial fulfilment
of the requirements for the
degree of Master of Science

UNIVERSITY OF TASMANIA
HOBART
1980

ABSTRACT

During the period in between February 1978 until October 1979, a geomagnetic variation study by means of eleven temporary field stations has been conducted covering the area of Launceston quadrangle, Tasmania Geological Atlas Series, sheet SK 55-4, scale 1 : 250 000. The study area is situated between latitude $41^{o}00$ and $41^{o}45$ south and between longitude $146^{o}15$ and $148^{o}00$ east, with a total area of about 12 700 sq. km.

The aim of this study is to record and analyse the behavior of geomagnetic variations which are related to lateral changes of electrical conductivity structure.

The coast effect similar to the one that was established in Hobart (Parkinson, 1962) is found in this area for longer periods greater than 64 minutes. And an anomalous local high conductivity zone is indicated by the directions of induction vectors at periods less than or equal to 48 minutes. This anomalous conductive zone is interpreted as caused by deep lateral variation of conductivity of sedimentary rocks ($\sigma = 0.54 \times 10^{-1}$ $S.m^{-1}$) with ages between Cambrian and younger and Devonian granodiorite ($\sigma = 0.54 \times 10^{-3}$ $S.m^{-1}$), both being covered by surface high conductive layer ($\sigma = 0.11$ $S.m^{-1}$) that extends from east of Deloraine to west of Scottsdale.

The occurence of a mineralized zone between Nabowla, Scottsdale and Tayene agrees with the direction of induction vectors at those stations.

LIST OF CONTENTS

This thesis contains no material which has been accepted for the award of any other degree or diploma in any University and to the best of my knowledge and belief, contains no copy or paraphrase of material previously published or written by another person, except where due reference is made in the text of this thesis.

Nazhar Buyung

March 7, 1980

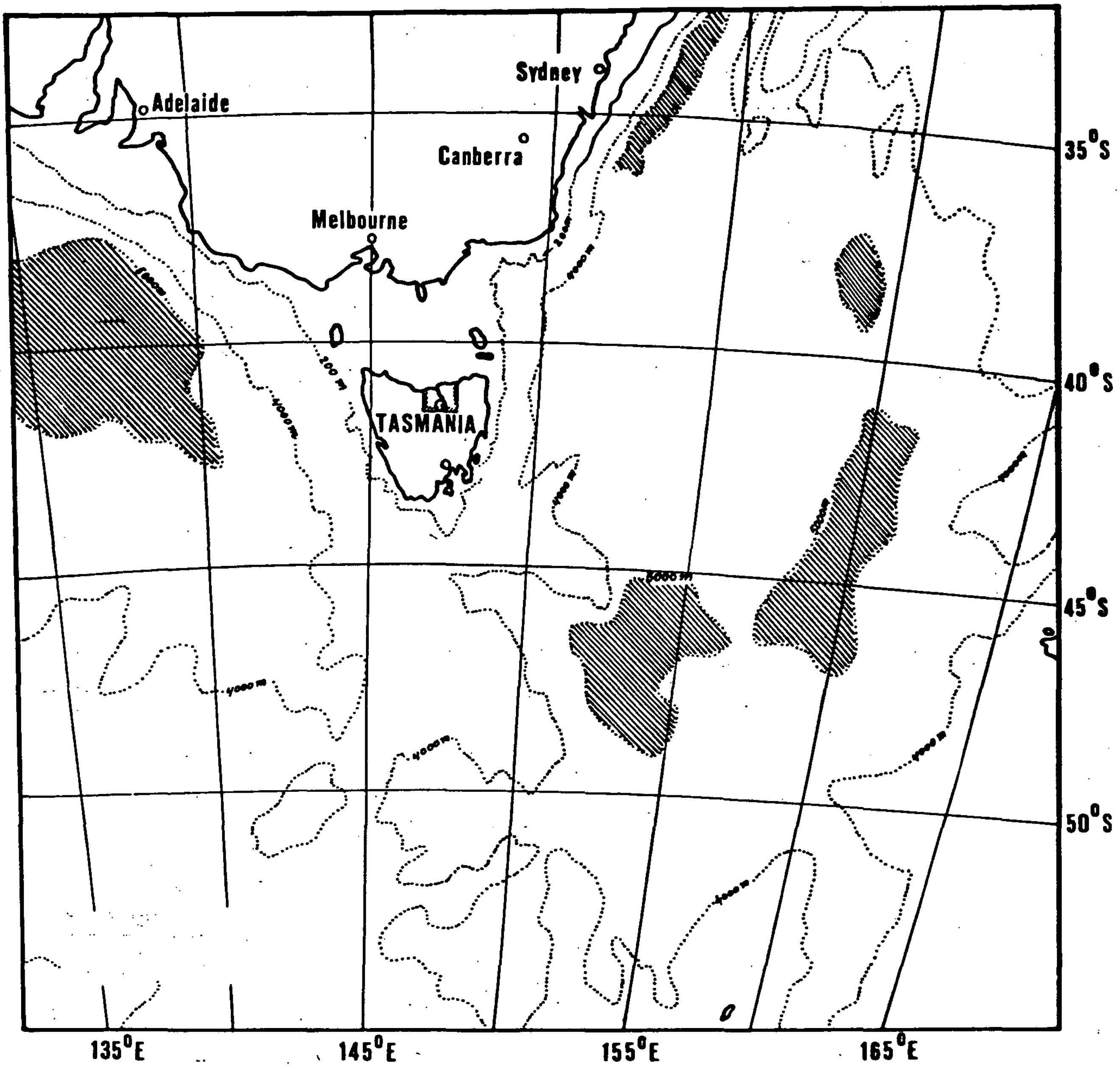

Fig. 1 Geographical location map of Tasmania and bathymetric contours around the south east of Australia.

Chapter I

MAGNETIC VARIATION STUDIES IN GENERAL

Many reports about the vertical conductivity distribution inside the earth have been published from the analysis of gemagnetic variations, since Schuster (1908) and Chapman (1919) recognized that there is a region of higher conductivity at a depth of some hundreds of kilometers inside the earth. The vertical conductivity distribution has been refined by the work of many researchers such as Lahiri and Price (1939), McDonald and Cantwell (1957) and Banks (1969).
The global average model suggests that conductivity value between depths of 0 and 400 kms would not exceed 0.10 $S.m^{-1}$, but the existence of material with conductivity in excess of that value has been reported. It is usually suggested that this is related to some factor such as saline water filled sediments, zone mineralization, or high heat flow. For greater depth, high conductivity anomalies are normally ascribed to partial melting of magma in the upper mantle (Banks, 1979).

I-1 LATERAL CONDUCTIVITY DISTRIBUTION

The lateral conductivity distribution is well indicated by the direction of induction vectors. The induction vector is a 2-D vector (A,B) where A and B are transfer functions describing the behavior of the vertical component as a function of the horizontal components. Its modern definition is given by

$$\underline{Z} = A.\underline{X} + B.\underline{Y} + ç$$

where $\underline{Z}, \underline{X}, \underline{Y}$ are (complex) Fourier transforms of the field components, and A and B are chosen to minimize ç. In general they are complex numbers, so we must deal with both a real and imaginary induction vector.

After the invention of induction vector by Parkinson (1962) and independently by Wiese (1962), the study of electrical conductivity distribution grew rapidly. Induction vectors introduced by Parkinson differ from those of Wiese; the direction of the former is toward higher conductivity, while the one introduced by Wiese is away from it. Throughout this paper the induction vectors pointing toward conductivity anomaly were adopted.

All over the world many areas have been intensively studied. Lilley(1975) and Adam (1976) summarized some of the areas studied to date. The response from all of those studies, have brought to light the behavior of magnetic variations at some particular areas. For some areas by noticing the characteristic of the directions and lengths of the induction vectors and the locality of the station observations concerned, the lateral effect of conductivity could be categorized into one of known effects such as coast, island, peninsula and strait effects. All of these effect are related to the influence of induced electric current flowing in the sea water and in fact are frequency dependent.

One classical example of the coast effect is shown on the induction vectors plotted around Australia and the region surrounding (Parkinson, 1962). All of the vectors point toward the adjacent deep ocean and perpendicular to the coast line. Other reports of the coast effect are in California by Schmucker (1963) and in Canada by Hyndman (1963) and by Lambert and Caner (1965).

On relatively uniform conductivity distributions, the coast effect causes the length of the induction vectors to be longer at stations on coast line and gradually to decrease inland. Longer induction vectors at inland stations compared to the one at coast line, indicate the land area is conductively anomalous.

The coupling between mantle and ocean conductivities weakens the electrical current intensity flowing in the ocean (Honkura, 1971), and will affect the bahavior of the vectors effected by the ocean.

An exceptional case of the induction vectors at a coast line is found in Peru, where the land anomaly is so strong that it causes the coast effect to vanish (Schmucker, 1969 and Aldrich et al., 1972).

The island effect differs slightly from the coast effect, since it is best seen at short period variations. Extensive studies about this effect have been done at Oshima (Sasai, 1967, 1968), Oahu (Klein, 1972), Miyake-jima (Honkura, 1971) and Hawaii (Klein, 1971). All induction vectors are characterized by the directions toward the sea away from the island.

The peninsula effect is considered as combination of coast and island effects which sometimes causes the amplitude of vertical variation (ΔZ) to be greater than the horizontal variations (ΔH and ΔD), although the coast effect itself sometimes also does this.

The strait effect is simply indicated by the direction of induction vectors on lands at both side of the strait point toward the strait. ~~that~~ This is caused by the induced electric current being channeled through the conductive strait.

I-2 INDUCTION VECTORS AROUND TASMANIA

Four induction vectors had already been established in Tasmania, before this study started in early 1978 (see figure 2). The induction vector at Hobart is one of the few induction vectors around the Australian coastal region. It was determined from bay type and similar geomagnetic fluctuations at period of 40 minutes. The direction of the vector is toward the deep ocean in the south east.

Three stations on the north coast of Tasmania, Bridport, Devonport and Smithton are part of magnetometer array stations at the south east Australia done by Lilley (1973-1974). The vectors are for periods of

5 - 20 minutes. The directions of induction vectors at Bridport and Devonport are toward a point slightly north of the line joining them. An indication of electric current with a direction northwest to south east passing

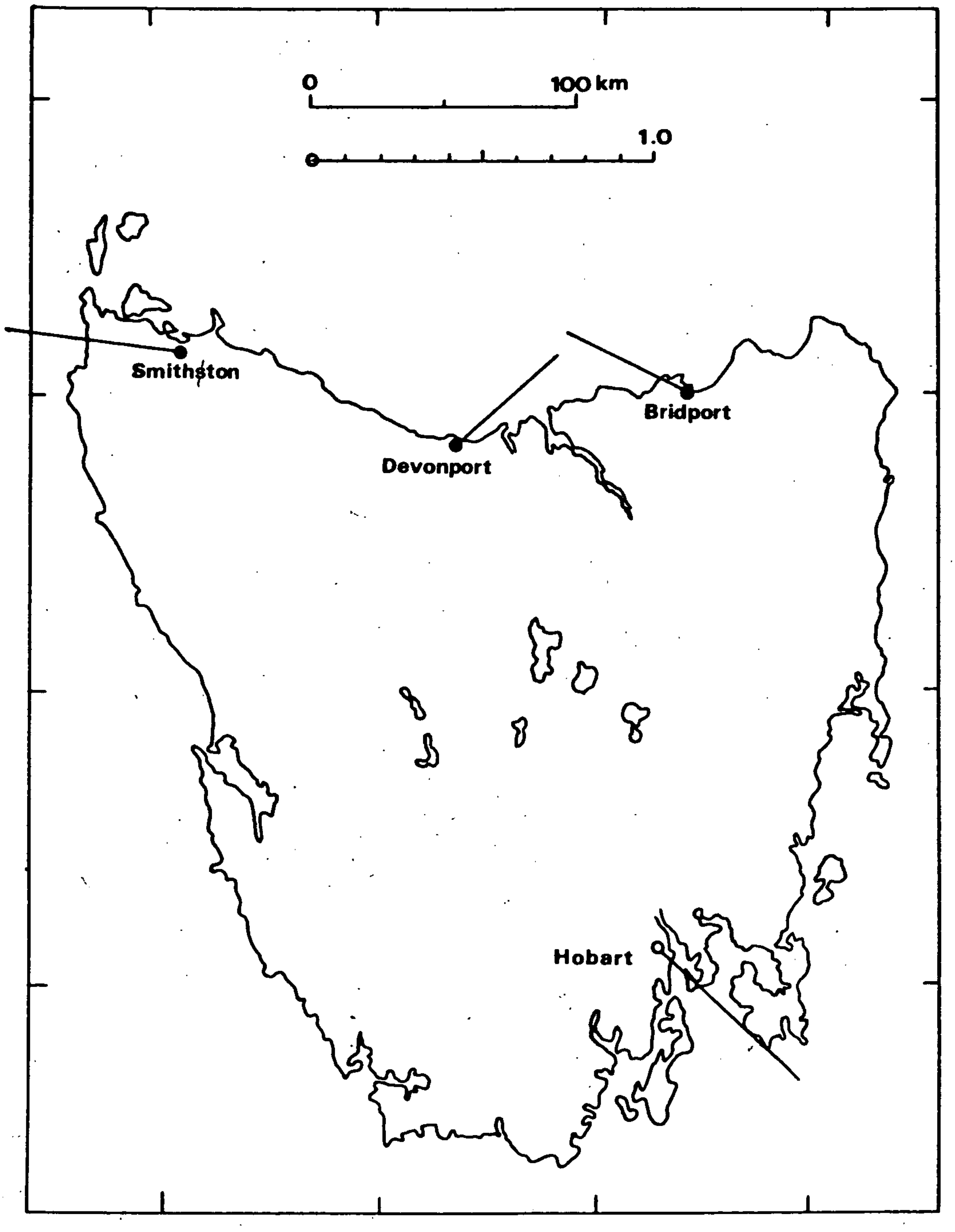

Figure 2 : Induction vectors around Tasmania. Hobart vector is for 40 minutes period, and Smithton, Devonport and Bridport vectors are for 5 - 20 minutes period.

● Lilley (1973 - 1974)

o Parkinson (1962)

through conductive zone inland could be assumed.

To understand the behavior of induction vectors and to interpret the possible conductivity structure of this area forms the objective of this study.

I-3 CONDUCTIVITY VALUES OF ROCKS

The important parameter involved in interpreting the subsurface structure derived from the geomagnetic variations is conductivity, i.e reciprocal of resistivity. Its unit in electromagnetic unit is emu, and in MKS units it is $mho.m^{-1}$ or $Siemen.m^{-1}$.

1 $Siemen.m^{-1}$ is equal to 10^{-11} emu.

Measurement of the conductivity value of rock in the laboratory was discussed in detail by Scott et al(1967) and Duba (1978).

The conductivity of a cylindrical sample can be simply calculated through measurement of its resistance in ohm, by the relation ;

$$R = \frac{L}{\sigma . A}$$

where R is the resistance in ohm, L is the length of sample in meter, σ is the conductivity and A is the surface area in m^2.

Laboratory results of conductivity values of rocks after being saturated in various saturants such as tap water ($\sigma = 0.95 \times 10^{-2}\ S.m^{-1}$), distilled water ($\sigma = 0.44 \times 10^{-3}\ S.m^{-1}$) and 0.1 M NaCl done by Duba (1978) are tabulated below.

TABLE 1 (after DUBA, 1978)

Lithology	Saturated in		
	Distilled water ($S.m^{-1}$)	Tap water ($S.m^{-1}$)	0.1 M NaCl ($S.m^{-1}$)
Kayenta sandstone (Triassic)	0.44×10^{-2}	0.18×10^{-2}	0.86×10^{-1}
St. Peters sandstone (Ordovician)	0.23×10^{-2}	0.11×10^{-2}	0.43×10^{-1}
Indiana limestone (Upper Ordovician)	0.56×10^{-3}	0.19×10^{-3}	0.12×10^{-1}

cont'd

Lithology	Saturated in		
	Distilled water ($S.m^{-1}$)	Tap water ($S.m^{-1}$)	0.1 M NaCl ($S.m^{-1}$)
Nugget sandstone	0.52×10^{-2}	0.30×10^{-2}	0.98×10^{-2}
Westerly granite (Upper Permian)	0.11×10^{-3}	0.39×10^{-4}	0.58×10^{-3}

Limestone and granite are known for their low porosity, thus the low conductivities after saturation are expected.

Measurement of conductivity values of various rocks from the study area were also done. The samples in the form of cylinders were clamped as five layers sandwiches (electrode - blotter - sample - blotter - electrode), and their resistances were measured using a Potentiometric Voltmeter ("PORTAMETRIC" PVB 300, serial no. 430057).

To make a good contact between the copper electrode and sample, wet blotting paper saturated with $CuSO_4$ solution was used. The results of measurement are tabulated in TABLE 2.

TABLE 2

MEASURED CONDUCTIVITY VALUES

Lithology	Not saturated ($S.m^{-1}$)	Saturated in tap water ($S.m^{-1}$)	Saturated in brackish water ($S.m^{-1}$)
Clayey sand	0.26×10^{-2}	-	-
Loose sand	0.33×10^{-2}	-	-
Sandstone	0.59×10^{-2}	-	-
Basalt porous	0.66×10^{-3}	0.27×10^{-3}	0.20×10^{-1}
Basalt compact	0.51×10^{-4}	0.77×10^{-3}	0.76×10^{-3}
Granodiorite	0.54×10^{-3}	0.28×10^{-2}	0.25×10^{-2}

Knowledge about measured conductivity values of rocks will give some help to generalize the conductivity distribution throughout the area. But since the conductivity values of rocks inside the earth are sensitive to temperature and compactness (related to water content), interpretation of conductivity structure on this basis need a high presumption.

Chapter II

LOCAL GEOMAGNETIC VARIATION STUDIES IN NORTH EAST TASMANIA

The location of the study area is shown in figure 3, and the distribution of the stations in figure 4.

Bass Strait with 200 meters deep sea water separates Tasmania from the mainland with a distance of about 400 kms.

Eleven temporary stations were distributed throughout the area. The names, abbreviations and geographic coordinates are tabulated on Table 3.

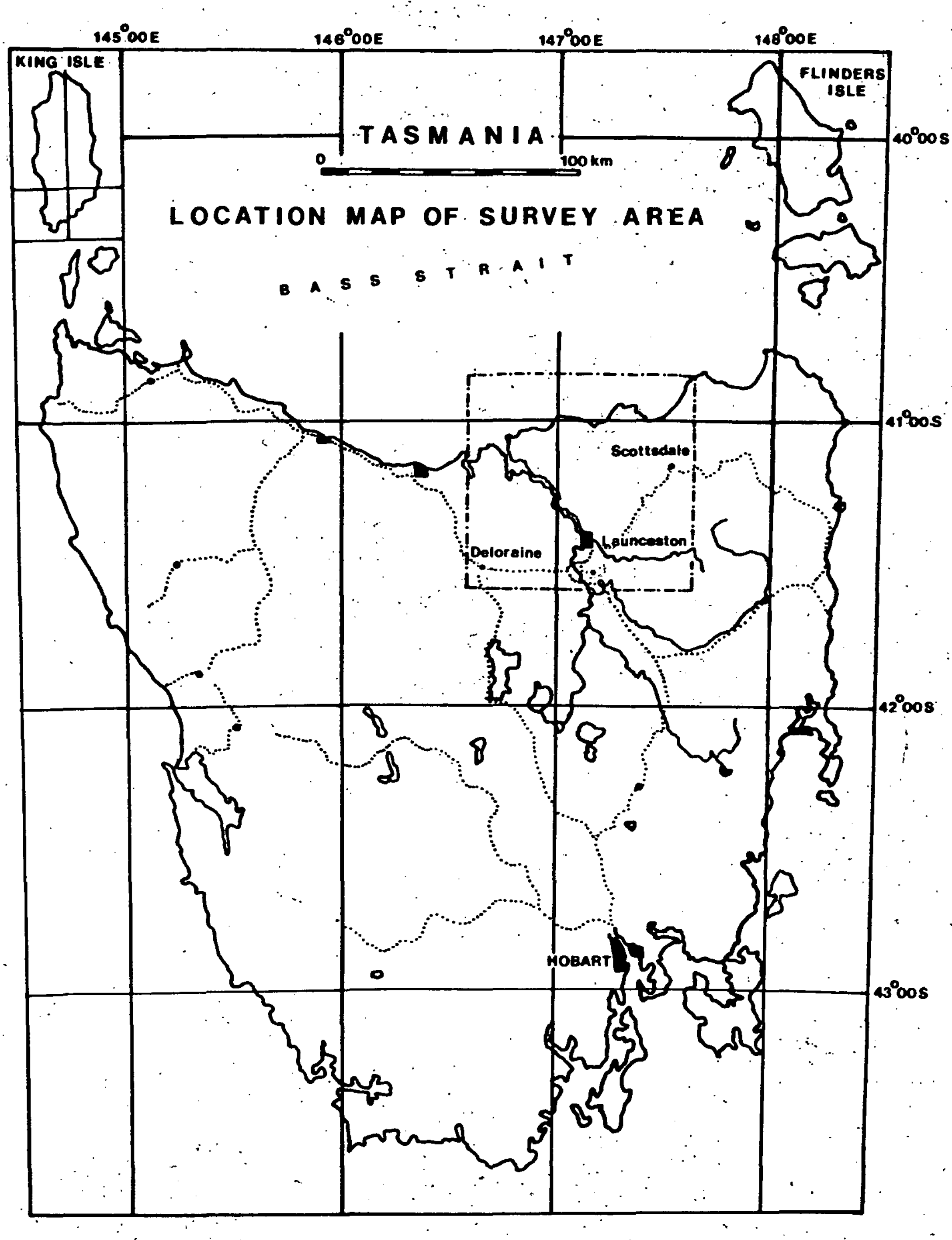

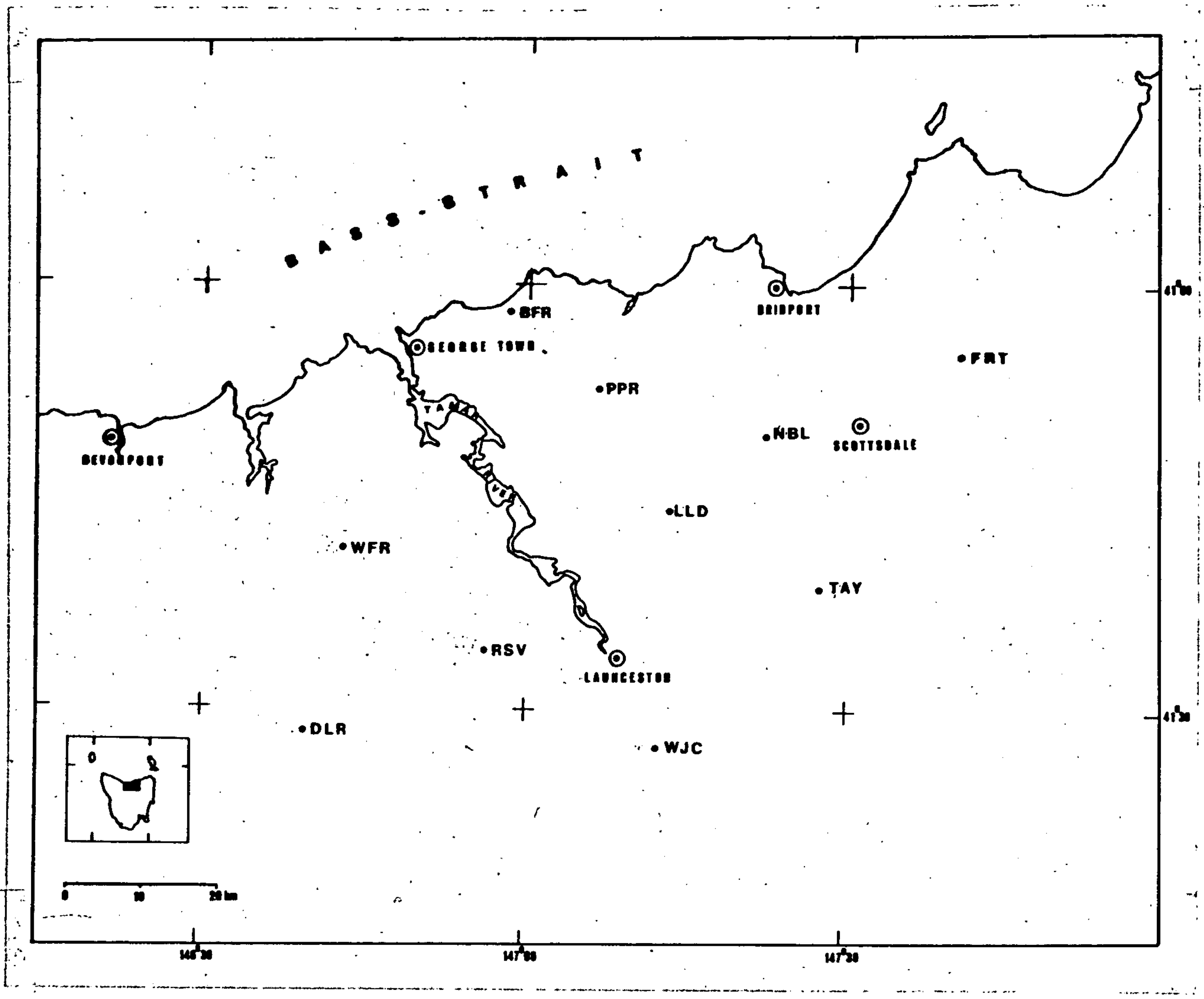

Figure 4 : Locations of geomagnetic observation points.

TABLE 3

	Station	Abbreviation	Latitude	Longitude
1.	Western Junction	WJC	41°32'45	147°12'24
2.	Scottsdale	SCD	41°09'47	147°31'02
3.	Deloraine	DLR	41°31'30	146°39'34
4.	Rosevale	RSV	41°25'39	146°55'58
5.	Lilydale	LLD	41°15'47	147°13'27
6.	Nabowla	NBL	41°10'34	147°16'58
7.	Forester	FRT	41°04'44	147°40'45
8.	West Frankford	WFR	41°18'33	146°42'56
9.	Pipers River	PPR	41°07'18	147°06'40
10.	Beechford	BFR	41°01'58	146°58'02
11.	Tayene	TAY	41°21'19	147°27'24

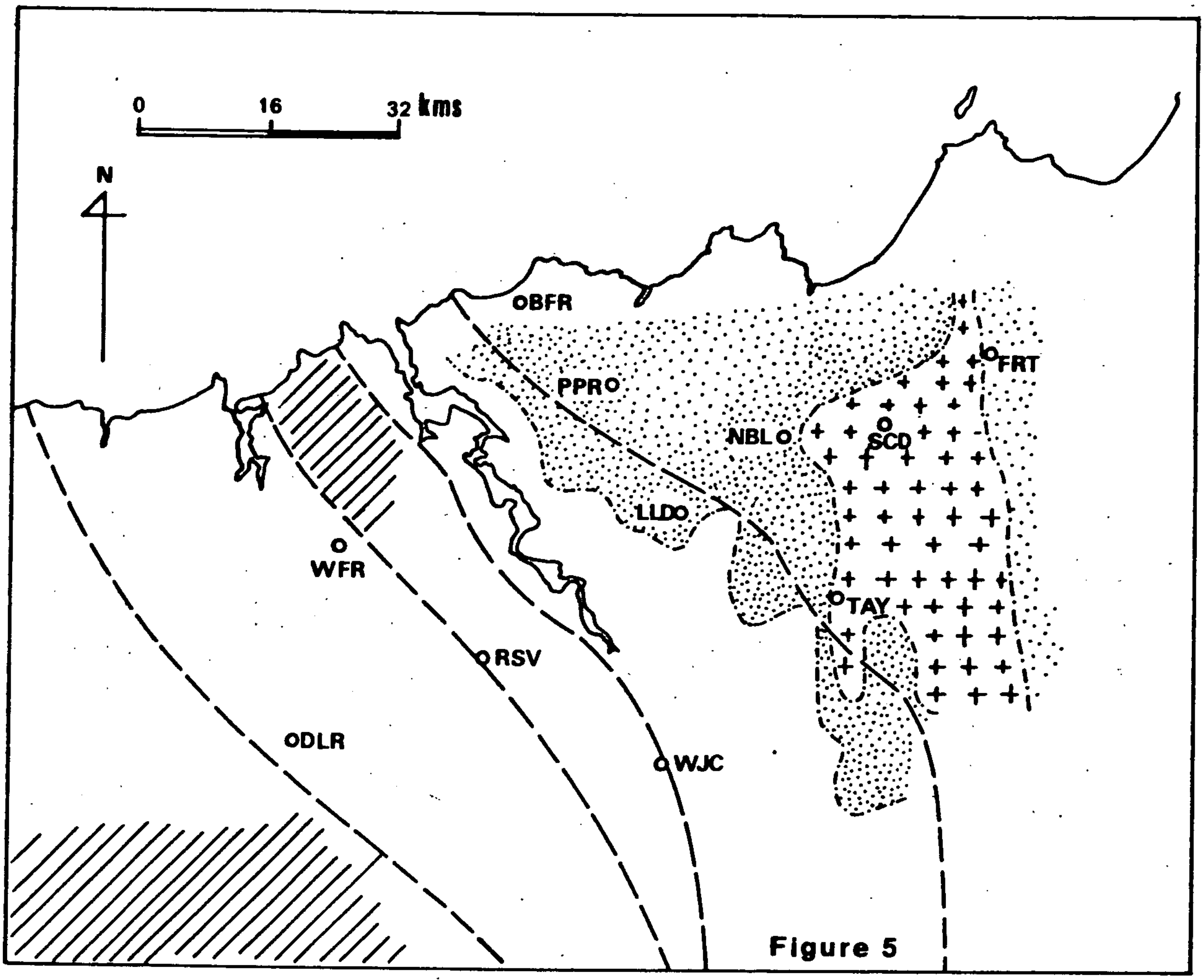

Figure 5

Legend

Parts of major Tertiary fault lines (Banks, 1962)

Cambrian and younger rock formations

Devonian granite - granodiorite

Siluro Devonian Mathinna Beds

Precambrian rocks

Four stations, WJC, RSV, DLR and WFR are located on the area that geologically has complicated structure with outcropped rocks ranging in age from Precambrian and younger and covered by Tertiary sediments filling a graben and relatively thin sills of Jurassic Dolerite.

The remaining seven stations, LLD, NBL, SCD, FRT, BFR, PPR and TAY are located on the area which has relatively simple major geological distribution of formations of Mathinna Beds and later intrusion of Devonian granite - granodiorite type. The Mathinna Beds have a thickness of at least 2 000 meters, but the total thickness is unknown (Banks, 1962).

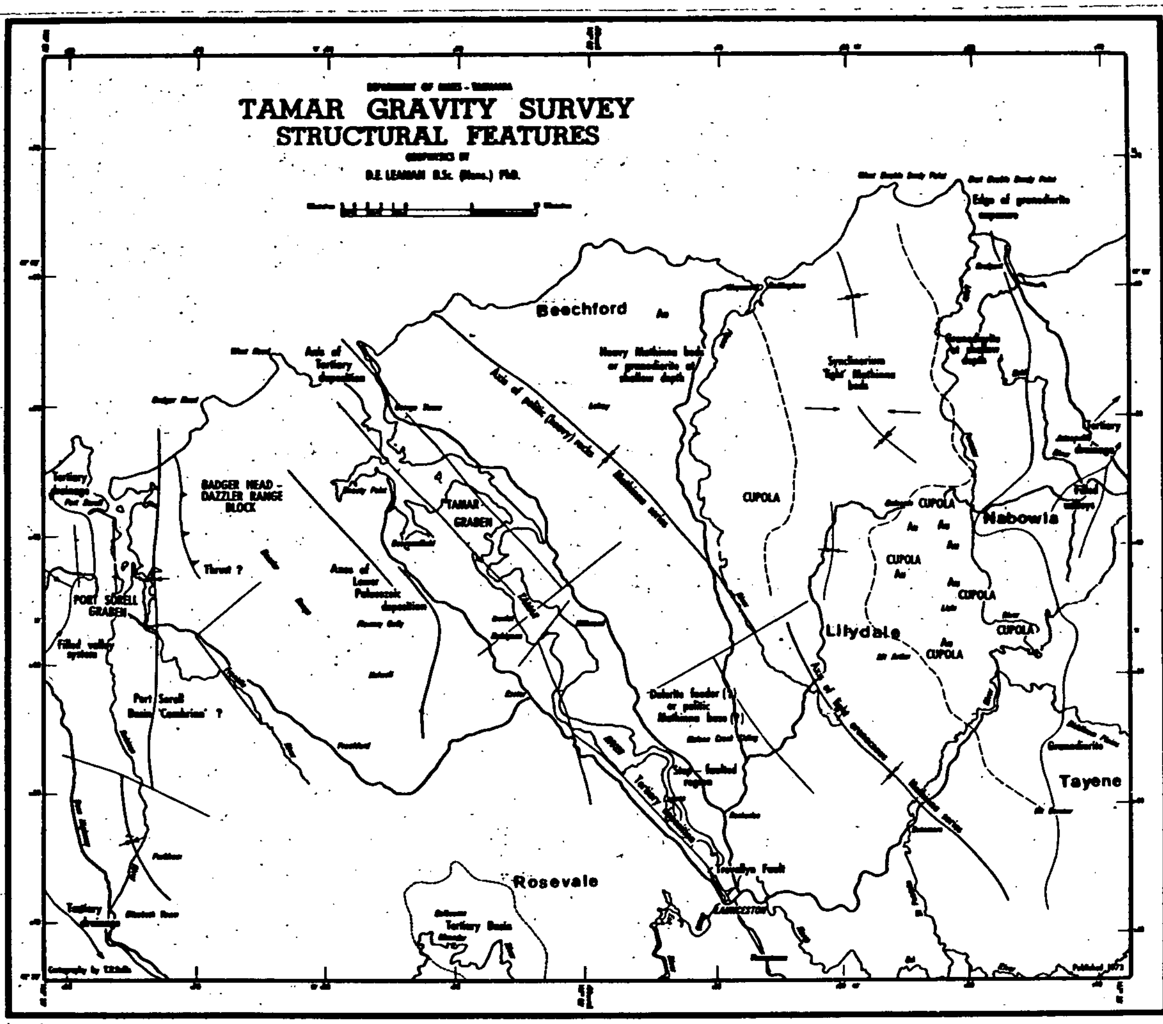

Fig. 6 Structural features of Tamar area derived from gravity anomaly (Leaman et al., 1976)

Gravity measurements have also been made over this area during the period 1971 to 1975 (Longman et al.,1971 and Leaman et al.,1976). Their regional gravity anomaly maps show a regional increase of anomaly toward the east that indicates a shallowing of the Moho. Noticed also that the structural features derived from gravity anomalies (see figure 6) show many cupolas at the area between Nabowla, Scottsdale and Tayene, that seem to associate with the existence of mineralization.

II-1 GEOMAGNETIC VARIATION MEASUREMENT AND CALIBRATION

The data of magnetic variations at Western Junction and half of Scottsdale were recorded using a 3-components Fluxgate magnetometer known as TOPMAG abbreviated from Tasmania Operation Magnetometer.
The magnetometer has no temperature control. To eliminate the effect of temperature variation between night and day, the detector was buried underground. From experience 50 cms of soil on top of the detector was enough to eliminate the temperature effect.
The magnetic variation data of the rest of the 9 stations and half of Scottsdale were recorded using a commercial Fluxgate (EDA instrument FM-100B, serial no. 2117). This magnetometer was put into operation on July 1978. The advantage of this new instrument is the built in temperature compensator; that means the detector does not have to be buried.

MAGNETOMETER CALIBRATION

TOPMAG : This magnetometer was calibrated using built in Helmholtz coils, in the form of two similar coaxial coils separated by a distance equal to their common radius and carrying current in the same direction. This formed the calibrating coil system for each component. The built in coils were tested and calibrated against a standard Helmholtz coil (Askania, serial no. 582047). It was found that the built in coils have the following values :

D = 27.5 nT/mA

H = 28.5 nT/mA

Z = 26.7 nT/mA

By applying known values of current into the coils, and measuring the needle deflection at chart recorder, the magnetometer sensitivity can be calibrated. The sensitivity values are :

D = 4.13 nT/mm

H = 4.28 nT/mm, Z = 4.01 nT/mm

FM 100 B FLUXGATE MAGNETOMETER

The value of 10 Volts output from magnetometer is specified by manufacture as more less equal to 1 000 nT (manual FM 100B).

To find the accurate value, a clibration was done using a square coils. The specific parameters of this square coils are ; each coils system has four separated coil, where the outer coils have more number of turns of wire than the inner coils, as specified below.

Vertical field coils :	Z outer coils	a = 0.27 m, N = 140, b/a = 1
	Z inner coils	a = 0.27 m, N = 60, b/a = 0.26
Horizontal field coils:	H outer coils	a = 0.25 m, N = 70, b/a = 1
	H inner coils	a = 0.25 m, N = 30, b/a = 0.26

where; a is half distance between the two outer coils, and b is half distance between the two inner coils.

The value of magnetic field intensity and current ratio, resulting if a current (I) is applied to the coils (4 square coils) is determined as :

$$\frac{B}{I} = 4 \times \frac{\mu_0}{\pi} \times \frac{a^2}{(a^2+b^2)\sqrt{2a^2+b^2}} \quad \text{in Tesla/Ampere}$$

All the parameters are known values. Thus the sensitivity of this square coils in term of nT/mA can be obtained.

The vertical Z field is 471.1 nT/mA

The horizontal H field is 254.4 nT/mA

The detector of particular component to be measured then oriented parallel to the magnetic field direction of the coils, and put right in the middle. By applying a known current value into the coils, the output voltage from magnetometer can be measured. From measurements were found the sensitivity value of magnetometer for each component as below :

H component = 92.2 nT/Volt

D component = 90.7 nT/Volt

Z component = 90.8 nT/Volt

II-2 DATA REDUCTION

The object of data reduction is to calculate the complex numbers of transfer function values A and B from the group of discrete events of three components of geomagnetic storms, that fit into the statistical relation : $\Delta Z = A.\Delta H + B.\Delta D$ at a particular frquency.
ΔZ, ΔH and ΔD are the amplitude variations of geomagnetic components on the directions vertical down, magnetic north and magnetic east respectively.

The particular events that were of interest in this study are the substorm type. Examples of the substorms are shown in Plate I.
It can be seen that the single event, which in particular so called bays provide an excellent signal which clearly stands out from the general background activity.

SAMPLING

Data in the analog forms which were recorded using two Rustrak type 288 and one Multiscript 3, were sampled partly by hand and partly by semi automatic scaler.

Hour marks are 2.5 cms apart and the full scale of the chart paper is equal to about 240 nT.

Because of the time resolution (2.4 minutes/mm) and the blurred image of some of traces, hand digitized samples are considered reliable only at 6 minutes intervals, allowing analysis of periods greater than or equal to 12 minutes.

Sampling using the scaler gives results that are consistent with those done by hand, except that the sample intervals can be shorter.

The output of the scaler is converted to digital form and fed into the computer. Values in between the scaled points are internally interlated. The relative values of every component (in nT) and at particular event were processed through INTERDATA 67/16 Computer and output in the form of 8 hole binary code in paper tape as a preparation for Fourier analysis.

A very important thing to notice is the polarity of the data being sampled, which means which is the direction of magnetic north, magnetic east or vertically down. These polarities are used to determine the direction of the induction vectors.

Determination of those polarities were done by the help of a permanent magnet being put at some distance from the detector. After the detectors have been set up with H detector pointing north, D detector pointing east and Z detector vertical, polarities are determined as follows :

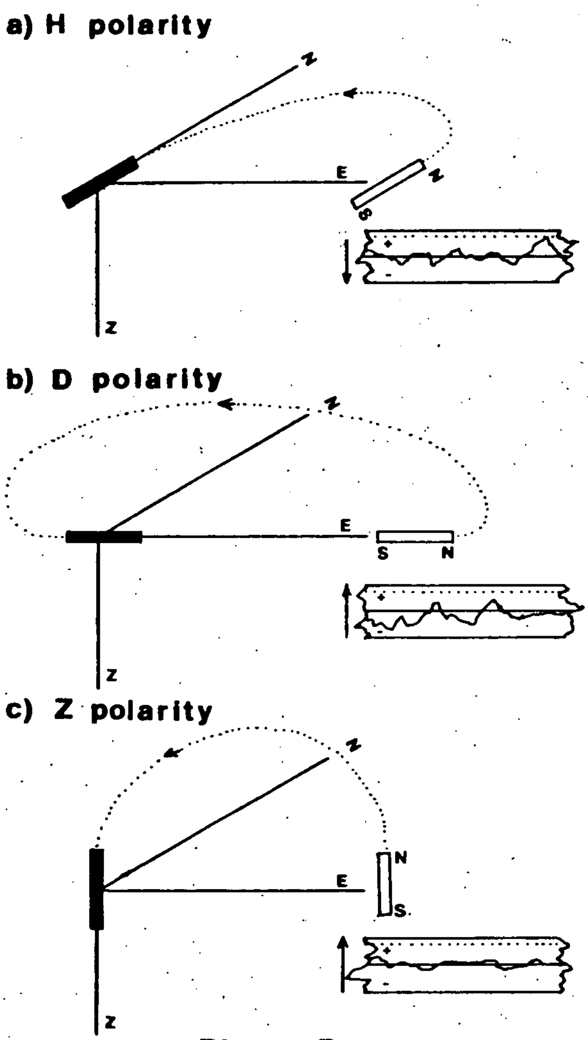

Figure 7

By applying the permanent magnet (N pole to north direction) parallel to detector, the direction of needle movement at recorder indicates south direction (i.e negative is south on chart in figure 7a).

By applying the permanent magnet (N pole to east direction) in line with the detector, the direction of needle movement at recorder indicates east direction (i.e positive is east on chart in figure 7b).

By applying the permanent magnet (N pole points up) vertically parallel to detector, the direction of needle movement indicates down direction (i.e positive down on chart in figure 7c).

II-2-1 FOURIER ANALYSIS

Before the sampled time series of data were transformed into the frequency domain, the amplitude data were calculated as the deviation from a straight line connecting the beginning and the end of the event. Also the mean of the first and the last few numbers were padded with zeros to 2^n values.

The calculation into the frequency domain was done in the INTERDATA 67/16 Computer, using the Fast Fourier Transform subroutine that already exists in the computer library, and output in the forms of Cosine (C) and Sine (S) functions of Fourier coefficients of various frequencies ranging from the first harmonic to the one that has period twice the sampling interval, into paper tape as data which are prepared for the next computing of the transfer function values A and B.

Example of computed amplitude and phase spectrums of H, D and Z components plotted against periods are shown in figure 8.

The relations between amplitude and phase spectrums with the Cosine (C) and Sine (S) functions are :

$$\text{Amplitude}(\omega) = (C^2 + S^2)^{1/2}$$

$$\text{Phase}(\omega) = \tan^{-1}\frac{S}{C}$$

Figure 8 is the plotted spectrums of the event at Rosevale for six hours from 16^{16} to 22^{16} in September 28 1978.

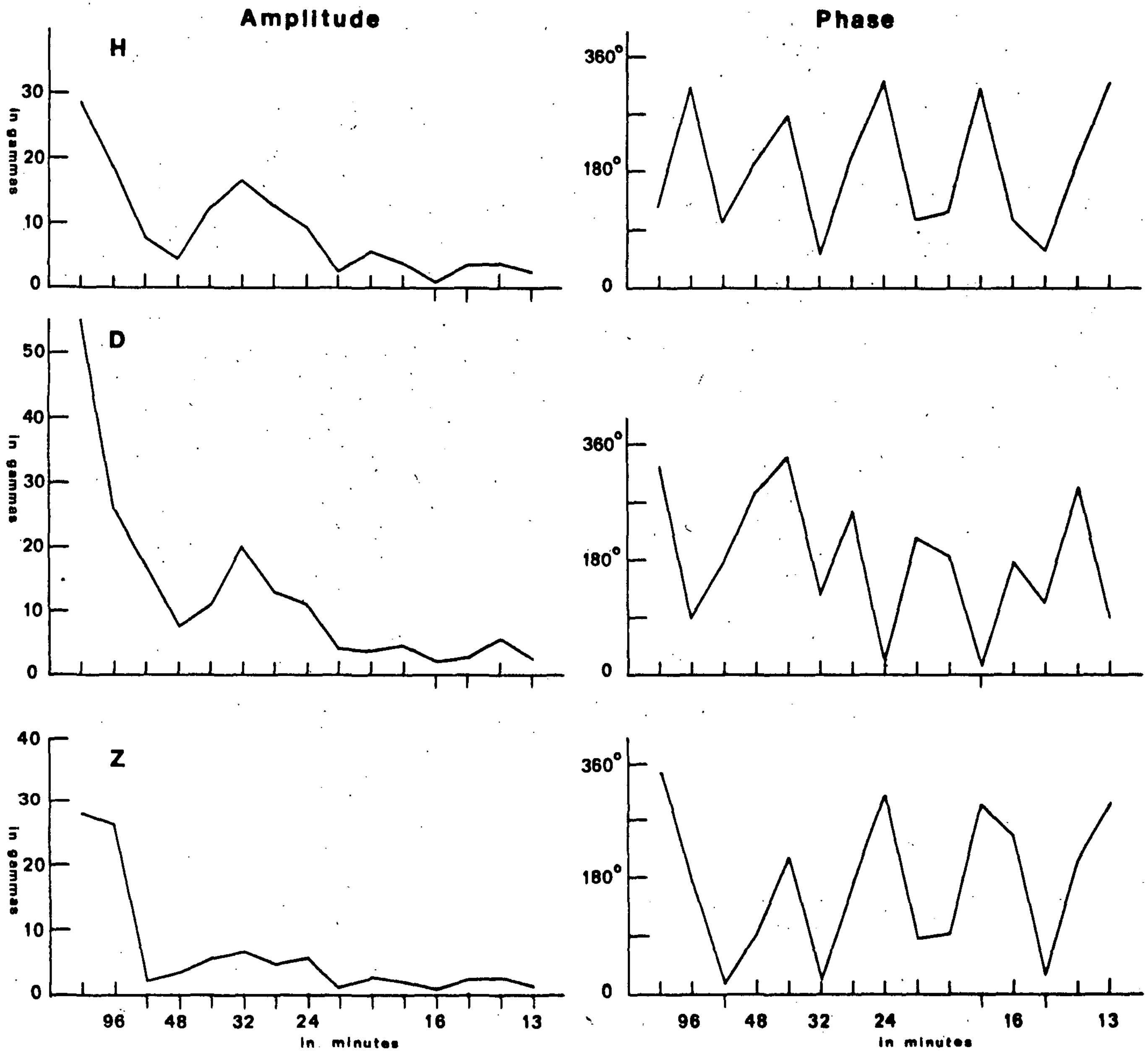
Amplitude
Phase
H
D
Z
in gammas
0
10
20
30
40
50
0
180°
360°
96
48
32
24
16
13
in minutes

Figure 8

II-2-2 COHERENCY

A check of coherency between the vertical and the horizontal components was done using the equation (Kanasewich, 1973) that was modified as :

$$C = \frac{\langle \underline{Z} \cdot \underline{B}^* \rangle^2}{\langle |\underline{Z}|^2 \rangle \cdot \langle |\underline{B}|^2 \rangle}$$

where : $\underline{Z}$ is the Fourier transform of Z component.

$\underline{B} = \underline{H} \cdot \cos\Theta + \underline{D} \cdot \sin\Theta$ ($\underline{H}$ and $\underline{D}$ are the Fourier transforms of H and D components respectively and Θ is the azimuth.

- The asterisk * indicates the complex conjugate of complex number concerned.
- The brackets $\langle\ \rangle$ indicate averaging over all events. Notice that averaging was done over events at constant period, not over the adjacent periods.

Expected value for C is close to one if $\underline{Z}$ is controlled by $\underline{B}$. The closer it is to one the more closely related are the two processes at particular period.

Coherencies were calculated for all values of Θ. The maximum values and the azimuth of the induction vectors are shown in Table 4.

The coherency values at periods 24, 32 and 48 minutes appear quite good at all stations, except values at 48 and 24 minutes at Scottsdale, and value at 48 minutes at Forester. The direction of induction vectors with relatively ~~maximum~~ large values generally coincide with the direction of either the real or imaginary induction vector whichever is larger.

The coherency values calculated between magnetic component are generally lower than between e.g E_x and H_y in magnetotellurics.

For longer periods, the azimuth Θ of maximum $|C|$ mostly coincides with the directions of the imaginary induction vectors, while at short periods it seem to associate with the real one.

TABLE 4

THE MAXIMUM VALUES AND PHASES OF COHERENCY AT VARIOUS PERIODS

	DELORAINE			ROSEVALE		
Period in min.	Direct. of Induction Vector	|C|	Phase of C	Direct. of Induction Vector	|C|	Phase of C
96	180°	0.77	60°	160°	0.78	68°
64	-	-	-	180°	0.71	88°
48	185°	0.76	88°	190°	0.74	112°
32	20°	0.82	-76°	190°	0.93	134°
24	195°	0.75	129°	190°	0.92	152°
16	30°	0.84	-55°	15°	0.47	-1°
13	195°	0.73	149°	30°	0.40	-162°

	LILYDALE			NABOWLA		
Period in min.	Direct. of Induction Vector	|C|	Phase of C	Direct. of Induction Vector	|C|	Phase of C
96	340°	0.51	-137°	330°	0.46	-120°
64	-	-	-	340°	0.70	-132°
48	340°	0.83	-121°	330°	0.83	-122°
32	340°	0.86	-109°	340°	0.79	-131°
24	320°	0.65	-71°	190°	0.70	2°
16	10°	0.55	-137°	350°	0.62	-154°
13	250°	0.33	-33°	200°	0.39	-1°

	SCOTTSDALE			FORESTER		
Period in min.	Direction of Induction Vector	|C|	Phase of C	Direct. of Induction Vector	|C|	Phase of C
96	180°	0.49	49°	180°	0.49	75°
64	170°	0.75	43°	180°	0.62	41°
48	320°	0.56	-156°	170°	0.29	52°
32	320°	0.67	-114°	170°	0.86	81°
24	170°	0.51	29°	170°	0.92	85°
13	290°	0.20	-11°	280°	0.67	6°
16	190°	0.40	9°	290°	0.68	-70°

II-2-3 DETERMINATION OF TRANSFER FUNCTIONS A AND B

Transfer function values A and B are used to determine the induction vector that has been often mentioned earlier. The early method is by a using polar diagram that was developed by Parkinson (1962), where the vector changes of the geomagnetic field tend to lie in a plane, called by Parkinson as "preferred plane" for the station.

Also Sasai (1967) has plotted the ratios of $\frac{\Delta Z}{\Delta H}$ against $\frac{\Delta D}{\Delta H}$ for geomagnetic variations that have period of 30 minutes and shorter. The plotted points seem to lie on a straight line. By taking two pairs of values on that line, and inserting them into the equation :

$$\frac{\Delta Z}{\Delta H} = A + B \cdot \frac{\Delta D}{\Delta H}$$

, the transfer functions A and B can be found. The two methods that have been discussed above deal only with the real part of transfer function. For few periods where the three components are often out of phase, the calculation of transfer function with this method becomes more complicated.

For more valid treatment and calculation with wide range of frequency, the determination of transfer functions that was developed by Everett and Hyndman (1967) was used. The records which contain geomagnetic activity (e.g substorm events) were selected and Fourier coefficients were obtained for the north, east and vertical components.

For each station a group of values at particular frequency thus obtained, and these values then were used to find the best fit to the equation : $\underline{Z} = A.\underline{H} + B.\underline{D}$. All of transform values consist of real and imaginary parts. The equations involved in the calculation are shown as below (Everett and Hyndman, 1967) :

$$A = \frac{\bar{P}E - \bar{Q}X}{NE - X\bar{X}} , \quad B = \frac{\bar{Q}N - \bar{P}X}{NE - X\bar{X}}$$

where : $N = \sum_1^n H \cdot \bar{H}$, $P = \sum_1^n H \cdot \bar{Z}$

$E = \sum_1^n D \cdot \bar{D}$, $Q = \sum_1^n D \cdot \bar{Z}$

$X = \sum_1^n H \cdot \bar{D}$

these values were summed over n events.

The bar above the letters indicates the conjugate of the complex number concerned. The transfer function values A and B calculated using this method are tabulated in Appendix 1 , and are plotted against periods and shown in Plate II.

TRENDS OF TRANSFER FUNCTIONS AGAINST PERIODS

There ~~are~~ two clear differences between the transfer function (TF) values in the areas east and west of the Tamar River, that can be seen especially from the real parts of the TF.

The variation trends of TF values plotted against periods are shown in figures 9 and 10. Most of the stations have TF trends varying smoothly with period. The stations with this condition are WJC, DLR, RSV, WFR, LLD, PPR and FRT (indicated by full circle in figure 11). The trends at SCD and BFR are drawn by interpolating between periods with ~~with the help of~~ relative low uncertainty at groups of TF at adjacent periods with small fluctuation (indicated by half full circles in figure 11). TAY and NBL trends are difficult to obtain, for they have big values of uncertainty, especially at periods in between 16 and 32 minutes at NBL (see Pl II-7, page 70).

The graphs of trend in figures 9 and 10 show the appearance of anomalous characteristic of this area. By knowing that the positive A of TF has the north direction, the negative A of TF has the south direction, as well as the B of TF has the east direction for positive value and west direction for negative B value of TF, thus by examining the trends of the graphs in figures 9 and 10 , some informations can be derived as follows.

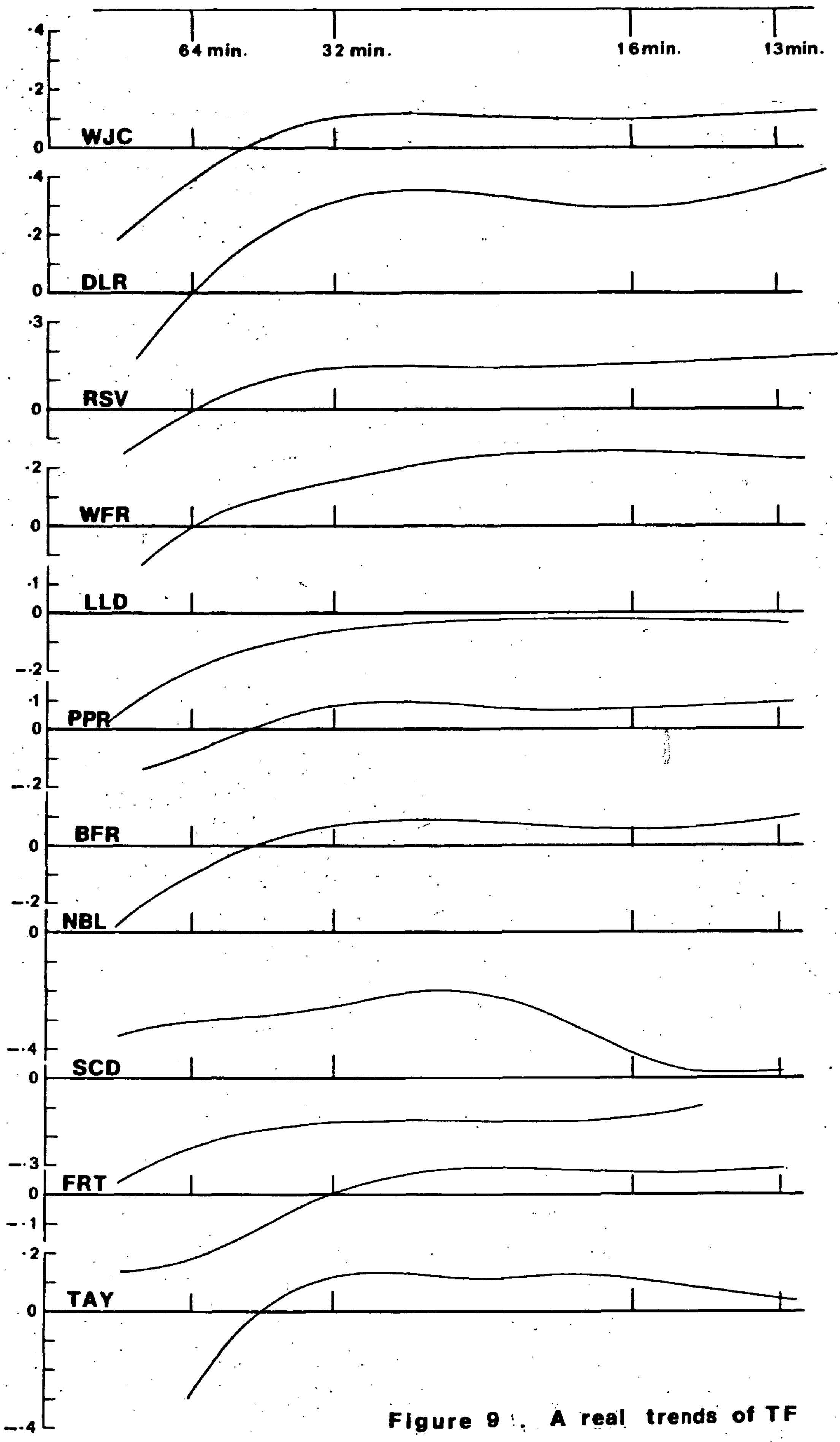

Figure 9 . A real trends of TF

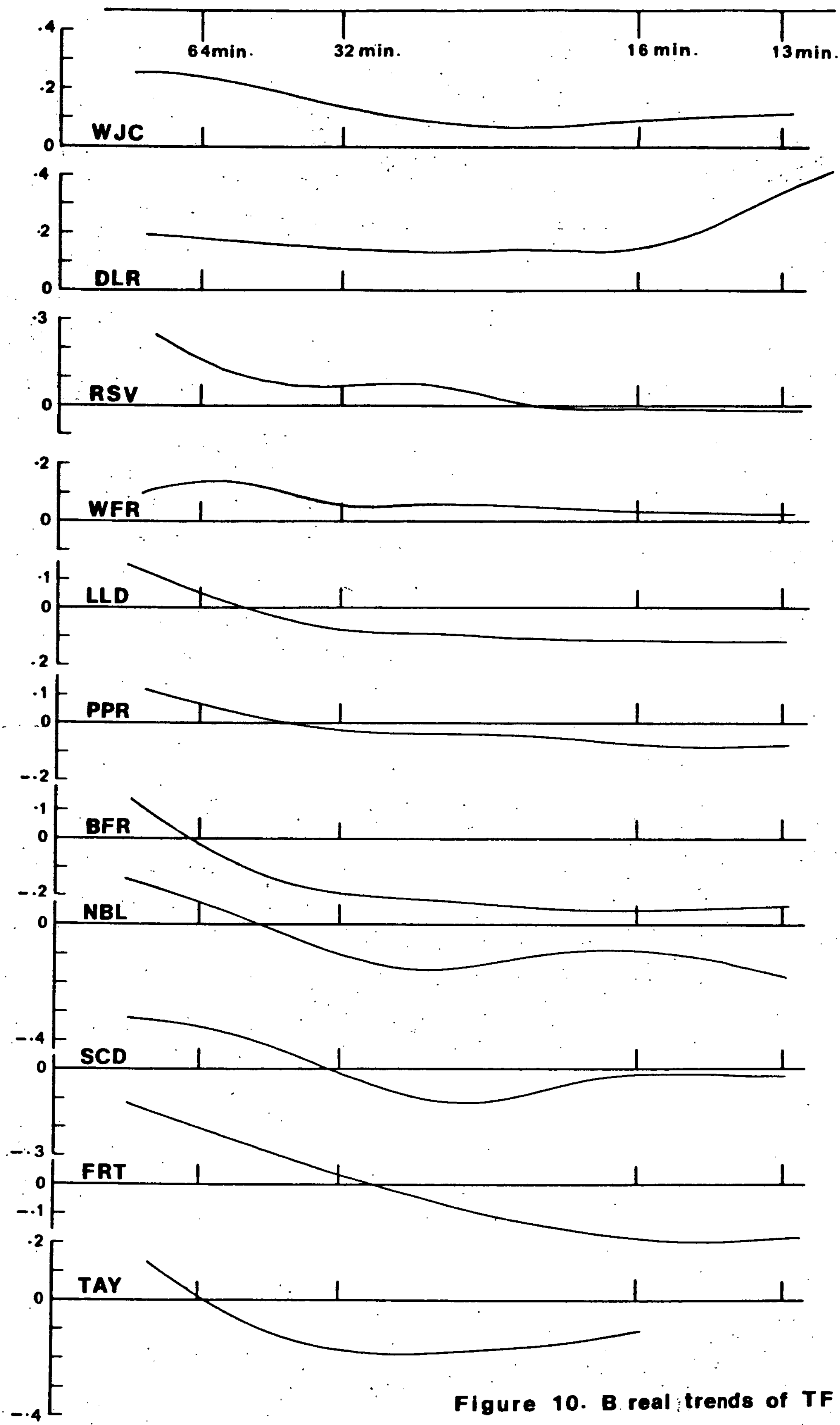

Figure 10. B real trends of TF

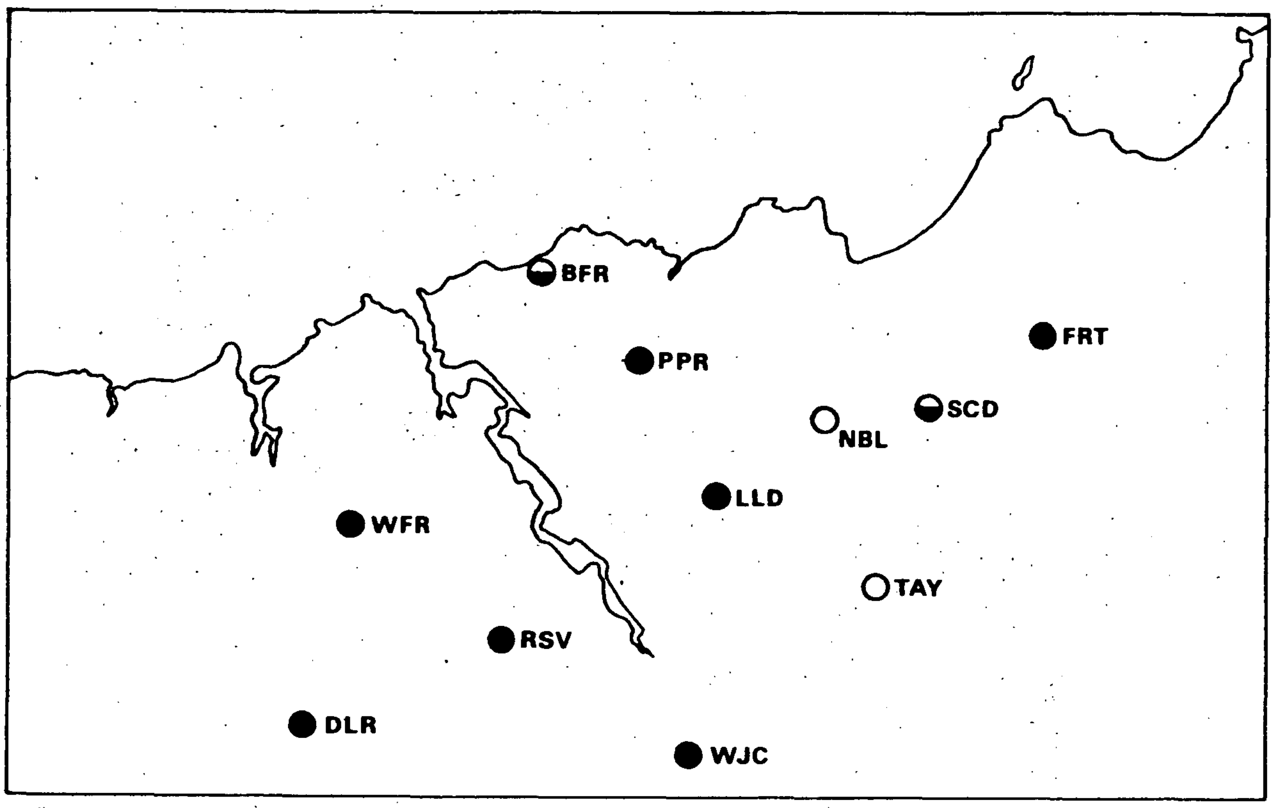

Figure 11

All of the west side stations at periods shorter than 32 minutes, have positive A real, and also positive B real (see figures 9 and 10, except a part of shorter period at RSV, thus the direction of the induction vectors will be to the north east.

At the east side, the stations LLD, NBL, and SCD have negative values of A real, but other stations such as PPR, BFR, FRT and TAY have positive values (fig. 10), meanwhile the B real at all stations in this side of area have negative values at periods less than 32 minutes (see fig. 10). Thus the directions of the induction vectors will be to the north west at PPR, BFR, FRT and TAY, and to the south west at

LLD, NBL and SCD.

By noticing that the west side stations have induction vectors point to the north east directions, and the east side stations point to the south west and north **west** directions. Thus the area in between east and west stations shows conductivity anomalies.

The detail explanations about informations that can be derived from induction vectors at various periods will be explained in Chapter III.

Chapter III

INDUCTION VECTORS ANALYSIS AND INTERPRETATION

III-1 INDUCTION VECTORS

Induction vectors applied in this analysis as has been mentioned earlier follow the one that was developed by Parkinson (1962), where the vectors point toward the high conductive zone. The results of calculation are tabulated in Appendix II. All the induction vectors at periods 96, 64, 51, 32, 24, 16 and 13 minutes are shown in figures 12 to 18.

INDUCTION VECTORS FOR PERIODS 64 AND 85 - 96 MINUTES (Figure 12,13) :

The effect of the coast from the deep ocean to the south east clearly influences the induction vectors at this range of period. Although the effect can be seen at all of the stations, the west side stations WJC, RSV, DLR and WFR are more stable in direction.

At all stations on the east side of the Tamar, as soon as the period decreases to 64 minutes, there is a slight rotation of the vectors to the west. This indicate that the effect of deep lateral variations of conductivity to the west of these stations has started to give some effect. Notice also that the length of the induction vectors are shorter at the stations on the north compared than those at the south, indicate the reducing of deep sea effect in the south east direction.

The centre of the survey area is about 185 kms from the continental slope. On the basis of average coast effect (e.g Parkinson and Jones, 1979) a transfer function values between 0.2 and 0.3 would be expected. The observed average value of transfer in the study area is 0.22.

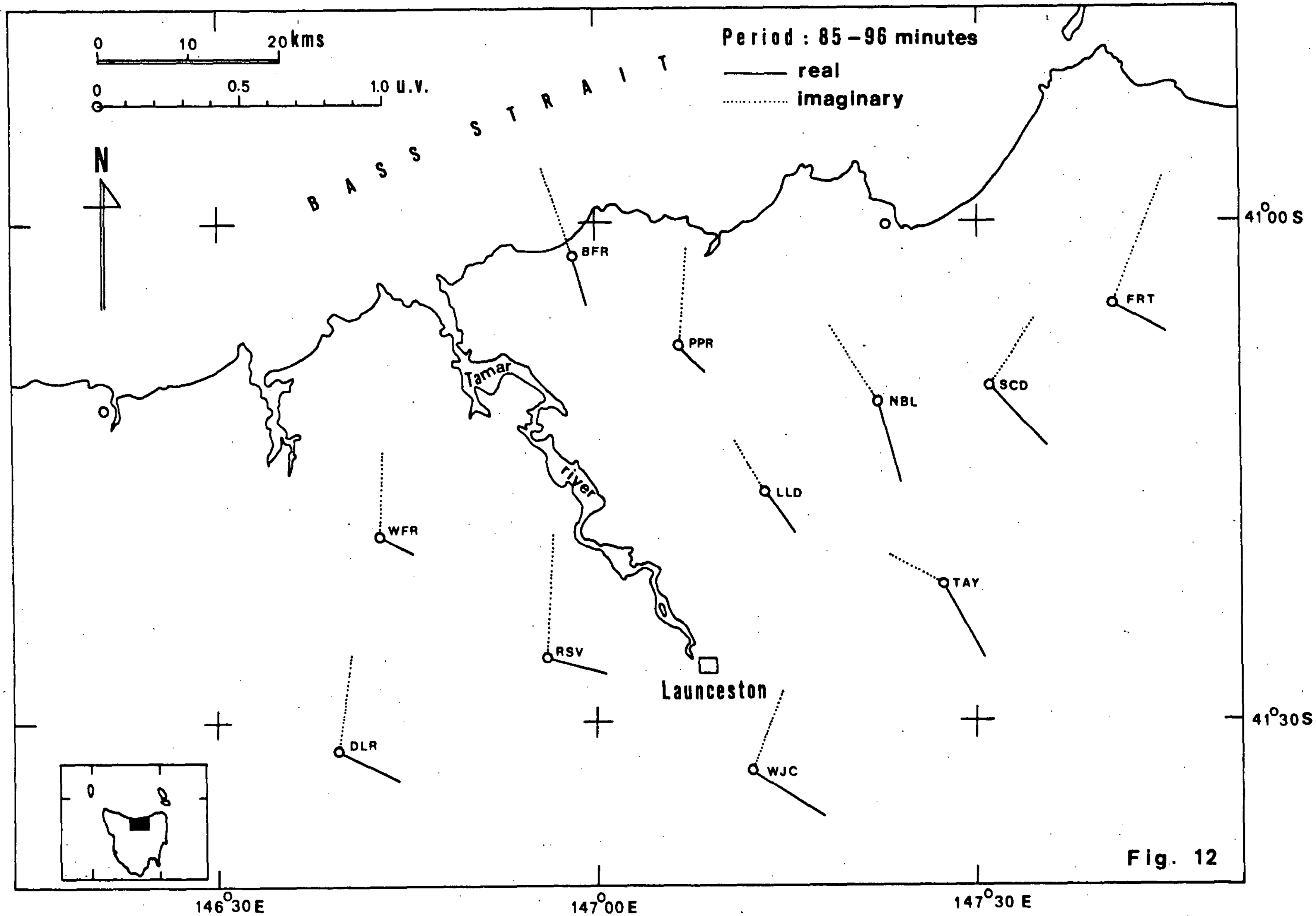

Period : 85 – 96 minutes
real
imaginary
0 10 20 kms
0 0.5 1.0 U.V.
N
BASS STRAIT
Tamar
river
Launceston
BFR
PPR
FRT
SCD
NBL
LLD
WFR
TAY
RSV
DLR
WJC
41°00 S
41°30 S
146°30 E
147°00 E
147°30 E

Fig. 12

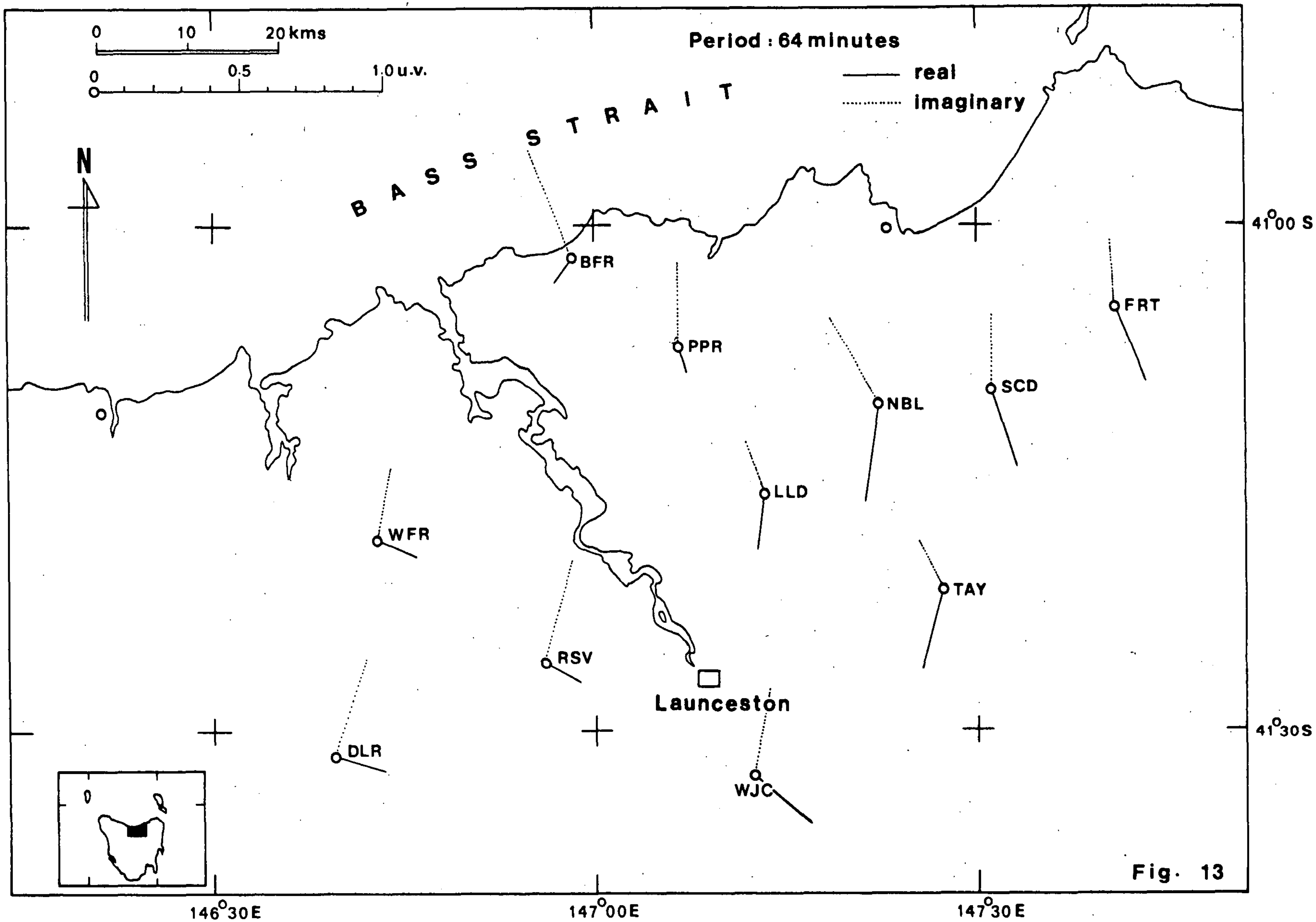
0 10 20 kms
0 0.5 1.0 u.v.
Period : 64 minutes
real
imaginary
N
B A S S S T R A I T
BFR
PPR
FRT
SCD
NBL
LLD
WFR
TAY
RSV
Launceston
DLR
WJC
41°00 S
41°30 S
146°30 E
147°00 E
147°30 E

Fig. 13

INDUCTION VECTORS FOR PERIOD 48 - 51 MINUTE (Figure 14) :

At this period the induction vectors at DLR, WFR and RSV are free from the influence of the southeast ocean effect that occurs at longer periods, and the deep local lateral conductivity structure effect dominates.

Induction vectors at LLD, NBL, SCD and FRT still have the same direction as the vectors of longer period.

Explanation for this is possibly another deep seated conductive zone which occurs south of these stations, and that is stronger than the effects of the known zone along the Tamar.

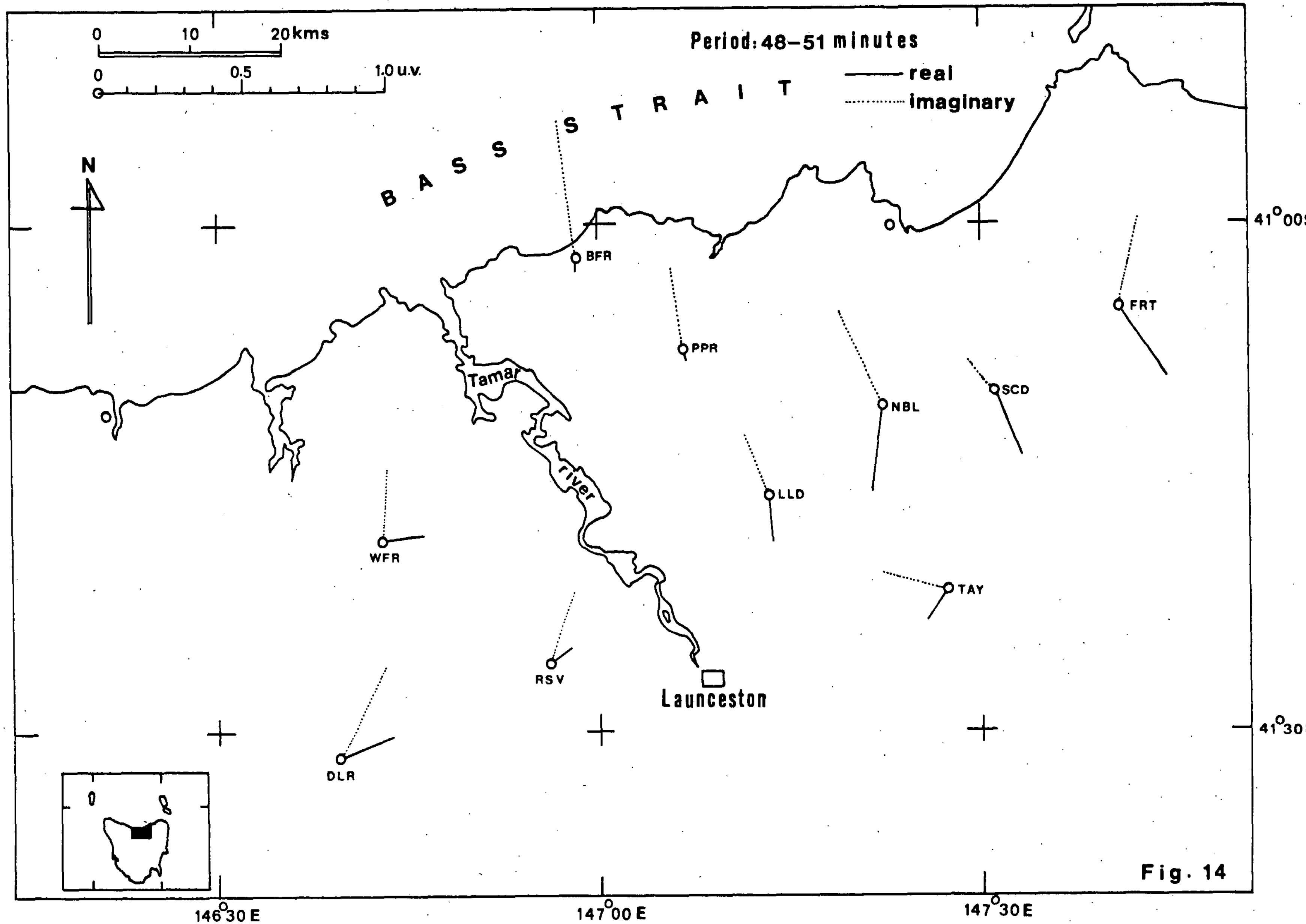
0 10 20kms
0 0.5 1.0 u.v.
Period: 48–51 minutes
real
imaginary
BASS STRAIT
N
BFR
PPR
FRT
NBL
SCD
LLD
WFR
TAY
RSV
DLR
Tamar
river
Launceston
41°00S
41°30S
146°30E
147°00E
147°30E

Fig. 14

INDUCTION VECTORS FOR PERIODS EQUAL TO AND LESS THAN 32 MINUTES

(Figures 15, 16, 17 and 18)

The induction vectors throughout this range of period are free from the south east coast effect, and the remaining factors other than inland anomaly is the influence of induced field from sea water in Bass Strait.

Vectors at all stations on the west side clearly show the effect of the induced electric current near the Tamar graben in the NW - SE direction, but at period less than 16 minutes those at WFR and RSV rotate nearly to the north direction, where the induced field of Bass Strait has a dominant influence.

This combination of land anomaly affected by induced fields in Bass Strait is also shown at FRT,PPR,BFR and Bridport (Lilley,1973-1974).

The direction of induction vectors at NBL, SCD,and TAY at three ranges of periods (32, 24 and 16 minutes) point toward a zone of mineralization (see figure 6, page 10 of this paper., Leaman (1976)).

The small lengths and more or less random directions of the induction vectors at PPR and LLD have been mentioned earlier appear to be situated right in the middle of a conductive zone.

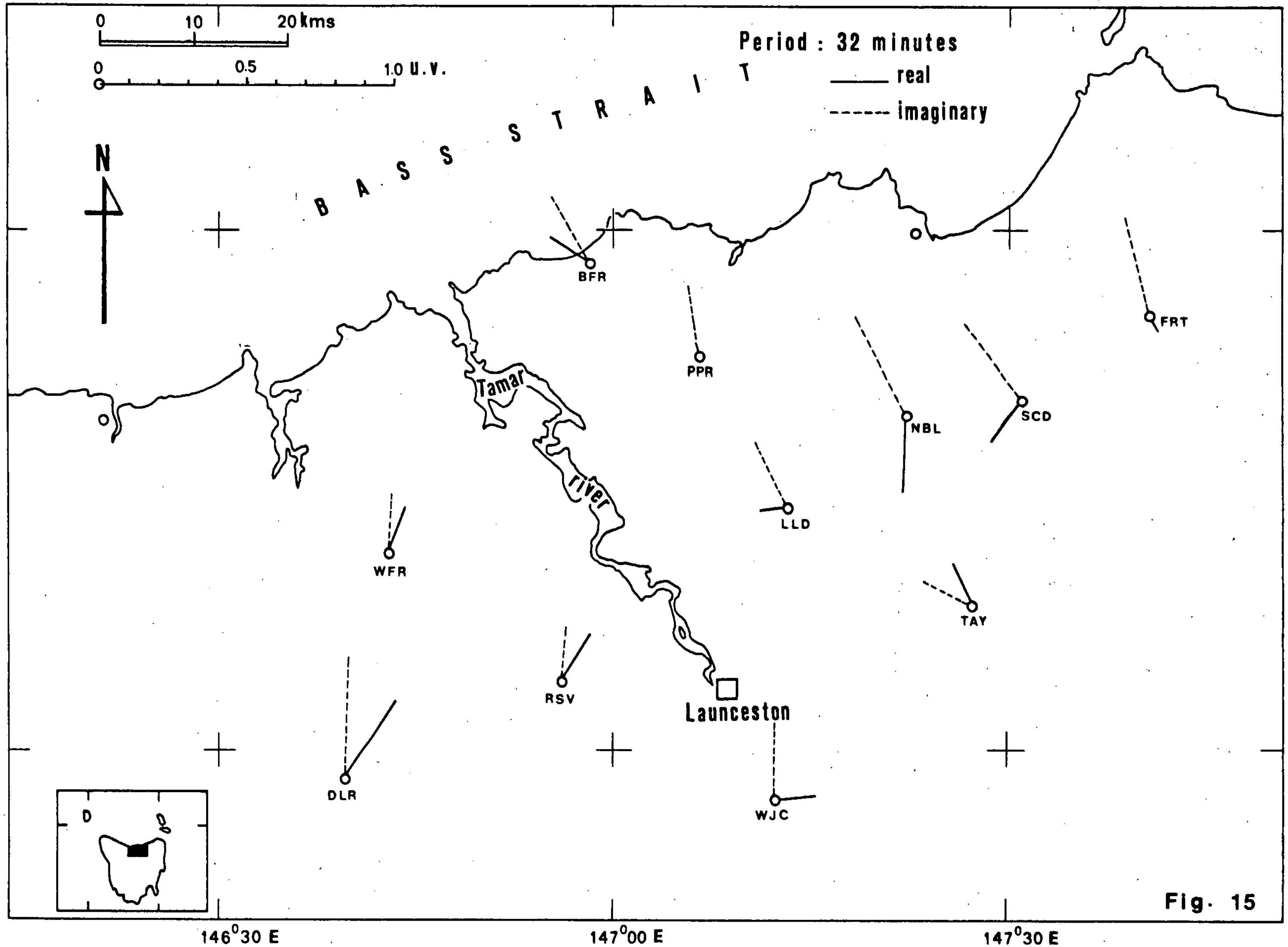
0 10 20kms
0 0.5 1.0 U.V.
Period : 32 minutes
real
imaginary
N
BASS STRAIT
Tamar
river
BFR
PPR
NBL
SCD
FRT
LLD
WFR
TAY
RSV
Launceston
DLR
WJC
D
41°00S
41°30S
146°30 E
147°00 E
147°30 E
Fig. 15

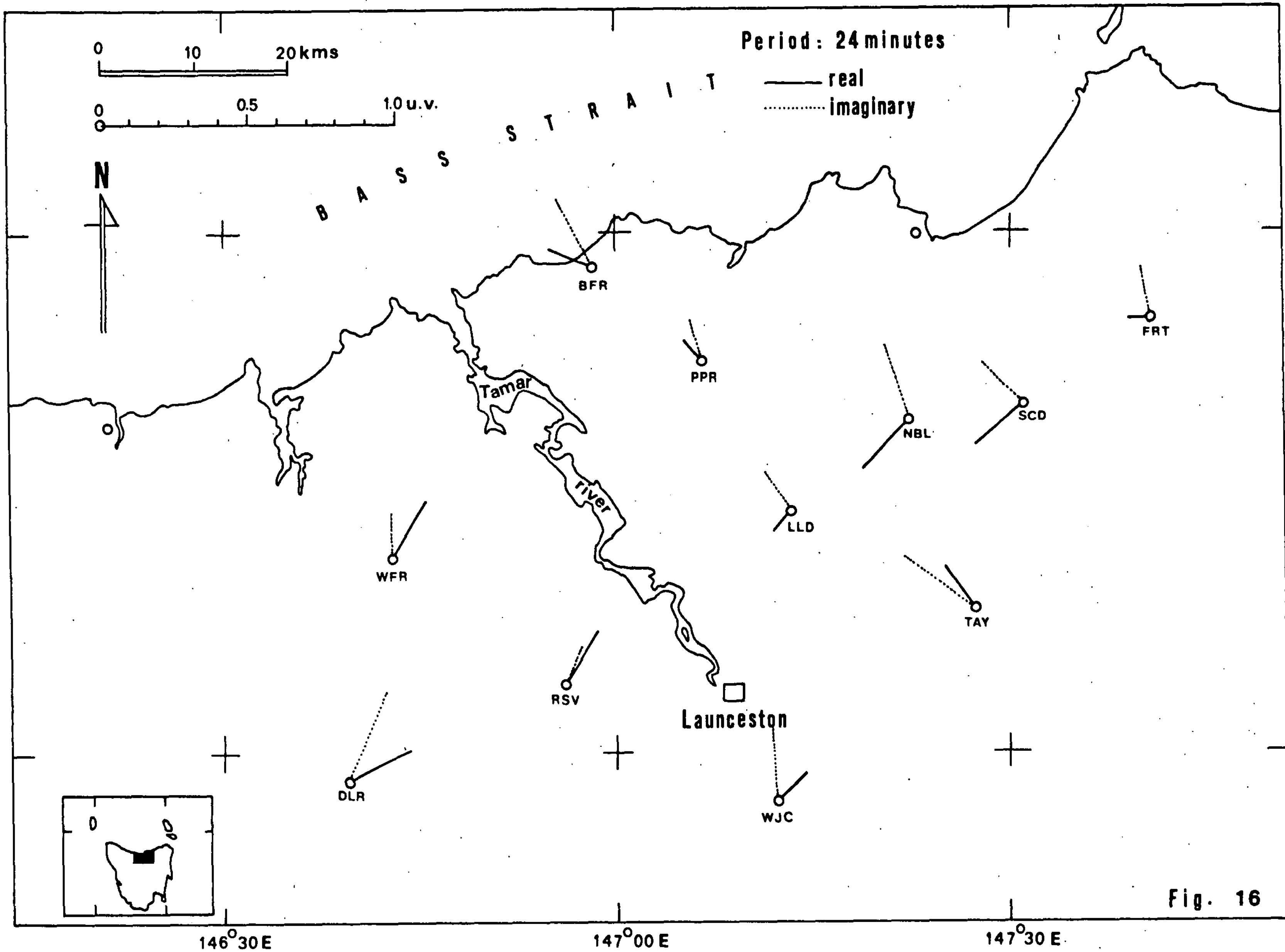

0 10 20kms
0 0.5 1.0 u.v.
N
Period: 24 minutes
real
imaginary
B A S S S T R A I T
Tamar
river
BFR
PPR
FRT
SCD
NBL
LLD
WFR
TAY
RSV
Launceston
DLR
WJC
41°00
41°30
146°30 E
147°00 E
147°30 E

Fig. 16

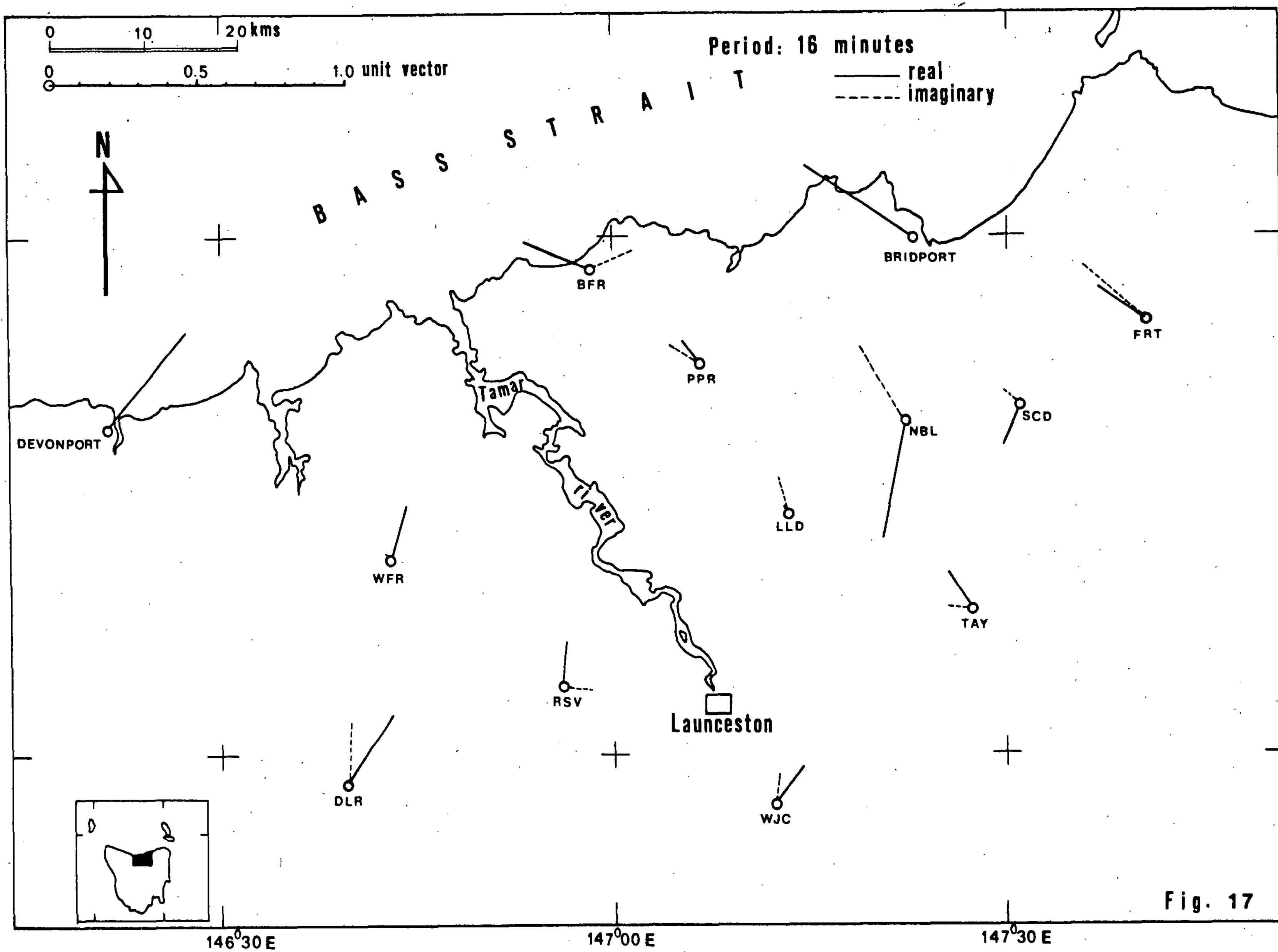

0 10 20 kms
0 0.5 1.0 unit vector
Period: 16 minutes
real
imaginary
N
BASS STRAIT
41°00 S
41°30 S
146°30 E
147°00 E
147°30 E
DEVONPORT
BFR
BRIDPORT
FRT
PPR
NBL
SCD
LLD
WFR
TAY
RSV
Launceston
DLR
WJC
Tamar
river

Fig. 17

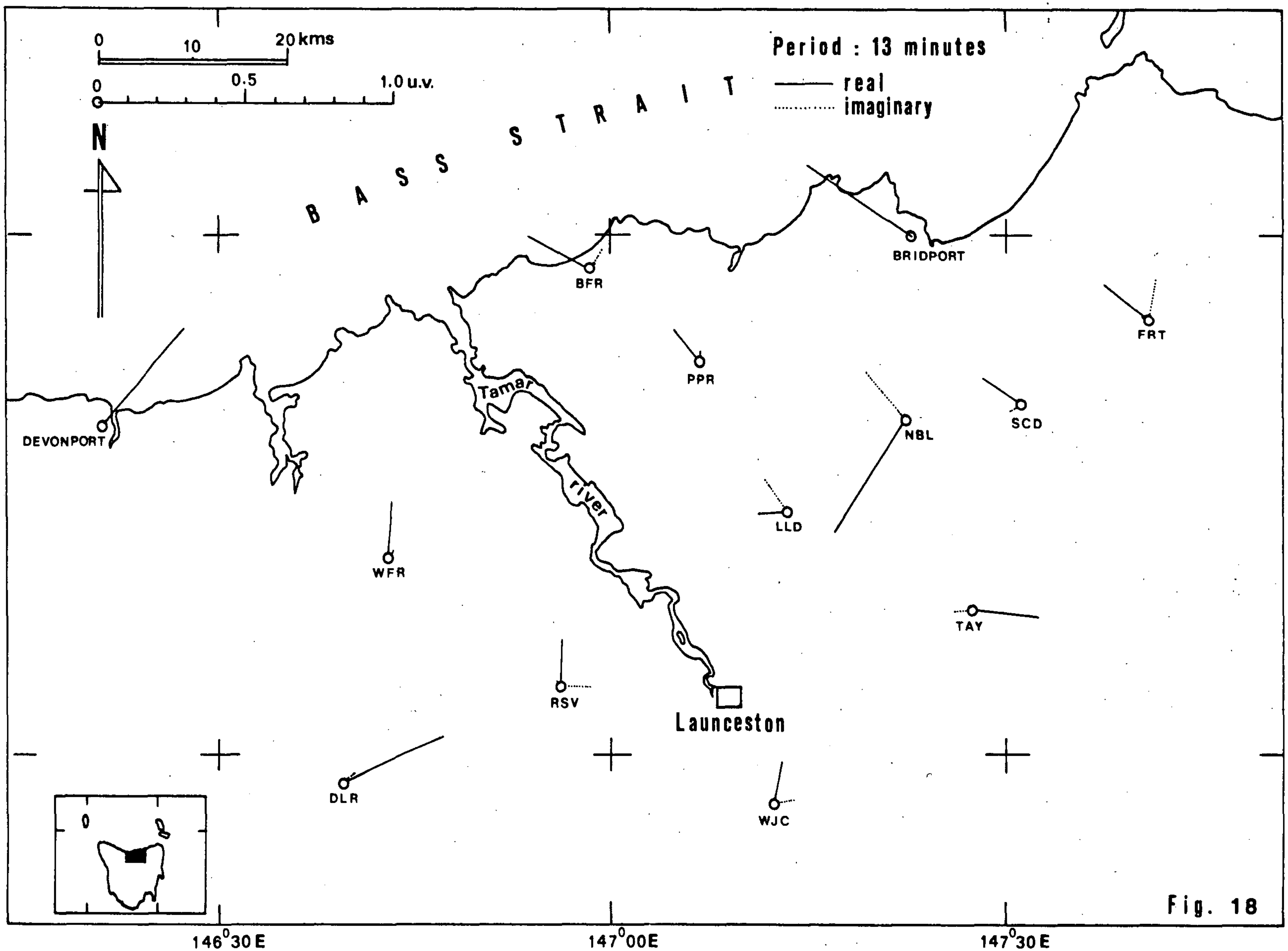

0 10 20 kms
0 0.5 1.0 u.v.
N
Period : 13 minutes
real
imaginary
BASS STRAIT
BRIDPORT
BFR
FRT
PPR
SCD
NBL
DEVONPORT
Tamar
river
LLD
WFR
TAY
RSV
Launceston
DLR
WJC
41°00 S
41°30 S
146°30 E
147°00 E
147°30 E

Fig. 18

III-2 SELECTION OF DATA FOR INTERPRETATION

Since the induction vectors especially at short periods (around 32 minutes) already show an indication of relatively highly conductive zone that influences the direction of the induction vectors, the possible electrical conductivity structure that is responsible has to be interpreted.

It has been assumed that the coastal effect of the ocean to the south east has already vanished at this range of period. Only the induced current from sea water in Bass Strait remainly influencing the induction vectors at this local area, and the influence is mainly on the imaginary transfer function.

The direction of the coast line of this area is about 35°north of east. It will be assumed that the predominant conducting zone is linear and oriented 35° west of north. This can be justified by the geological structure and grain of the area, and the direction of induction vectors of long period west of the Tamar.

At a period of 24 minutes (see figure 16, page 32) the induction vectors at LLD, NBL and SCD point toward a conducting zone in a WSW direction. However the random directions at other stations on this east side show that this area has complicated conductivity structure.

Induced electric currents in the pressumed conducting zone, with a trend NNW-SSE, cause magnetic field vectors in the direction 35° north of east. This is parallel to the coast line and perpendicular to the regional structure of geology as well as the direction of the conducting zone. The data used in a two-dimensional interpretation are the components of the induction vectors projected onto a line bearing 35° north of east. The stations used are those along the traverse from DLR to FRT.

Considering the projections of vectors onto a line bearing 35°north of east is equivalent to considering a "virtual event" in which the horizontal field is linearly polarized in the direction E 35° N and has unit amplitude.

The projections of the real and imaginary vectors then indicate the amplitudes of the in phase and out of phase parts of the vertical field.

Over a wide range of frequencies the imaginary transfer function vectors tend to lie in fairly uniform direction (between N and NW), and vary in amplitude rather than direction. This is shown in figures in Plate II, by the imaginary parts of A and B appearing as mirror images of each other.

The imaginary transfer function vectors seem to be controlled by induction in the shallow water of Bass Strait, and only the real transfer function vectors are controlled by conductivity variations on land. For these reasons only the real part of the transfer function will be taken more attention in the interpretation of inland anomaly. The contour maps of the observed vector components at periods of 85 - 96, 64, 48, 32, 24 and 16 minutes are shown in figures 19 to 21.

At all periods these contour maps show that there is an approximately two dimensional conductivity structure on the west side, while on the east side a more complex structure is involved. A possible reason for the complicated structure of conductivity in the area to the east is a complicated boundary between the granite - granodiorite mass and the thick sedimentary Mathinna Beds. This would involve an edge effect between the low conductive igneous rocks and high conductive sedimentary rocks.

The observed vector components that will be used as surface field observations for the interpretation are shown in figure 22. These values then have to be fitted to the calculated values from models of conductivity structure.

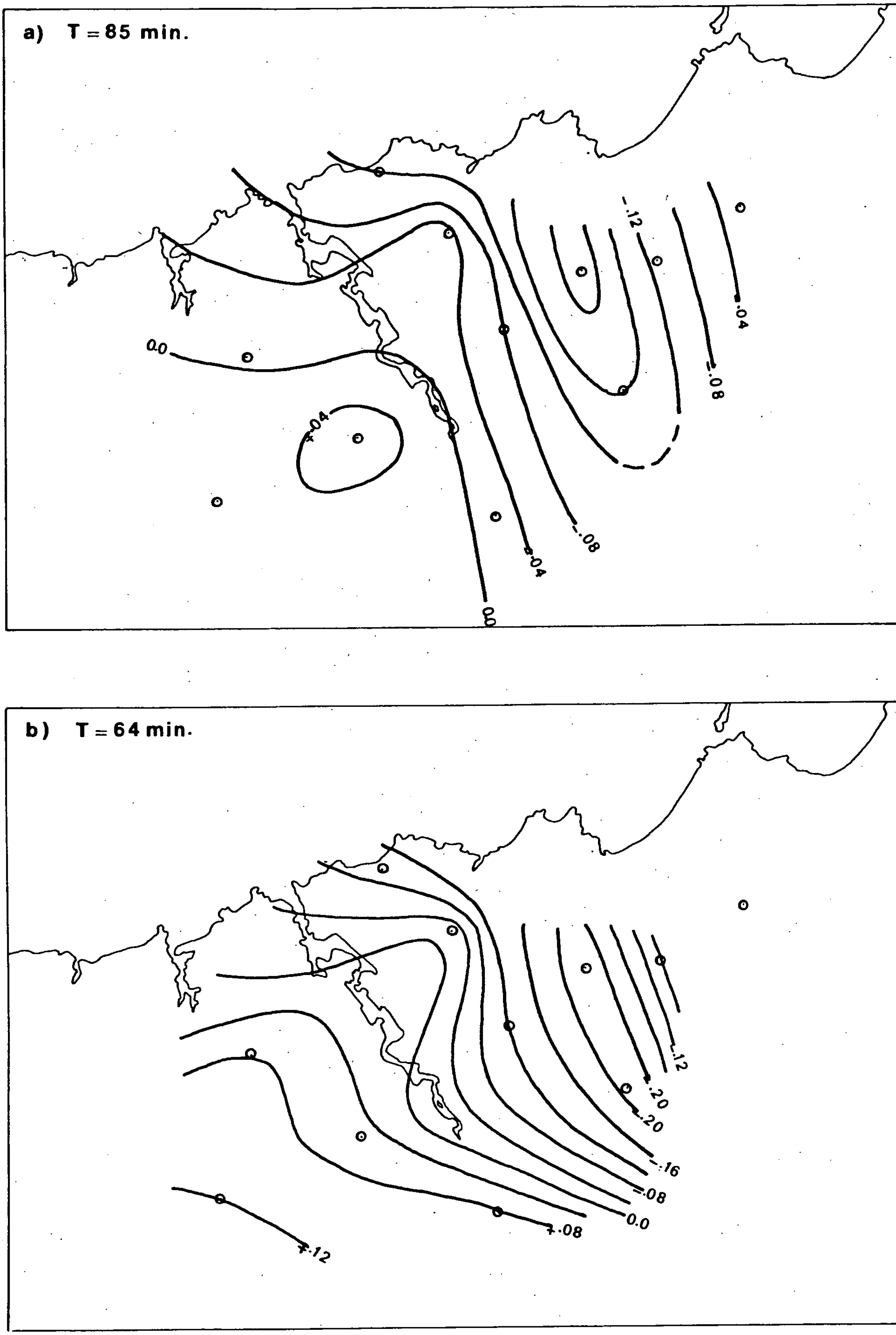

Fig. 19

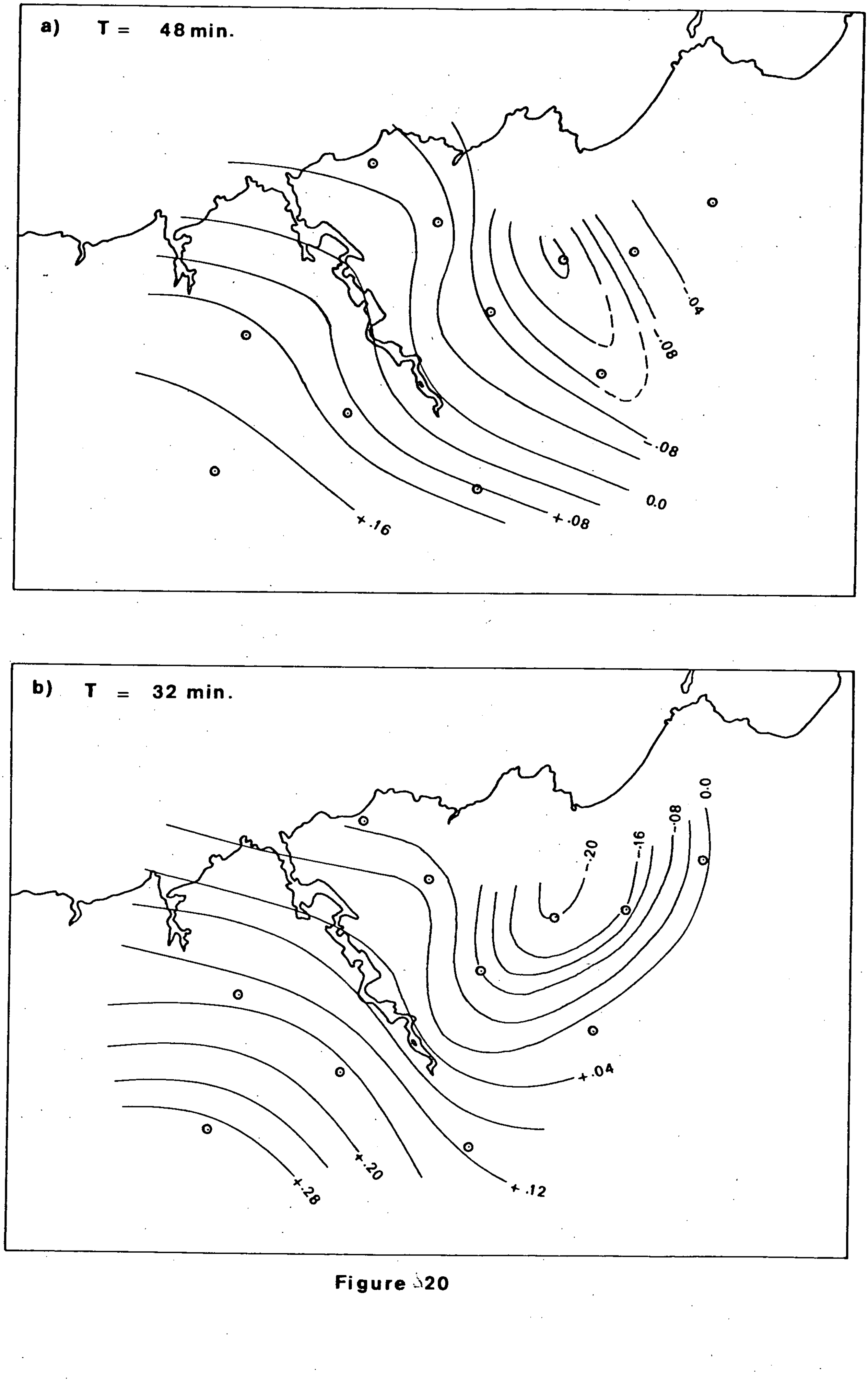

Figure 20

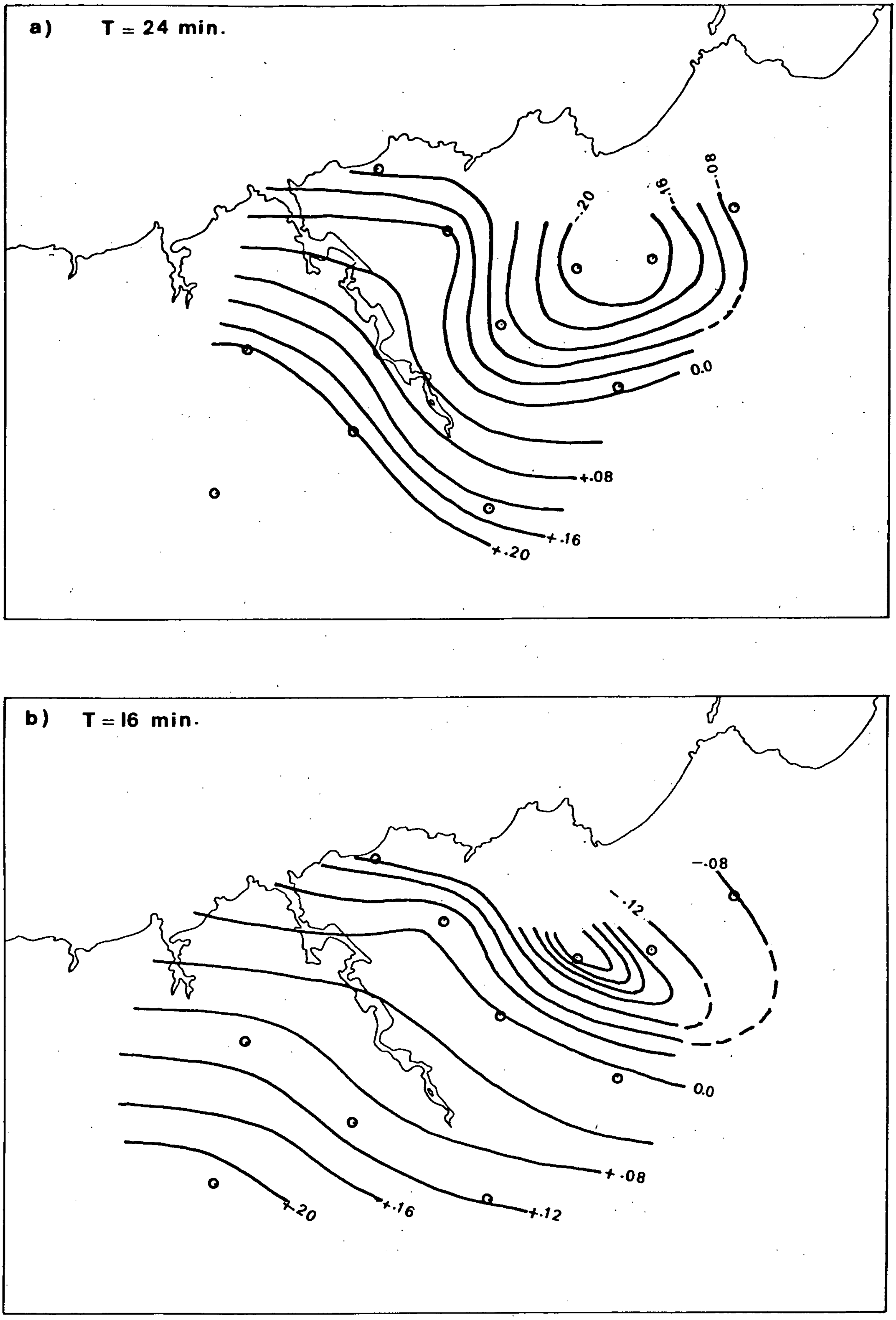

Fig. 21

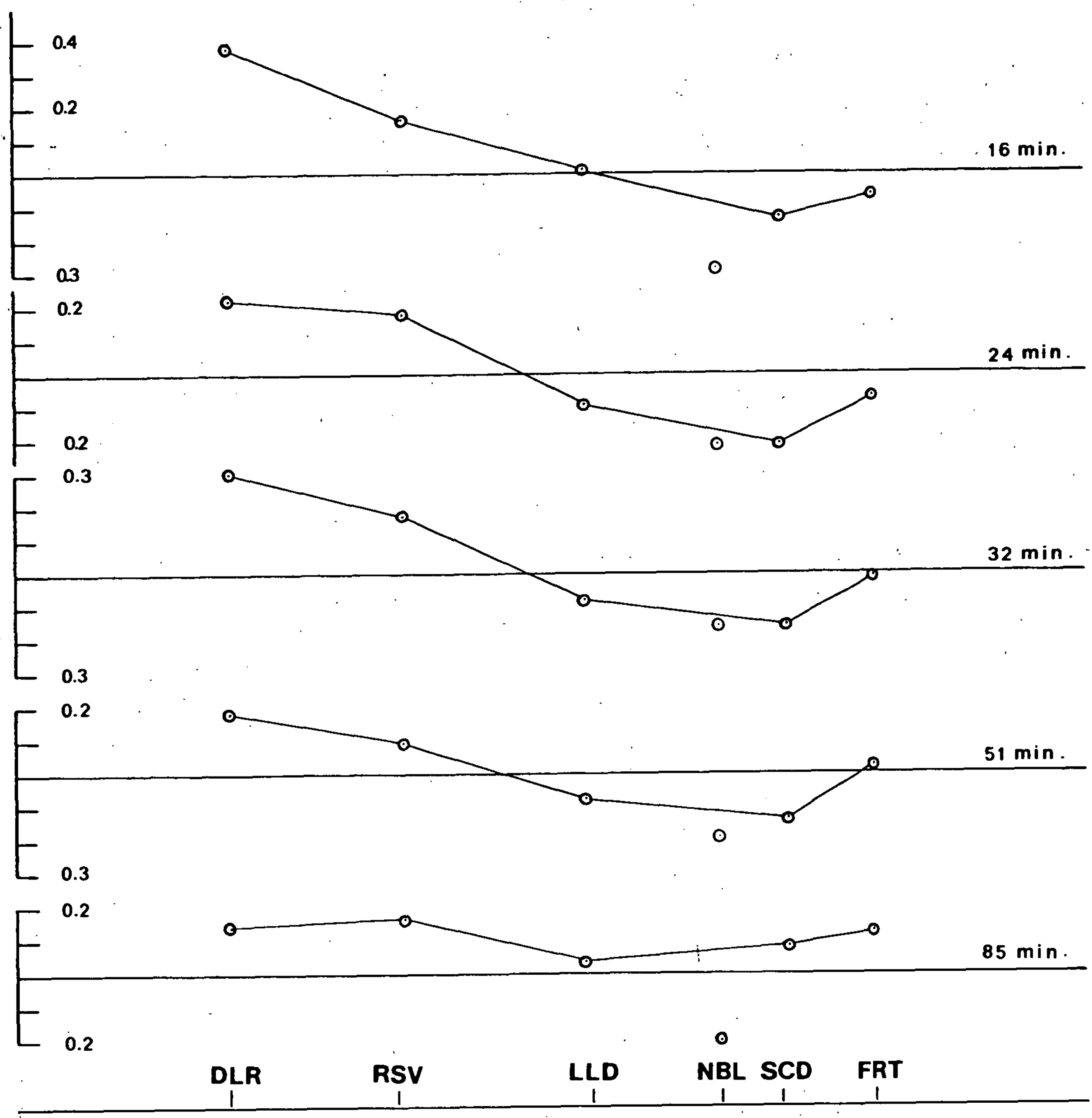
0.4
0.2
0.3
16 min.
0.2
0.2
24 min.
0.3
0.3
32 min.
0.2
0.3
51 min.
0.2
0.2
85 min.
DLR
RSV
LLD
NBL
SCD
FRT

Figure 22

III-3 GEOLOGICAL INFLUENCE IN DESIGN OF MODELS

On the basis of magnetic field variations alone, the distribution of lateral conductivity that fits the field observation in this region consists simply of a high conductive zone lying between Deloraine and Scottsdale. This follows from the high values of the components of transfer functions with positive value (e.g +0.30 for 32 minutes period at Deloraine), and gradually decreasing to east - northeast direction and reaching zero around Lilydale, and becoming high negative at Scottsdale (e.g -0.16 for 32 minutes period), and toward Forester the value increase again.

Because the geology shows that this region consists of several major rock formations which have clear surface boundaries, the surface distribution of formation needs to be taken into consideration in the interpretation of magnetic variations.

The surface distribution of rock formations on the profile Deloraine Forester basically follows the general distribution of major rock formations that dominantly cover this area (see figure 5, page 9). From southwest to northeast there is Precambrian basement at southwest of Deloraine, followed by complicated structure of Cambrian and younger formations, Mathinna Beds and Permian sedimentary rocks, and granodiorite.

Based on geological evolution, a deep conductivity contrast situated between Lilydale and Rosevale was assumed. This contrast zone is consistent with the boundary between contrasting types of Precarboniferous rocks (William, 1978); those to the east include turbidite type of rocks as well as micaceous quartzwacke and mudstone sequence, of which the Mathinna Beds are typical and those to the west are stable shelf deposits such as interbedded quartz sandstone and mudstone and marine and terrestrial sediments, quartz sandstone and conglomerate.

This boundary may be related to the slight rotation of the induction vectors to the west for the east side stations for period 64 minutes, compared to the one with 85 - 96 minutes period.

III-4 METHOD OF INTERPRETATION

The computer program developed by Jones and Pascoe (1971) and Pascoe and Jones (1972) were used to calculate the response at the Earth's surface of two-dimensional conductivity structure. The program has been modified due to errors that were pointed out by Williamson et al. (1974), by some changes to the subroutine ITERE (iteration) from Jones and Pascoe (1971). Brewitt-Taylor et al. (1976) argued that the E-polarization formulas in Jones and Pascoe are inaccurate when the step-sizes of the numerical grid around the point are uneven.

By taking into account the arguments above and by following the suggestion of Jones and Thomson (1974) a modification is used in which the calculated results will be sufficiently accurate when the numerical grid spacings are not too irregular. Also the program was slightly modified so as to compute the amplitude ratio and phase difference between the vertical component and the horizontal component of the field at each station, which enables a direct comparison to be made between the observed response components and the surface values of a model calculation.

The computation was made first for 32 minutes period, where the response appears to vary fairly uniformly with frequency, and the values at 32 minutes period seem to represent the frequency range between 0.03 cycle.min^{-1} to 0.06 cycle.min^{-1}

In planning the model of conductivity structure from Deloraine to Forester, the two-dimensional model with dimension 180 kms and 333 kms for horizontal and vertical dimension respectively was taken.

The top 110 kms of the vertical dimension was taken to represent the zero conductivity of the atmosphere up to the base of ionosphere, where the source of the primary field that is responsible for inducing currents in the conductive zone is located.

The surface lateral variations of conductivity in general follow the major geological formations in this area, and the conductivity values which were taken in the computation are as follows. The value of granodiorite is taken to be 0.54×10^{-3} S.m^{-1}, based on laboratory measurements reported earlier, and this value is also in the range of conductivity value of crystalline rocks (granite, basalt etc) at the temperatures and pressures applicable to the crust (Keller and Frischknecht, 1966). The conductivity value for Precambrian basement is taken to be 0.11×10^{-3} S.m^{-1}, which is also close to the range of conductivity value for the crust based on laboratory measurement of crustal rocks by Brace (1971), which is range in between 0.10×10^{-3} to 0.10×10^{-4} S.m^{-1}. The conductivity of the underlying deep structure that is probably upper mantle, is taken to be 0.20×10^{-2} S.m^{-1}, which is similar to the conductivity value at depth 20 - 30 kms under south eastern Australia according to Woods (1979). These values are reasonable as long as the effects such as partial melting of magma in the upper mantle or strong mineralization in the crust are not involved. The conductivity of the Cambrian sedimentary rocks have been chosen to fit the observed transfer functions. The best value of conductivity for the Cambrian rocks that crop out at Deloraine (figure 28) is 0.54×10^{-1} S.m^{-1} based on the longer period variations. The shorter period variations require a conductivity of 0.11 S.m^{-1} for the superficial layer of Siluro - Devonian Mathinna Beds to Tertiary sediments.

Several attempts have been made in modelling the conductivity

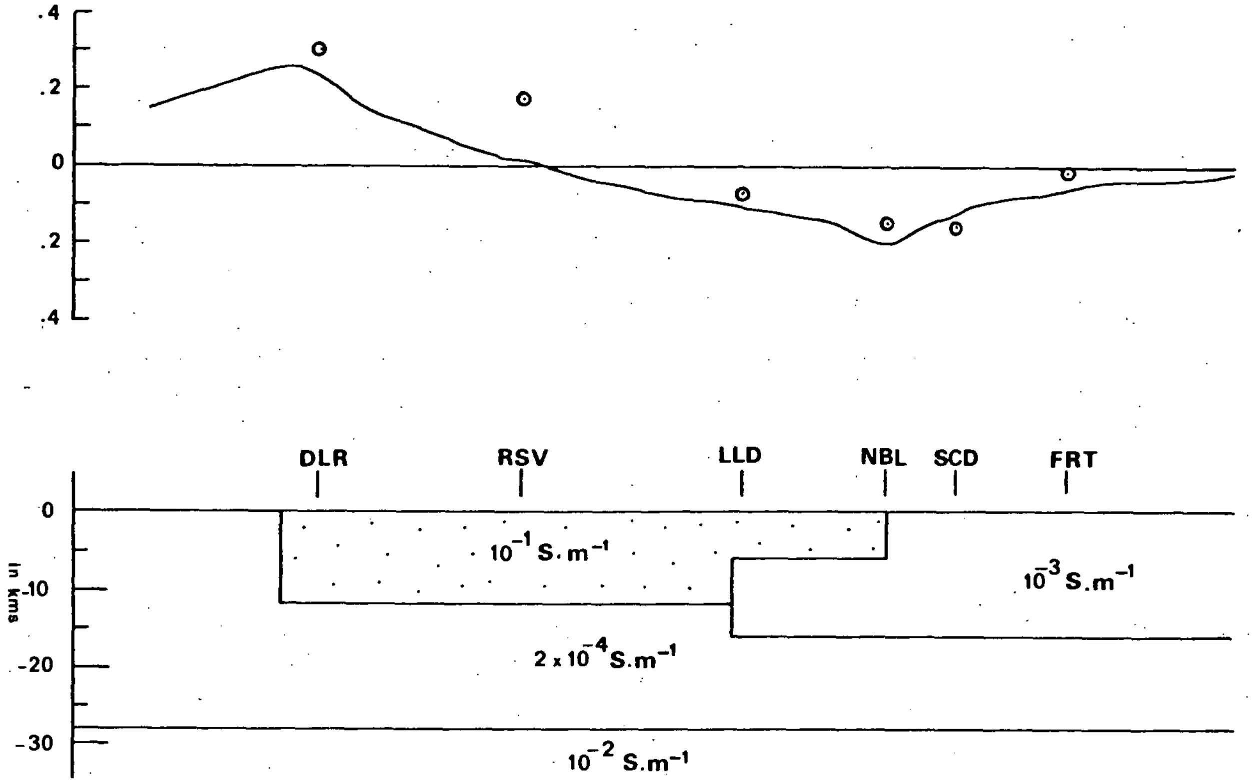

Figure 23

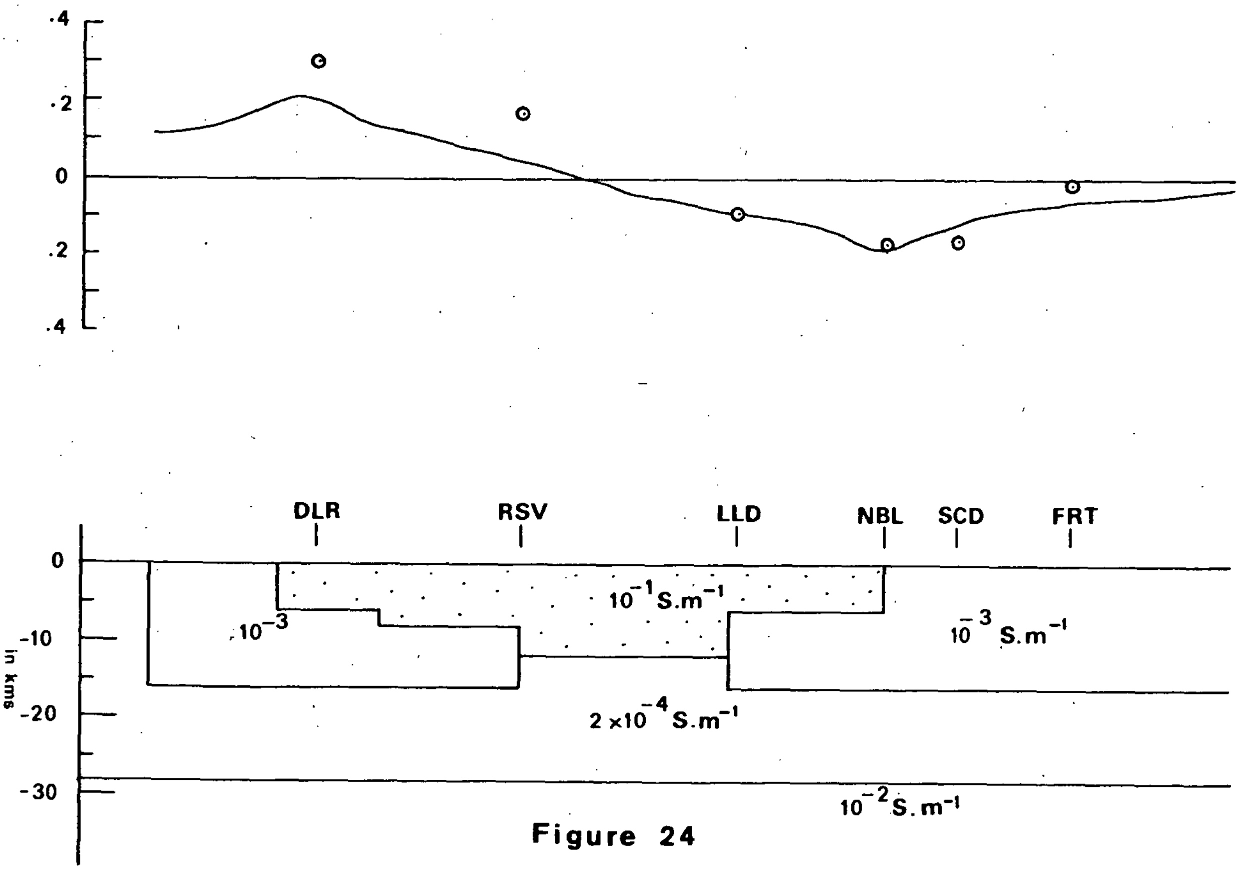

Figure 24

structure to find the best fit to the observed data.
An early model was done by assuming that the highly conductive zone between Nabowla and Deloraine, was bounded to the east by a granodiorite mass with lower conductivity, and that these two formations were underlain by Precambrian basement as the lowest conductive formation (see figure 23). The calculated surface values at the east side show better consistency than the west side.

In the second attempt(see figure 24), a higher conductive zone at the west side that possibly represents the Cambrian formation, was assumed to have the same conductivity as the east conductor. The results show that the east side responses fit fairly well to the observed data, but the west side response is still lower than was expected. At RSV the calculated response has increased slightly as a result of gradually increasing the conductivity of the western formation from low to high value.

The third attempt was by setting a fault in the deep structure with downthrow to the west (see figure 25). The result improved the response value at the west side, but reduced it to the east.
From here was derived a conclusion that the deep structure with relatively high conductive was upthrow at the east area which underlies the low conductive zone at this region. A higher conductivity value to the west has to be taken to reach the high observed values at DLR and RSV, as well as to match the observed values in the east stations.
The conductivity structure as shown in figure 26 which includes a highly conductive surface layer lying in between RSV and NBL is fairly consistent with all observed data.

By realizing that the east side conductor is dominated by granite-granodiorite type of rocks with known value of conductivity. The ratios

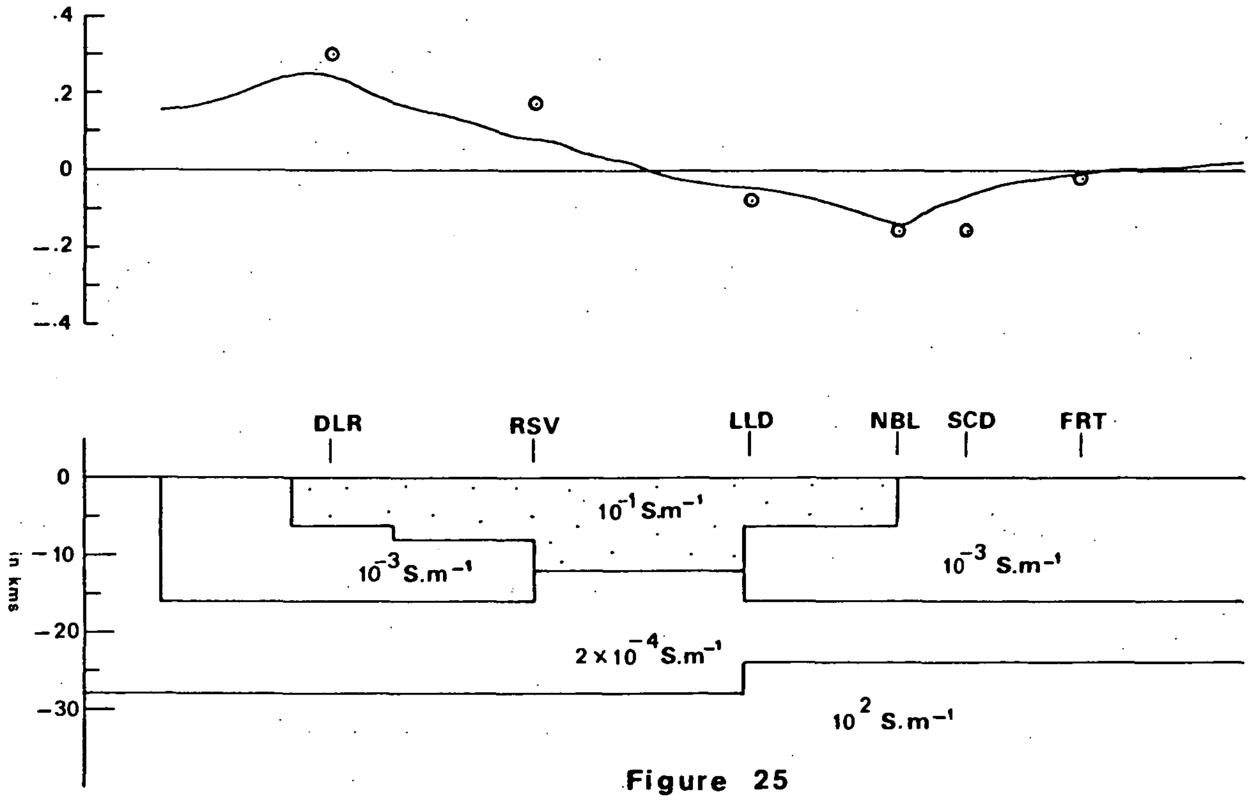

Figure 25

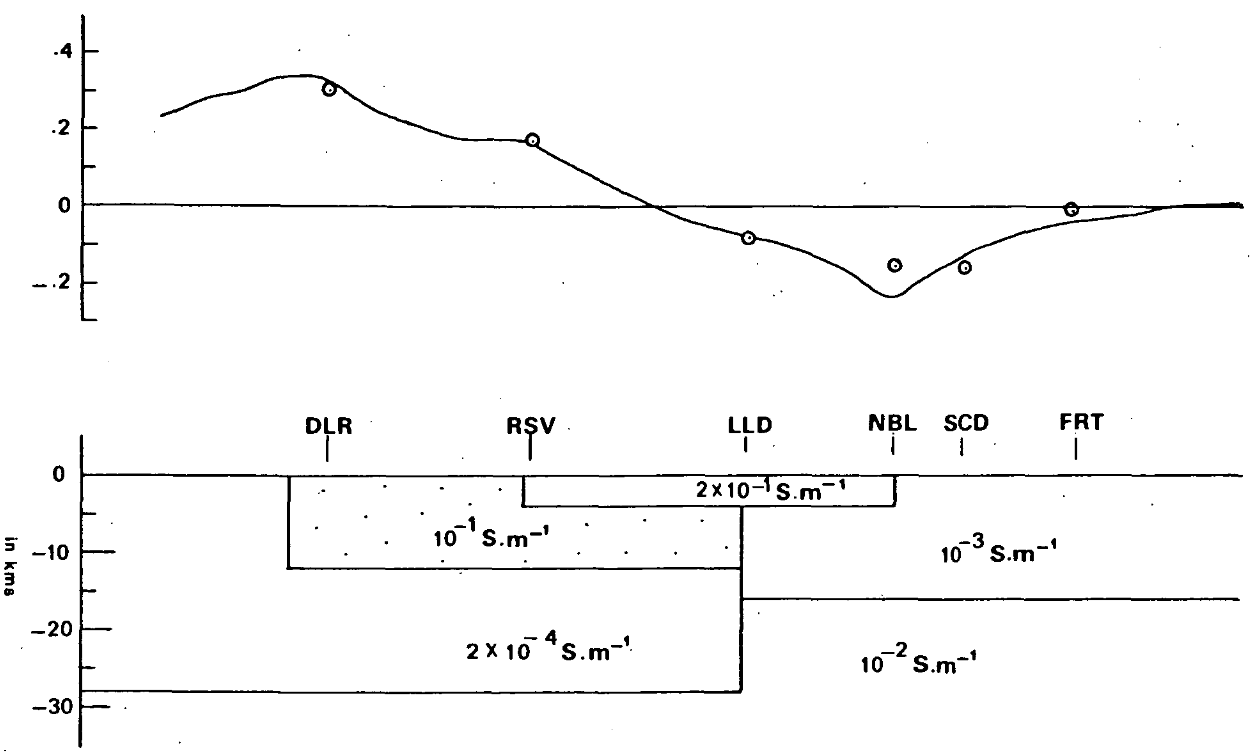

Figure 26

of conductivities in the model shown in figure 26 seem satisfactory. The correct actual conductivities can be found by assigning a value to one rock formation and changing all the others in proportion. The best determined conductivity is considered to be that of granodiorite is taken as 0.54×10^{-3} S.m^{-1}. A closer fit to observations is obtained if the conductivity of the basement is changed to 0.20×10^{-2} S.m^{-1}. This increases the conductivity contrast on the east side.

The best fitting model to the 32 minutes period data for this area is shown in figure 27. To compare this structure with other possible structure that could be fitted to the 32 minutes data, a calculation for every possible frequency response was done. Results are shown in figure 28. Considering the uncertainties of the observations data, this fit seems satisfactory. Only the real parts of the induction vector have been matched, because the imaginary parts seem to be dominated by induction from the Bass Strait.

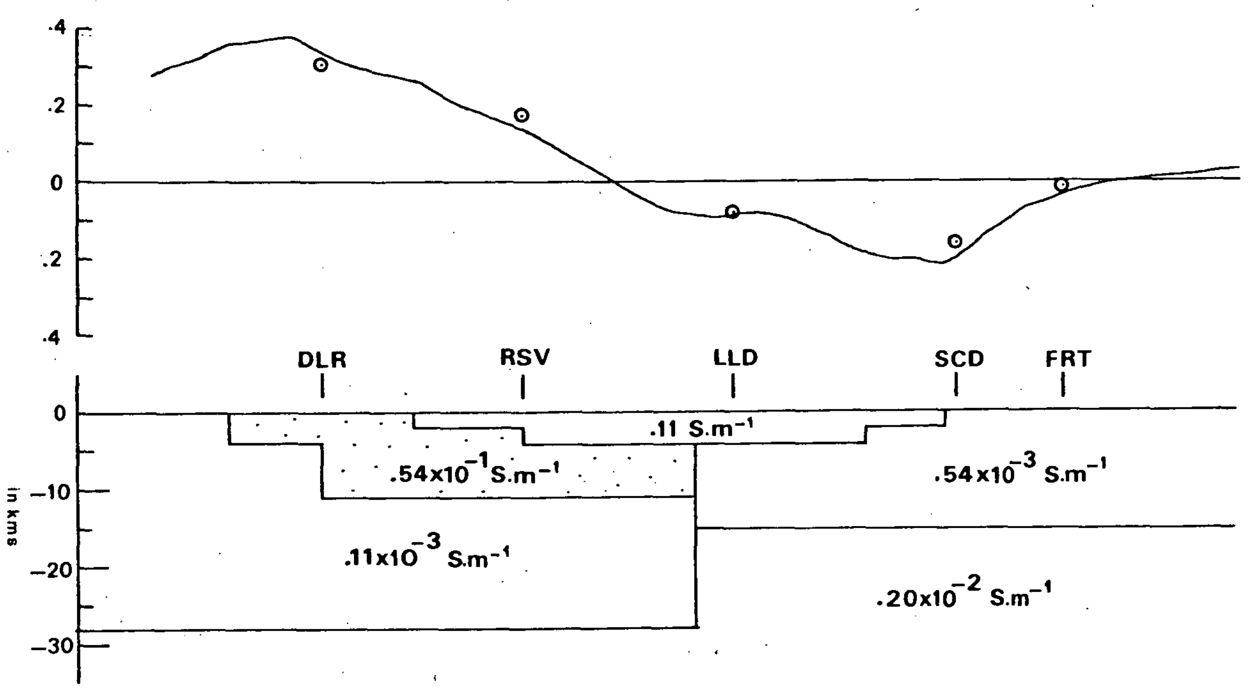

Figure 27

III-5 INTERPRETATION OF STRUCTURE

The conductivity structure derived from geomagnetic variation study as shown in figure 28, shows five different conductivities which have been applied to satisfy the observed magnetic variations as well as other results such as geology and gravity. Although the determination of the depth, thickness and conductivity of the formations involved are subject to considerable uncertainty, the few structural features that are responsible for the anomaly are probably fairly well defined. For example, the deep structure at a depth of 15 kms in the east side, that has a conductivity of about 20 times that of the Precambrian basement, is responsible for complicating the conductive anomaly in the east side, where the induction vectors have relatively small amplitudes and random in directions, compared to the induction vectors in the west side.

There is no obvious reason why the conductivity of the basement rock should be higher than either the Precambrian or granodiorite. The assumption in gravity interpretation is that it is denser than the overlying rocks, which suggests a lower porosity. It is unlikely, but perhaps not impossible, that its increased conductivity is due to higher temperature.

To the west side the later sedimentations are underlain by Precambrian crust that has the lowest conductivity value in this region. Since there is no control of the observed anomaly to the west of Deloraine, the base of this Precambrian crust in that region is left in question.

The conductivity structure clearly shows that the area in the vicinity between Scottsdale and some kilometers west of Deloraine has the form of a basin, where sedimentation occured since Cambrian times. Two highly conductive layers were interpreted in this area. One overlies the Precambrian basement, being mainly Cambrian in age, and the other is the highest conductive layer, probably because of the high quatity of water filling porous sediments.

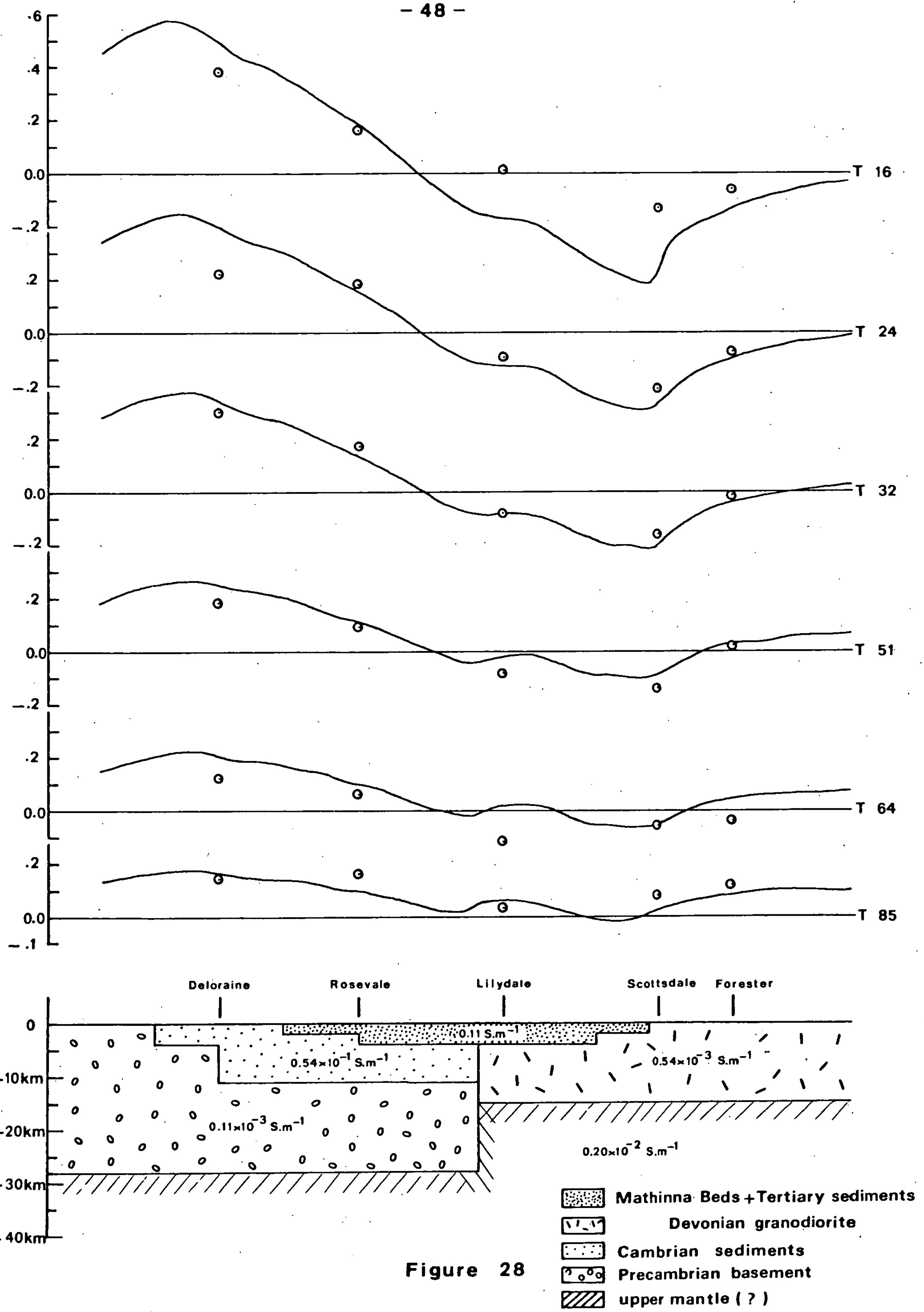
.6
.4
.2
0.0
-.2
T 16
T 24
T 32
T 51
T 64
T 85
-.1
Deloraine
Rosevale
Lilydale
Scottsdale
Forester
0
-10km
-20km
-30km
-40km
0.11 S.m⁻¹
0.54×10⁻¹ S.m⁻¹
0.54×10⁻³ S.m⁻¹
0.11×10⁻³ S.m⁻¹
0.20×10⁻² S.m⁻¹
Mathinna Beds + Tertiary sediments
Devonian granodiorite
Cambrian sediments
Precambrian basement
upper mantle (?)

Figure 28

Chapter IV

CONCLUSIONS

Some significant indications have been gained from this geomagnetic variations study ;

1. Local conductivity anomalies control the variations at periods less than or equal to 48 minutes, while the deep sea effect gives a more or less uniform direction of the real induction vectors for periods greater than 64 minutes. The induced current at sea water from the Bass Strait effects on the imaginary induction vectors at all periods greater than 16 minutes.
2. The surface high conductive zone with NNW - SSE trend, suspected from earlier results has been confirmed between east of Deloraine and west of Scottsdale.
3. There is a deep vertical boundary that separates east formation from west formation under the Tamar zone. To prove the continuation of this boundary, more stations to the south are needed.
4. The regional gravity trend in the area indicates a fault at depth with downthrow side to the west. The derived conductivity structure is consistent with this assuming that the lower layer (perhaps upper mantle) is a better conductor.
5. A localized zone of mineralization in between Nabowla, Scottsdale and Tayene shows strong influence on the local conductivity anomaly.
6. Magnetic variation surveys always have small precision in determination of depth. One of the functions of this survey is to indicate locations at which magneto-telluric measurements should be done in the future, and how differences is such measurements may be linked. The area east of the Tamar River where Z variations are small, should be suitable for magneto-telluric investigations.

ACKNOWLEDGMENTS

I would like to express my sincere thanks to Dr. W. D. Parkinson for his encouragement and continuous effort in completing this project, and also for his suggestions and discussions during its preparation. To Dr. R. J. G. Lewis, for his useful help in computing is so much appreciated.

To all property owners and school masters where I set up the instruments, for their help in allowing me to use their electric power and their land for the sites, are gratefully appreciated. Thanks are also due to Mr. Paul Waller for his useful help in setting up the instruments and transportation during the field operation.

REFERENCES

Adam, A., 1976. Geoelectric and Geothermal Studies - KAPG, Monograph Series, Akademiai Kiado Budapest.

Banks, M. R., 1962. Journal of The Geological Society of Australia., volume 9, part 2., The Geology of Tasmania.

Banks, R. J., 1969. Geomagnetic variations and the Electrical Conductivity of The Upper Mantle. Geophys. J. Roy. astr. Soc., vol. 17, 457.

Brewitt, C.R - Taylor and Weaver, J.T.,1976. On the finite difference solution of two-dimensional induction problems. Geophys.J.R.astr.Soc., vol. 47, 375 - 396.

Banks, R.J., 1979. The use of Equivalent Current Systems in the interpretation of Geomagnetic Deep Sounding data. Geophys.J.R.astr.Soc., vol. 56, 139 - 157.

Chapman, S., 1919. The Solar and Lunar diurnal variations of terrestrial magnetism. Phil. Trans. Roy. Soc. A., vol. 218, 1.

Duba, A., Piwinskii, A.J., Santos, M., and Weed, H.C., 1978. The Electrical conductivity of Sandstone, Limestone and Granite. Geophys.J.R.astr.Soc., vol. 53, 583 - 597.

Everett, J.E., and Hyndman, R.D., 1967. Geomagnetic variations and the electrical conductivity structure in south-western Australia. Phys. Earth Plan. Int., vol. 1, 24 - 34.

Hyndman, R.D., 1963. Unpublished M.Sc Thesis (Institute of Earth Sciences : University of British Columbia).

Honkura, Y., 1971. Geomagnetic variation anomaly on Miyake-jima Island, Jour. Geomag. Geoelectr., vol. 23, 307 - 333.

Jones, F.W. and Pascoe, L.J., 1971. A general computer program to determine the perturbation of alternating currents in a two-dimensional model of region of uniform conductivity with an embedded inhomogeneity.
Geophys. J. R. astr. Soc., vol. 24, 3 - 30.

Kanasewich, ., 1973. Time Sequence Analysis in Geophysics., The University of Alberta Press, pp. 120.

Klein, D. P., 1971. Geomagnetic time - variation on Hawaii Island and mantle electrical conductivity., AGU Meeting, 1971.

Klein, D. P., 1972. Geomagnetic time - variations, the Island Effect, and Electromagnetic Depth Sounding on Oceanic Island. Thesis, Univ. Hawaii.

Lahiri, B. N., and Price, A. T., 1939. Electromagnetic Induction in non-uniform conductors, and the determination of the conductivity of the Earth from terrestrial magnetic variations.
Phil. Trans. Roy. Soc. A, vol. 237, 64.

Lilley, F. E. M., 1975. Magnetometer array studies : A Review of The Interpretation of Observed Fields.
Physics of The Earth and Planetary Interiors, vol.10, pp. 231 - 240.

Lilley, F. E. M., 1976. A magnetometer array Study Across Southern Victoria and the Bass Strait area, Australia.
Geophys. J. R. astr. Soc., vol. 46, pp. 165 - 184.

Leaman, D. E., Symonds, P. A., and Shirley, J. E., 1973. Gravity Survey of the Tamar Region, Northern Tasmania., Geological Survey Paper No. 1., Tasmania Department of Mines.

Leaman, D. E., and Symonds, P. A., 1975. Gravity Survey of North-Eastern Tasmania. Geological Survey Paper No. 2., Tasmania Department of Mines.

Lambert, A., and Caner, B., 1965. Geomagnetic depth-sounding and the coast effect in Western Canada.
Can. Jour. Earth Sci., vol. 2, 485.

McDonald, K. L., 1957. Penetration of the geomagnetic secular variation through a mantle with variable conductivity.
J. Geophys. Research., vol. 62, 117.

Parkinson, W. D., 1959. Directions of Rapid geomagnetic fluctuations., Geophys. J. Roy. astr. Soc., vol. 2, 1.

Parkinson, W. D., 1962. The influence of continents and oceans on geomagnetic variations.
Geophys. J. Roy. astr. Soc., vol. 4, 441 - 449.

Pascoe, L. J., and Jones, F. W., 1972. Boundary Conditions and Calculation of Surface Values for the General Two - Dimensional Electromagnetic Induction Problem.
Geophys. J. Roy. astr. Soc., vol. 27, 179 - 193.

Parkinson, W. D., and Jones, F.W., 1979. Review of Geophysics and Space Physics, vol. 17.

Schuster, A., 1908. The diurnal variation of terrestrial magnetism.
Phil. Trans. Roy. Soc. A. 208, 163.

Schmucker, U., 1964. Anomalies of Geomagnetic variations in the South Western United States.
J. Geomag. Geoelectr., vol. 15, 193 - 221.

Sasai, Y., 1967. Spatial Dependence of Short-period geomagnetic Fluctuations on Oshima Island. Bulletin of The Earthquake Res. Inst., vol. 45, pp. 137 - 157.

Sasai, Y., 1968. idem ditto., vol. 46, pp. 907 - 926.

Wiese, H., 1962. Geomagnetische Tiefentellurik, Teil II, Geofis. Pura appl., vol. , 83 - 103.

William, E., 1978. Structural Map of Pre-Carboniferous Rocks of Tasmania, Department of Mines, Tasmania.

Brace, W. F. (1971) Reistivity of saturated crustal rocks to 40 km based on laboratory measurements. In THE STRUCTURE AND PHYSICAL PROPERTIES OF THE EARTH'S CRUST, Ed. John G. Heacock. Amer. Geophys. Un. Monograph 14.

Jones, F. W., and Thomson,D. J., 1974. A Discussion of the Finite Difference Method in Computer Modelling of Electrical Conductivity Structures. A Reply to the Discussion by Williamson, Hewlett and Tammemagi.
Geophys. J. R. astr. Soc. (1974), vol 37, pp. 537 - 544.

Keller, G. V., and Frischknecht, F. C., 1966. Electrical methods in geophysical prospecting. Chapter 1, Pergamon Press Ltd, Oxford.

Williamson, K., Hewlett, C. and Tammemagi, H. Y., 1974. Computer modelling of electrical conductivity structures, Geophys. J. R. astr. Soc., vol 37, 533.

Woods, D. V., 1979. Thesis, Australian National University.

PLATE I

EXAMPLES OF THE SUBSTORM EVENTS

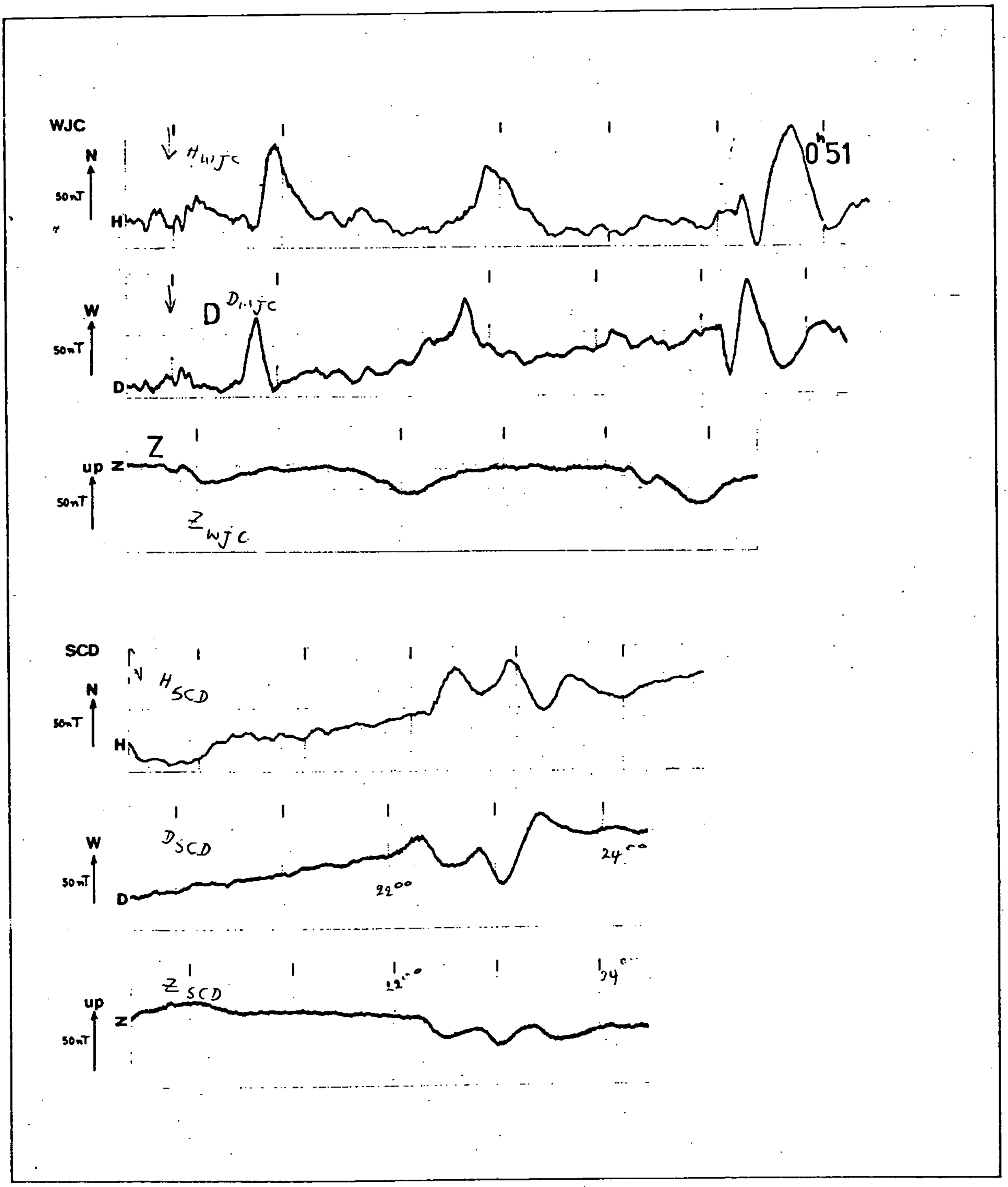

Plate I-1

Substorm type variations from Western Junction (WJC) and Scottsdale (SCD)

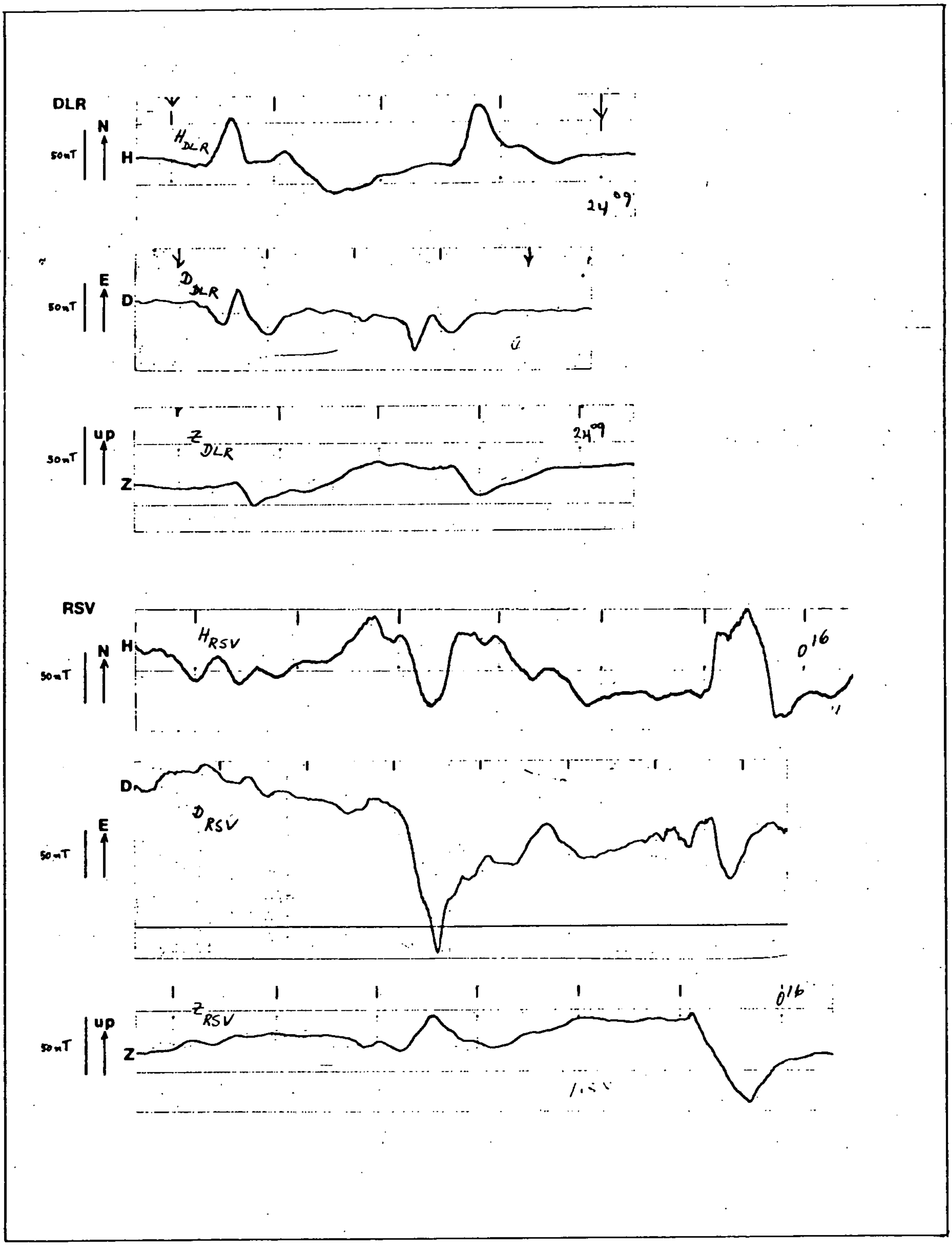

Plate I-2

Substorm type variations from Deloraine (DLR) and Rosevale (RSV).

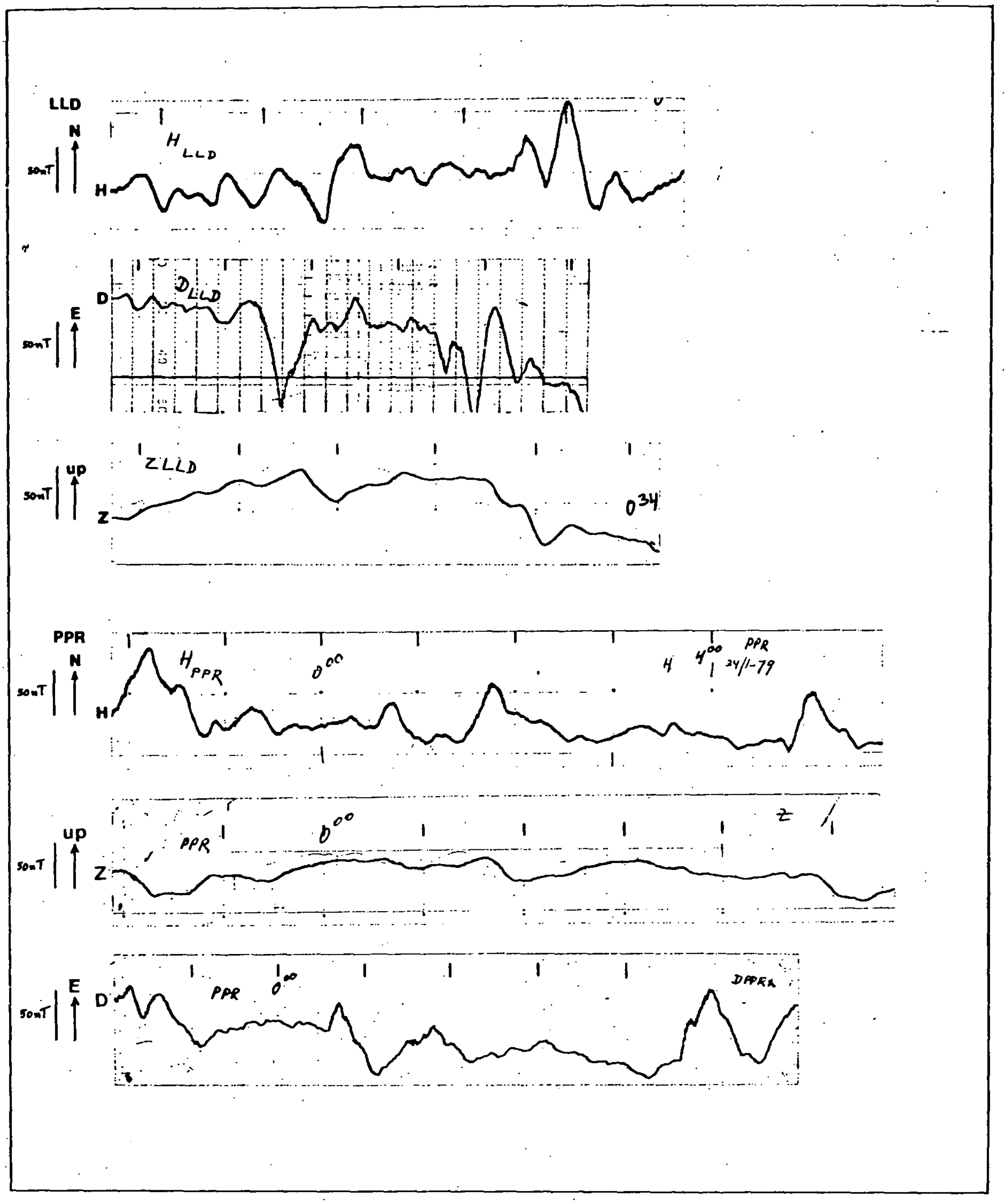

Plate I-3

Substorm type variations from Lilydale (LLD) and Pipers River (PPR).

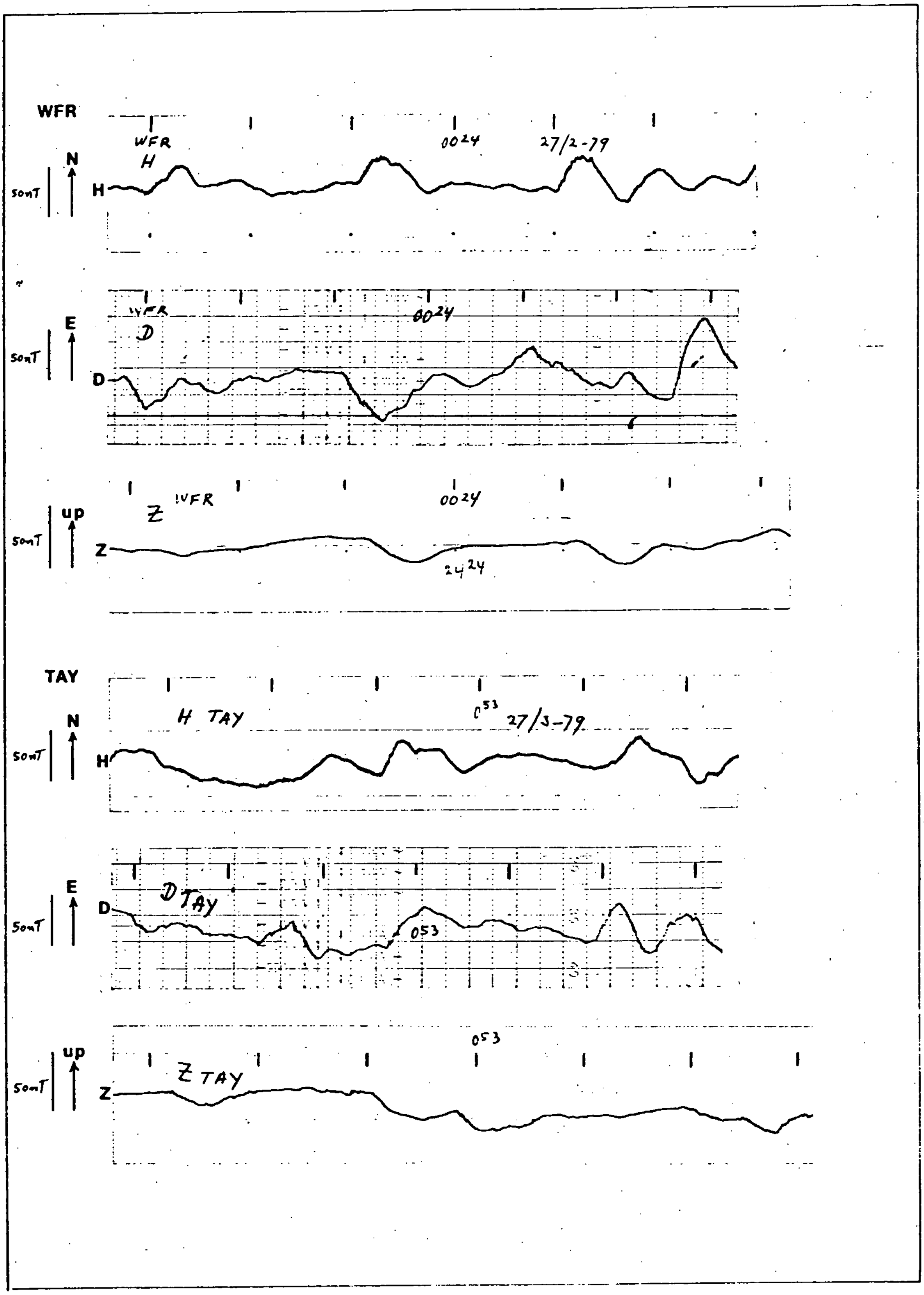

Plate I-4

Substorm type variations from West Frankford (WFR) and Tayene (TAY).

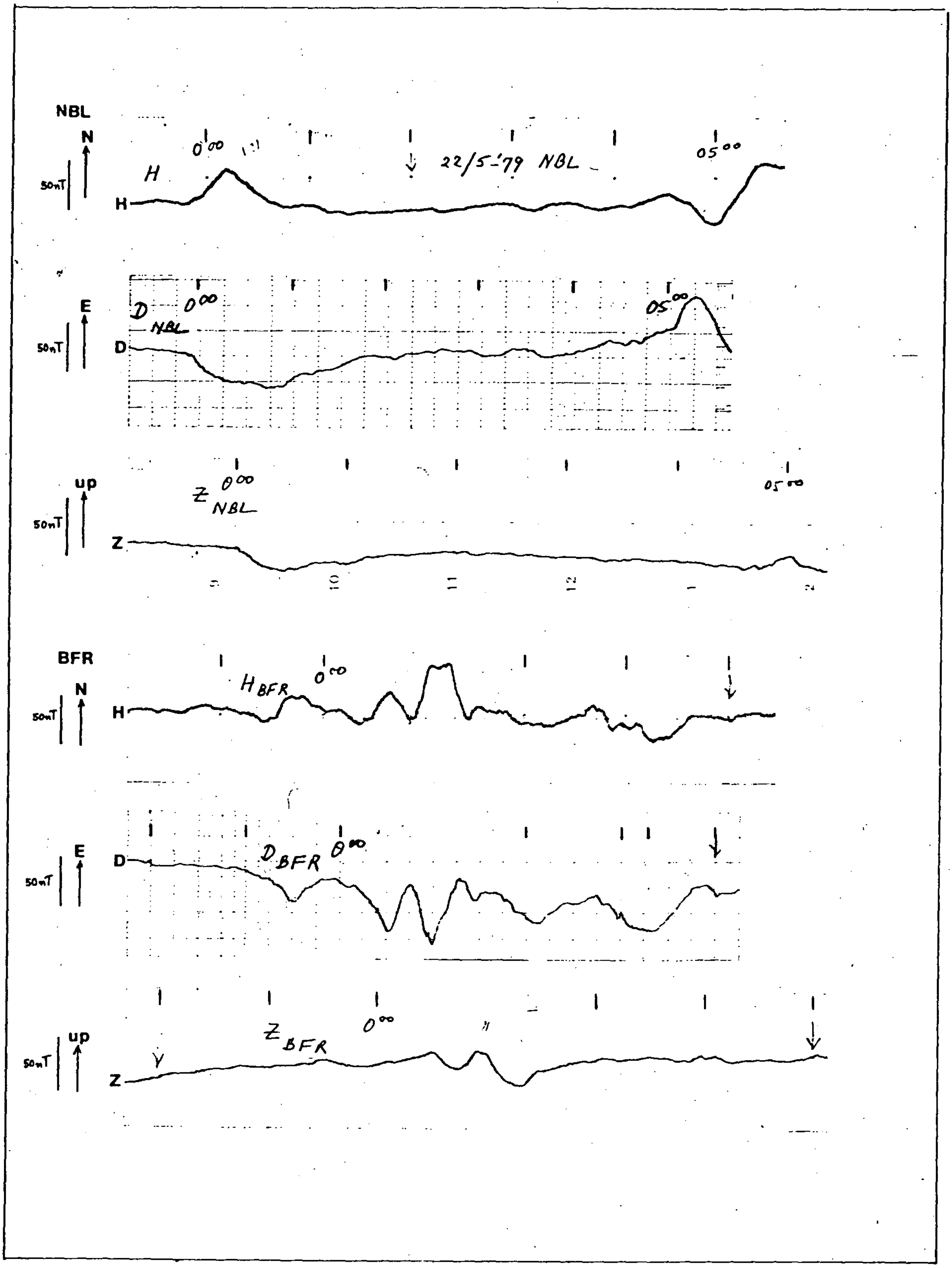

Plate I-5

Substorm type variations from Nabowla (NBL) and Beechford (BFR).

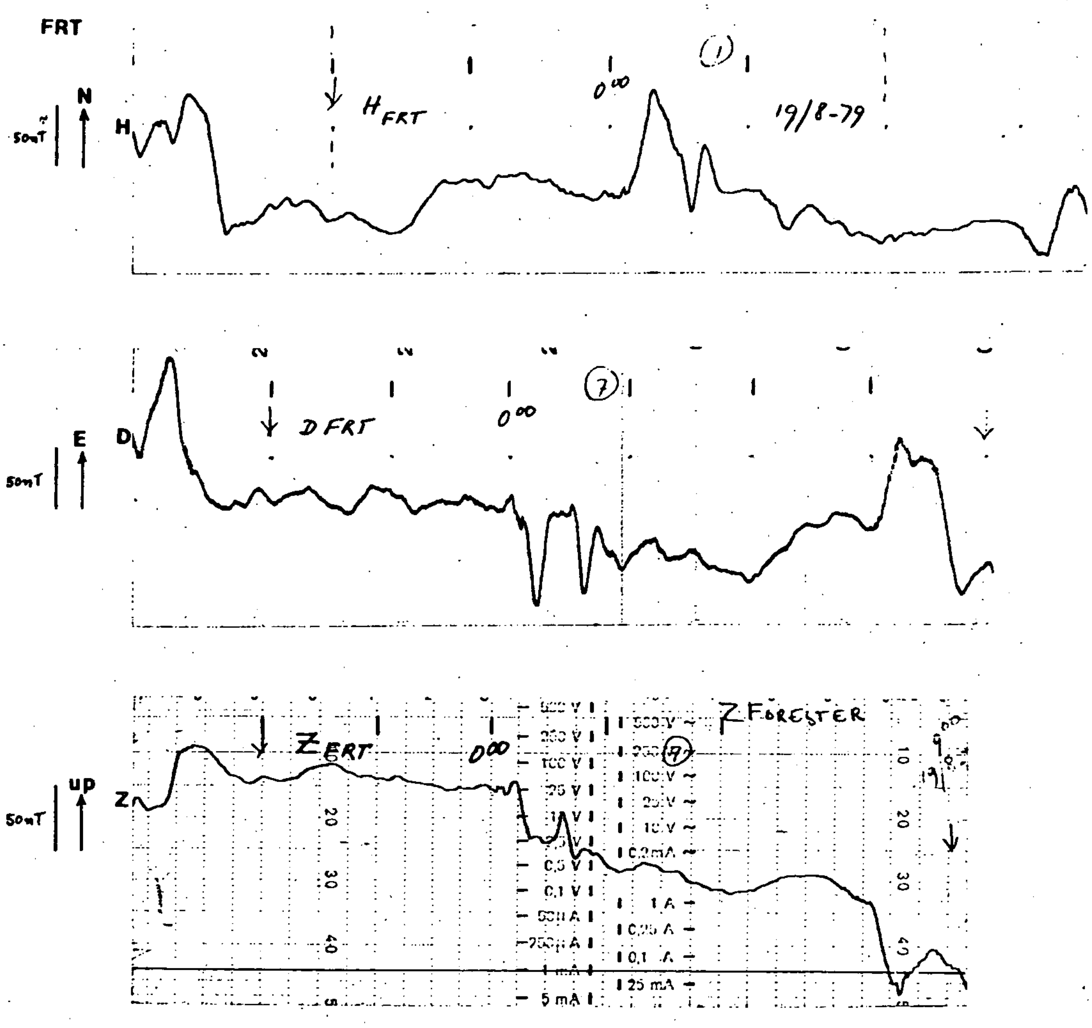

Plate I-6

Substorm type variations from Forester (FRT).

PLATE II

PLOTTED TRANSFER FUNCTION VALUES AGAINST PERIODS

Remarks : A_r is the real part of A transfer function (T.F).
B_r is the real part of B transfer function (T.F).
A_i is the imaginary part of A transfer function (T.F).
B_i is the imaginary part of B transfer function (T.F).

A_r and B_r are plotted as a function of periods (T), and the vertical bars indicate the uncertainty of T.F at a particular period.

A_i and B_i are plotted as a function of periods (T), both in one T.F - T profile, to show the mirror image characteristic between A and B imaginary at almost all stations.

Notice that the uncertainty values for A and B imaginary are the same as A and B real, but are not drawn to avoid a mess.

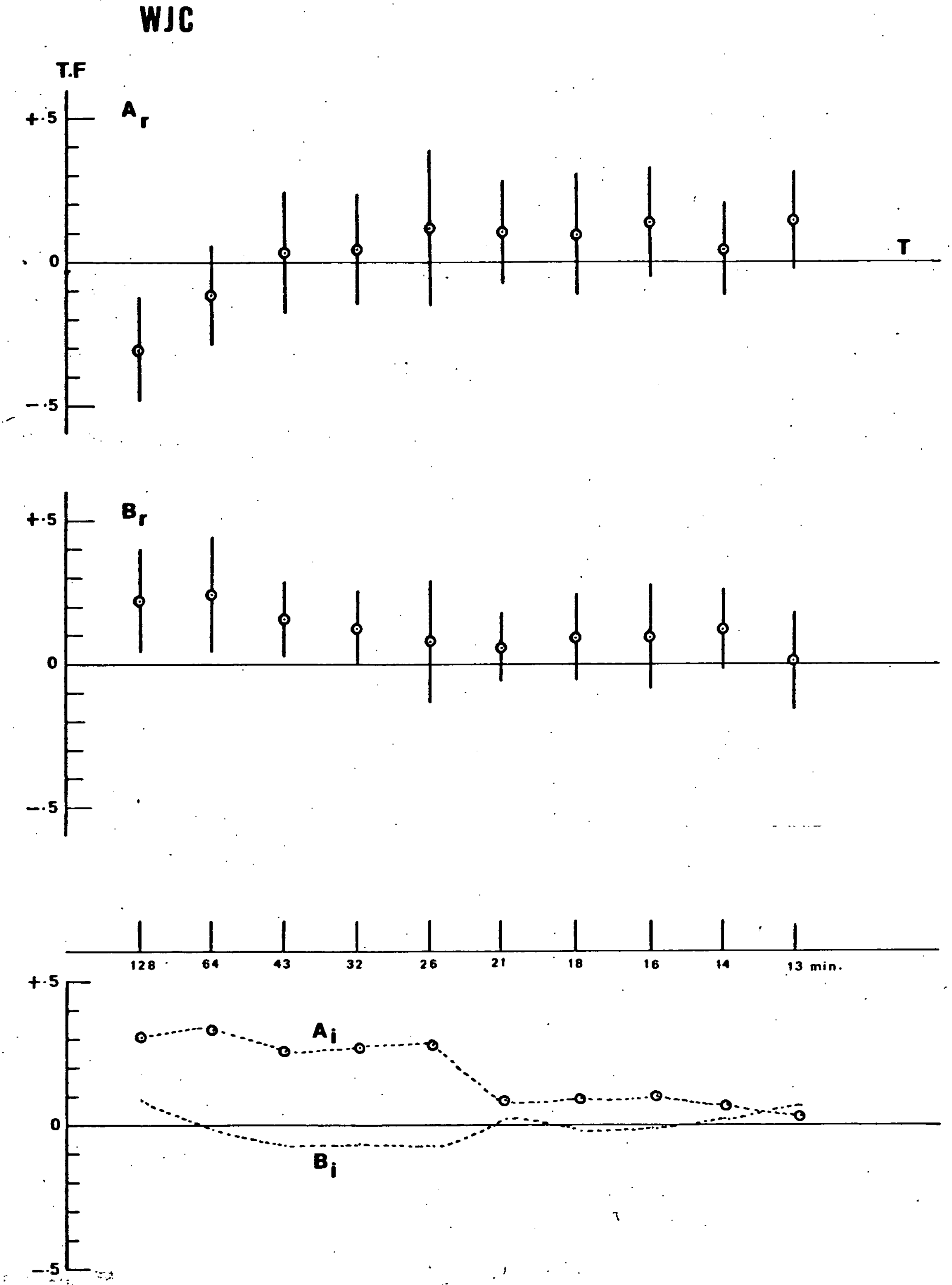

Plate II-1

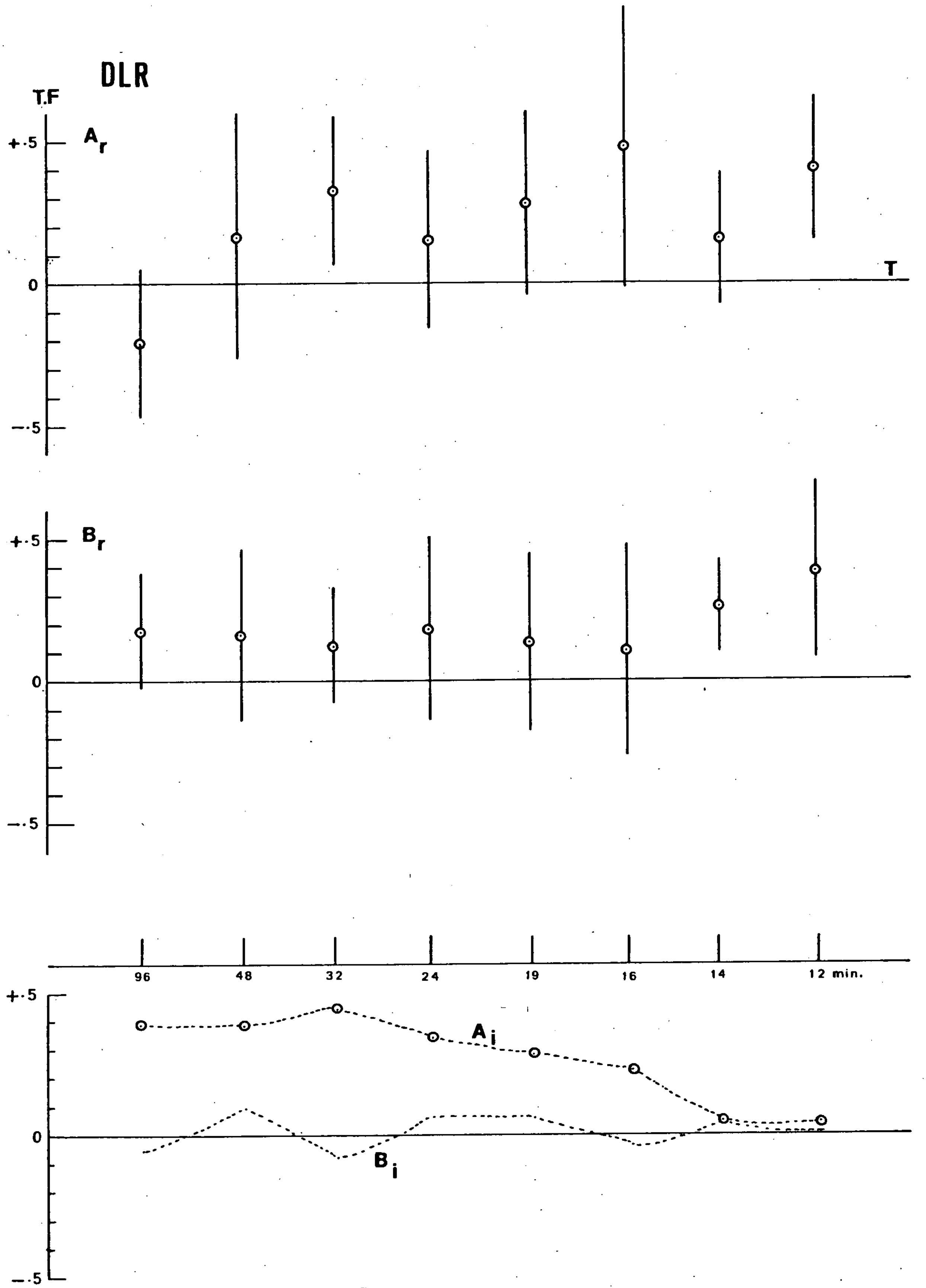

Plate II-2

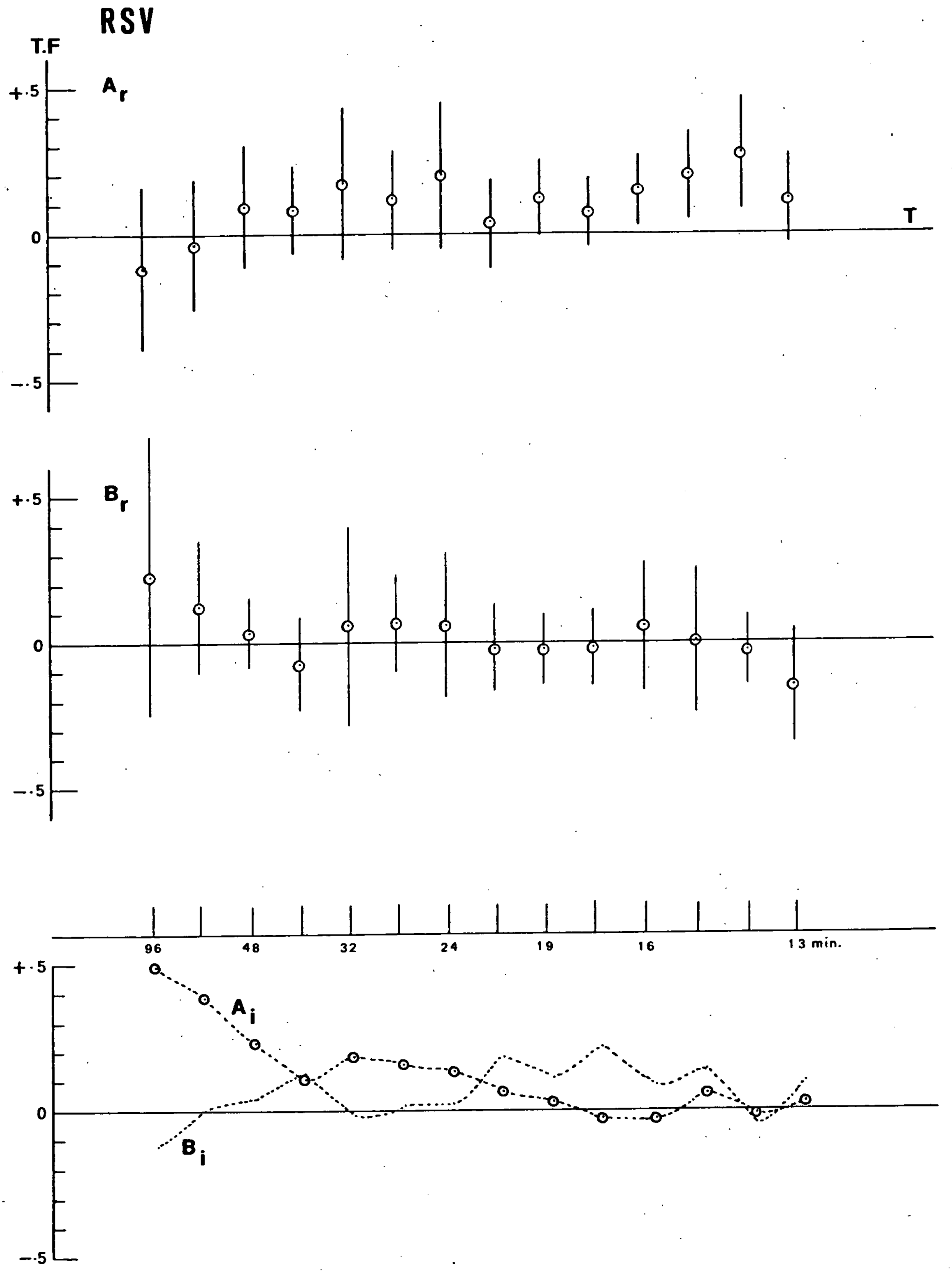

Plate II-3

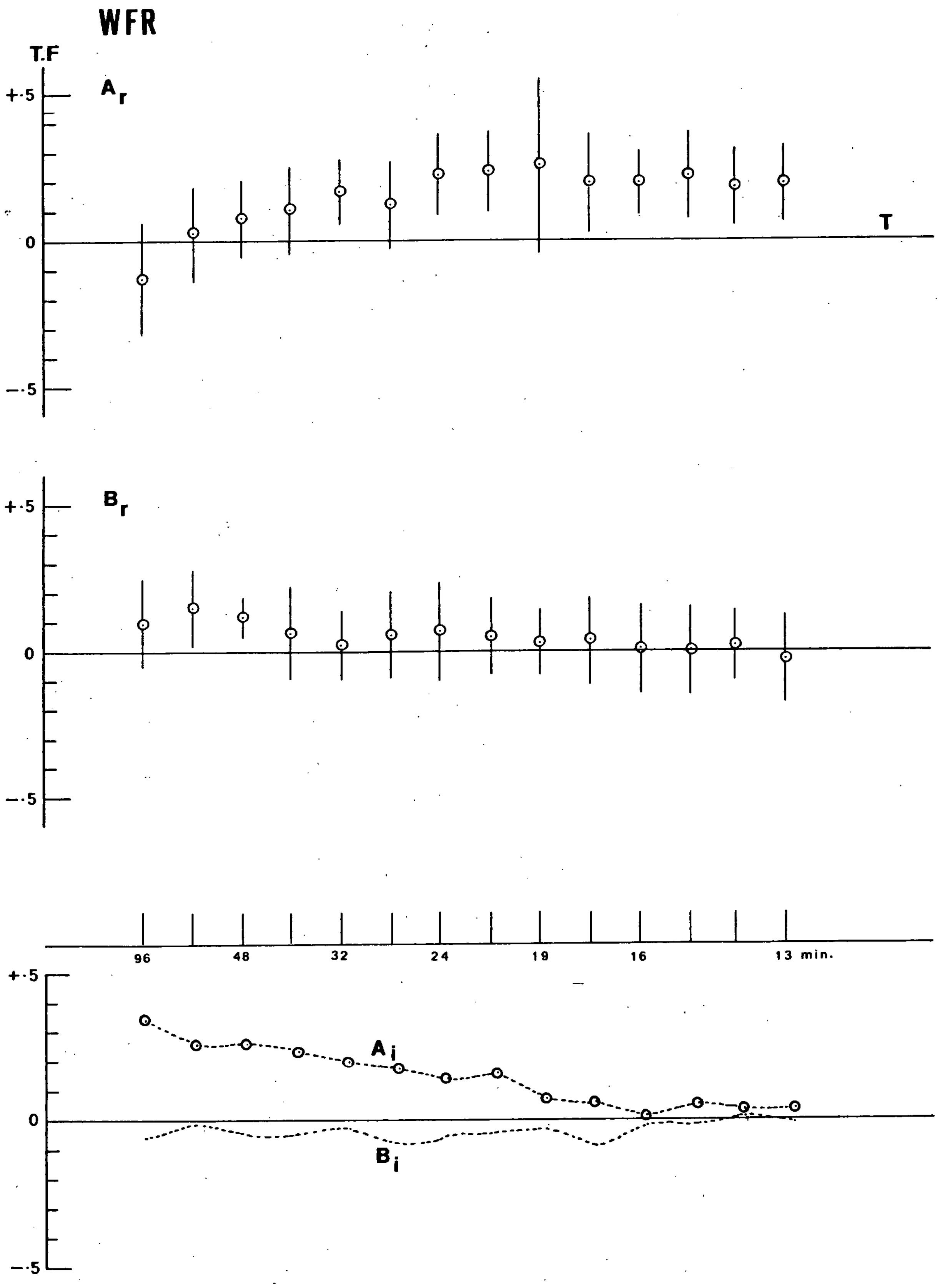

Plate II-4

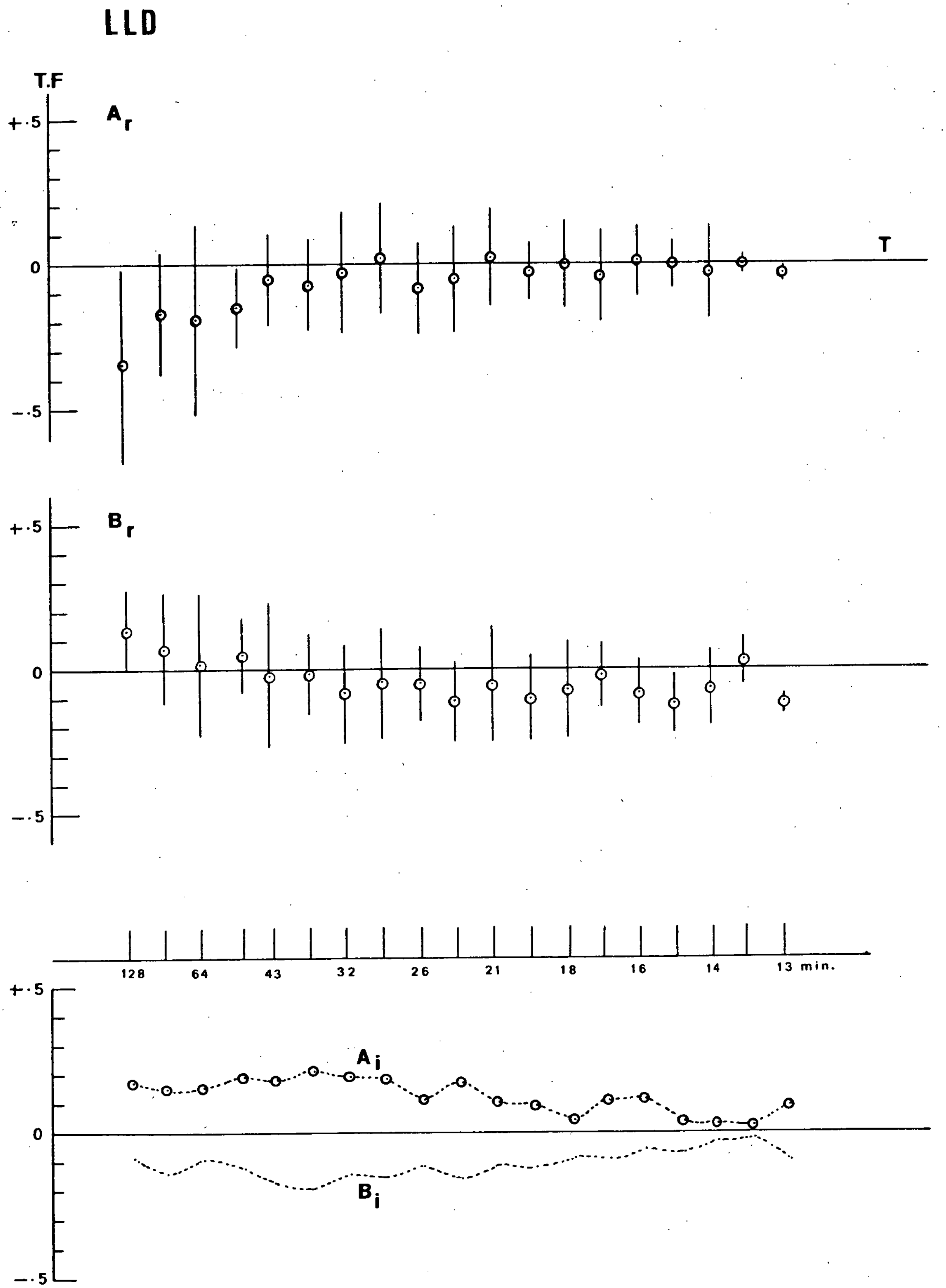

Plate II-5

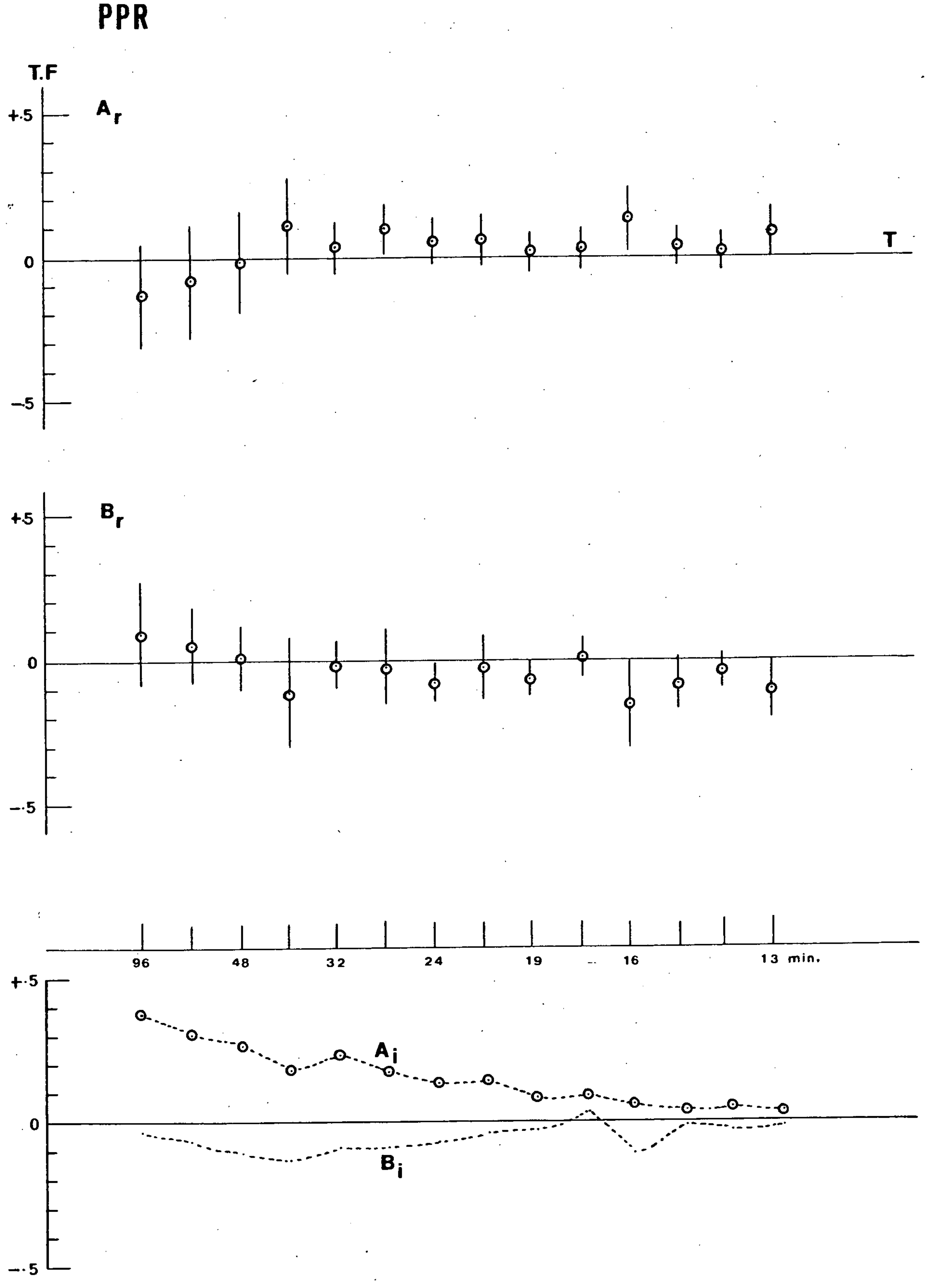

Plate II-6

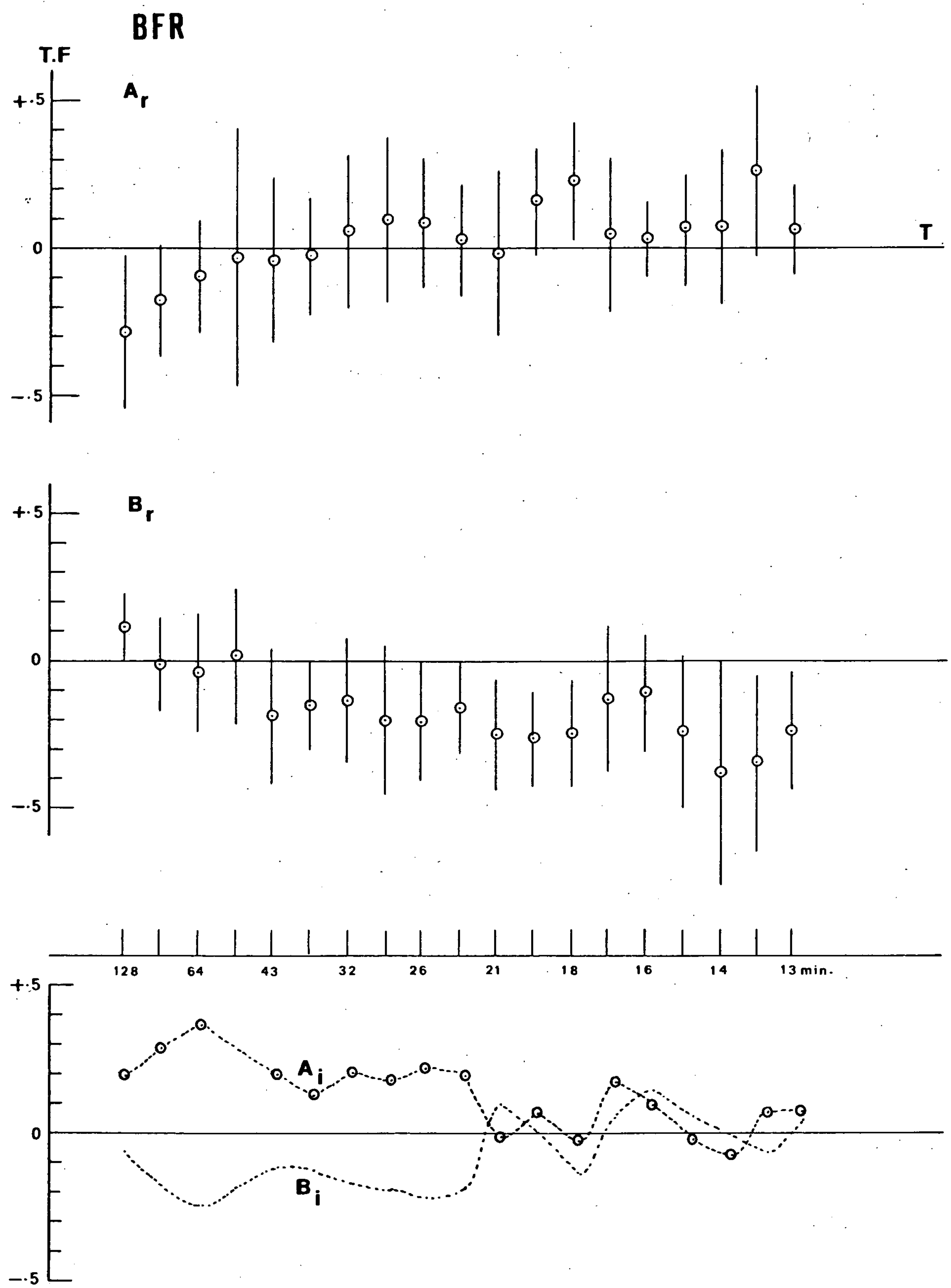

Plate II-7

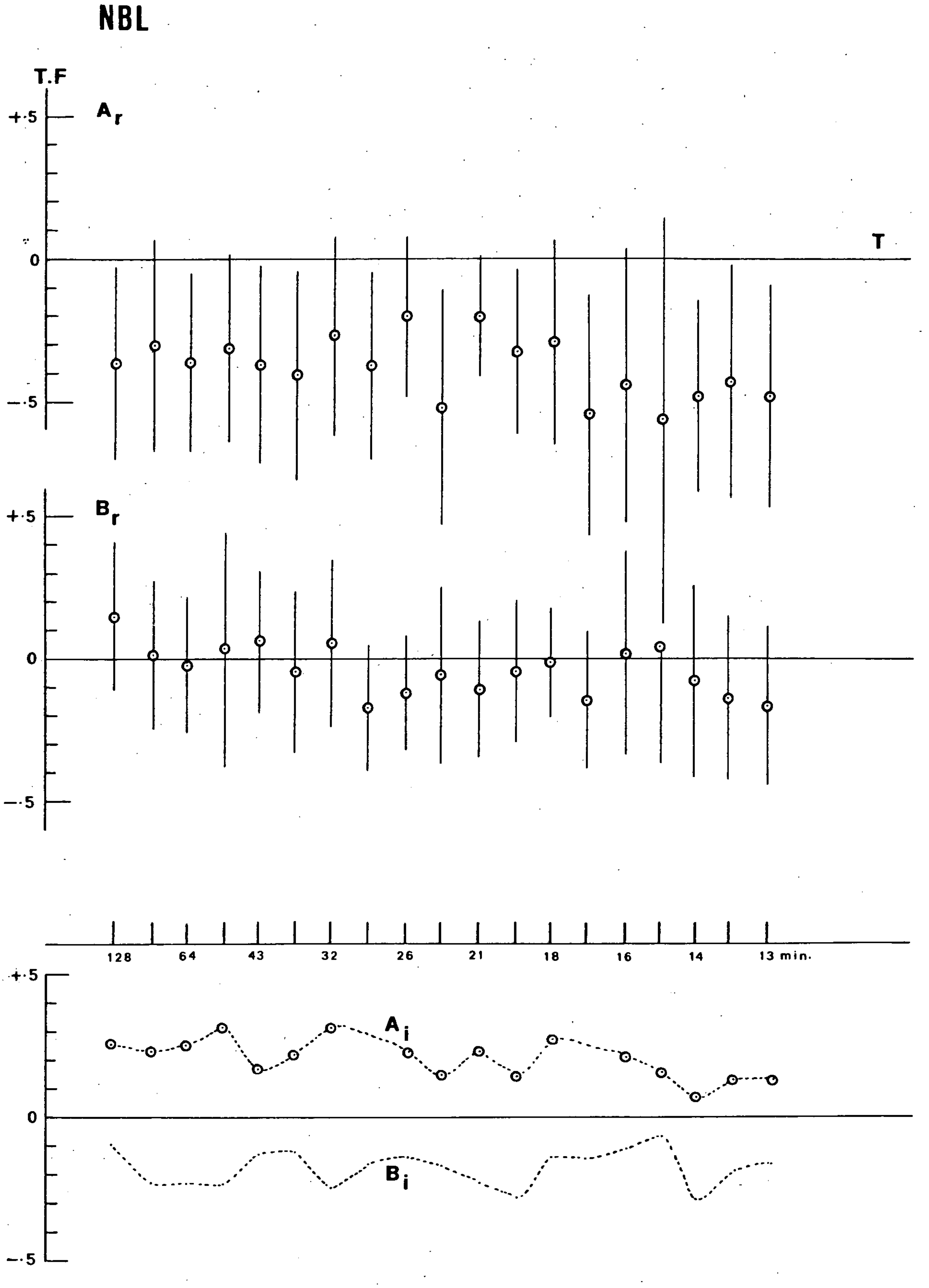

Plate II-8

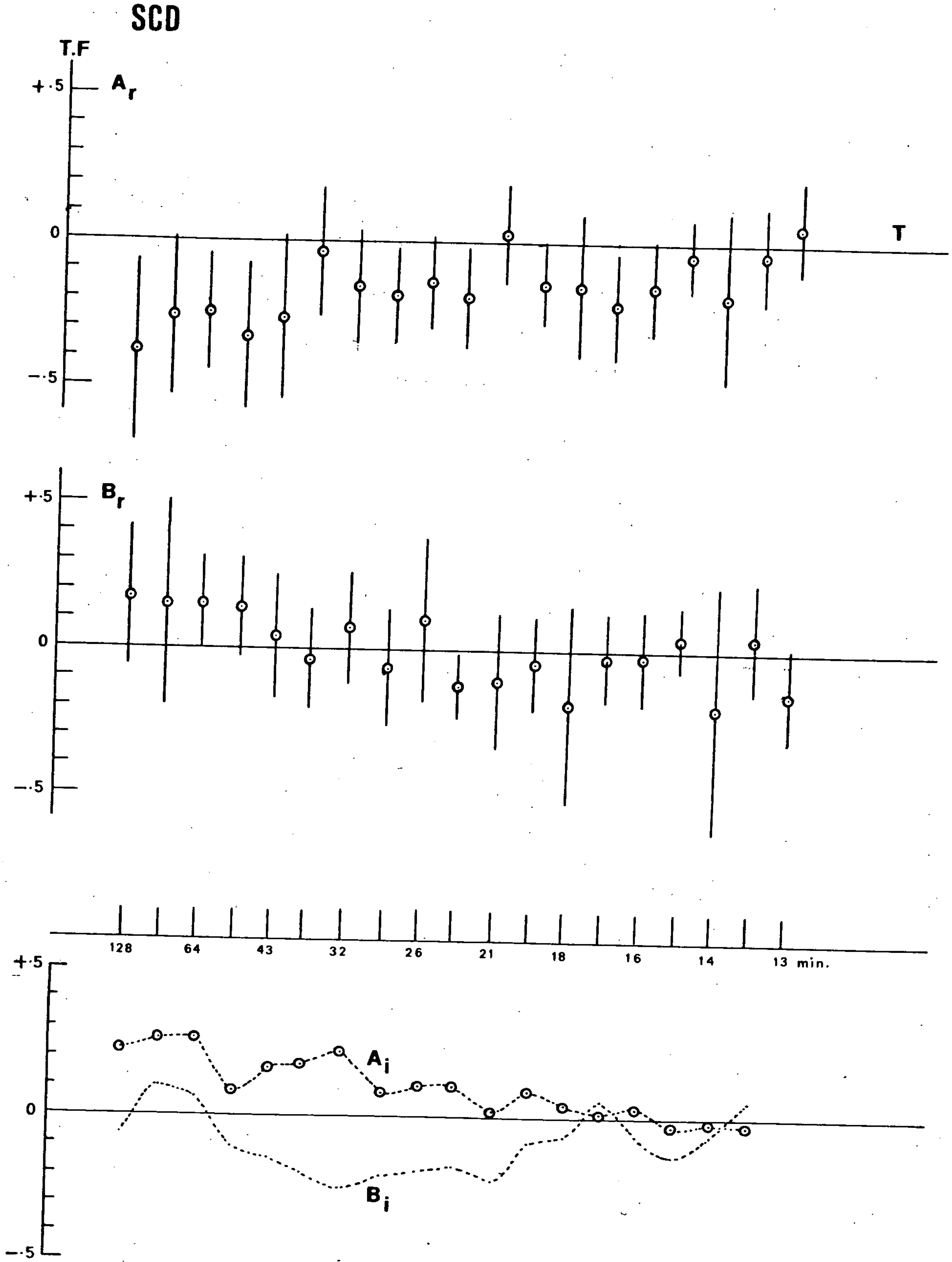

Plate II-9

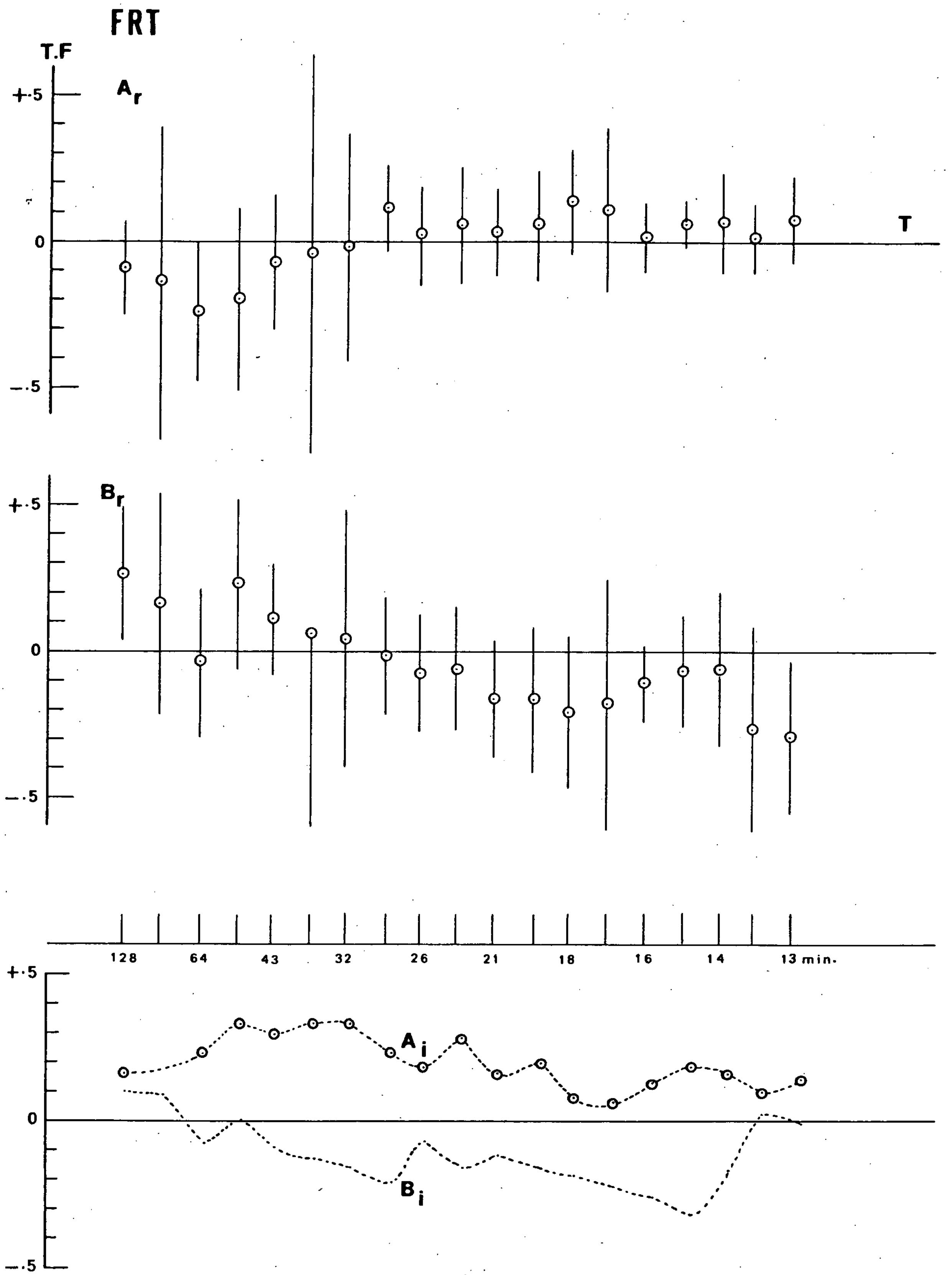

Plate II-10

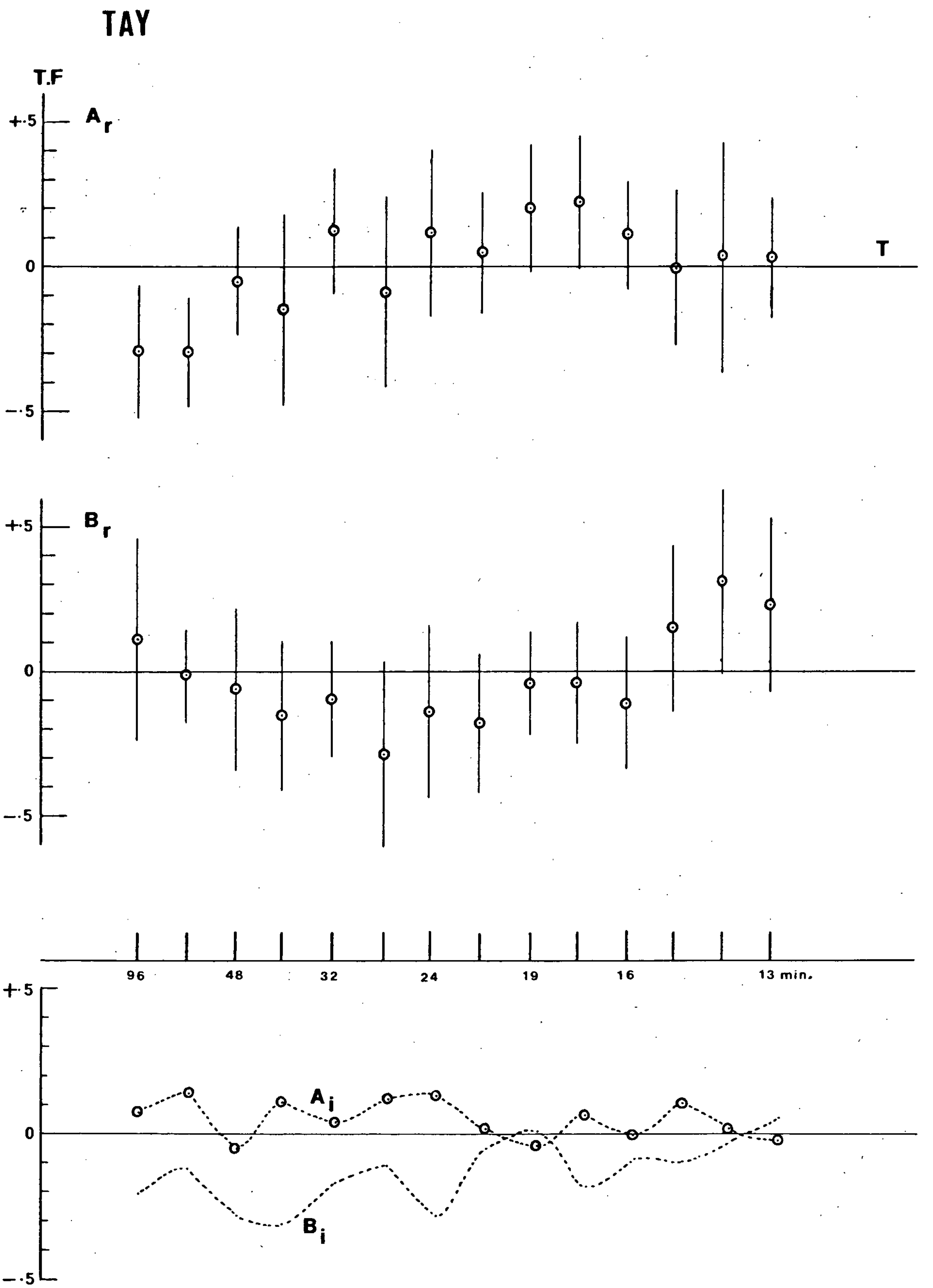

Plate II-11

PLATE III

COMPUTED SURFACE VALUES FOR PERIODS 85, 64, 51, 32, 24 AND 16 MINUTES FOR THE BEST FITTED MODEL OF CONDUCTIVITY STRUCTURE DELORAINE - FORESTER 2 - D PROFILE.

```
/* THE CONDUCTIVE CONFIGURATION */

 1  0000000000000000000000000000000000000000
 2  0000000000000000000000000000000000000000
 3  0000000000000000000000000000000000000000
 4  0000000000000000000000000000000000000000
 5  0000000000000000000000000000000000000000
 6  2211111555555555555555555555555544444444
 7  2211111555555555555555555555555544444444
 8  2211111111155555555555555555544444444444
 9  2211111111155555555555555555544444444444
10  2222111111155555555544444444444444444444
11  2222111111111111111144444444444444444444
12  2222111111111111111144444444444444444444
13  2222111111111111111144444444444444444444
14  2222222222222222222244444444444444444444
15  2222222222222222222233333333333333333333
16  2222222222222222222233333333333333333333
17  2222222222222222222233333333333333333333
18  3333333333333333333333333333333333333333
19  3333333333333333333333333333333333333333
20  3333333333333333333333333333333333333333
21  3333333333333333333333333333333333333333
22  3333333333333333333333333333333333333333
23  3333333333333333333333333333333333333333
24  3333333333333333333333333333333333333333
25  3333333333333333333333333333333333333333
26  3333333333333333333333333333333333333333
27  3333333333333333333333333333333333333333
28  3333333333333333333333333333333333333333
29  3333333333333333333333333333333333333333
30  3333333333333333333333333333333333333333
31  3333333333333333333333333333333333333333
32  3333333333333333333333333333333333333333
33  3333333333333333333333333333333333333333
34  3333333333333333333333333333333333333333
35  3333333333333333333333333333333333333333
36  3333333333333333333333333333333333333333
37  3333333333333333333333333333333333333333
38  3333333333333333333333333333333333333333
39  3333333333333333333333333333333333333333
40  3333333333333333333333333333333333333333

   SIGMA        SKIN DEPTH

0   0.            ********
1   .5400E-12   154.70
2   .1100E-14  3427.64
3   .2000E-13   803.85
4   .5400E-14  1547.02
5   .1100E-11   108.39
6   0.            ********
7   0.            ********
8   0.            ********
9   0.            ********
A   0.            ********
B   0.            ********
C   0.            ********
D   0.            ********
E   0.            ********
F   0.            ********
```

Plate III-1

Conductivity model representing the structure of the area

CALCULATED SURFACE VALUES COMPUTED FOR MODEL WITH 85 MINUTES PERIOD AND STOPPED ON 66 ITERATIONS

	AME	AMHY	AMHZ	HZHY	DPHASE	DPHAHY	DPHAHZ	APPRES	TREAL	TIMAG
2	0.998	0.993	0.120	0.121	0.014	-2.401	-2.128	.545E+14	0.12	0.03
3	0.997	1.014	0.180	0.177	0.011	-2.379	-1.937	.521E+14	0.16	0.08
4	0.996	1.069	0.201	0.188	0.009	-2.300	-1.900	.468E+14	0.17	0.07
5	0.995	1.092	0.179	0.164	0.007	-2.281	-1.942	.448E+14	0.15	0.05
6	0.995	1.108	0.169	0.152	0.006	-2.267	-1.966	.435E+14	0.15	0.05
7	0.995	1.121	0.166	0.148	0.005	-2.259	-1.974	.424E+14	0.14	0.04
8	0.994	1.139	0.166	0.145	0.004	-2.243	-1.974	.411E+14	0.14	0.04
9	0.994	1.165	0.149	0.128	0.003	-2.214	-2.019	.393E+14	0.13	0.02
10	0.993	1.178	0.128	0.109	0.002	-2.207	-2.096	.383E+14	0.11	0.01
11	0.993	1.185	0.120	0.101	0.002	-2.207	-2.138	.379E+14	0.10	0.01
12	0.993	1.197	0.116	0.097	0.001	-2.197	-2.157	.371E+14	0.10	0.00
13	0.992	1.213	0.103	0.085	0.001	-2.182	-2.245	.361E+14	0.08	-0.01
14	0.992	1.222	0.083	0.068	0.000	-2.176	-2.442	.356E+14	0.07	-0.02
15	0.992	1.226	0.068	0.055	0.000	-2.174	-2.759	.353E+14	0.05	-0.03
16	0.991	1.227	0.062	0.051	0.000	-2.170	-3.096	.352E+14	0.03	-0.04
17	0.991	1.221	0.063	0.052	0.000	-2.177	2.948	.355E+14	0.02	-0.05
18	0.991	1.215	0.064	0.053	0.000	-2.181	2.866	.359E+14	0.02	-0.05
19	0.991	1.207	0.066	0.054	0.000	-2.185	2.794	.363E+14	0.01	-0.05
20	0.991	1.198	0.067	0.056	0.000	-2.192	2.730	.369E+14	0.01	-0.05
21	0.990	1.187	0.065	0.054	0.000	-2.199	2.836	.375E+14	0.02	-0.05
22	0.990	1.179	0.063	0.053	0.000	-2.213	-3.004	.381E+14	0.04	-0.04
23	0.990	1.170	0.065	0.055	0.000	-2.219	-2.866	.386E+14	0.04	-0.03
24	0.990	1.162	0.068	0.059	0.000	-2.225	-2.735	.391E+14	0.05	-0.03
25	0.990	1.155	0.072	0.062	0.000	-2.234	-2.631	.396E+14	0.06	-0.02
26	0.989	1.152	0.071	0.061	0.000	-2.232	-2.666	.397E+14	0.06	-0.03
27	0.989	1.149	0.065	0.057	-0.000	-2.233	-2.845	.399E+14	0.05	-0.03
28	0.989	1.144	0.062	0.054	-0.000	-2.235	3.129	.402E+14	0.03	-0.04
29	0.988	1.135	0.067	0.059	-0.000	-2.240	2.724	.409E+14	0.01	-0.06
30	0.988	1.116	0.081	0.072	0.000	-2.258	2.432	.423E+14	-0.00	-0.07
31	0.988	1.091	0.088	0.081	0.000	-2.287	2.336	.442E+14	-0.01	-0.08
32	0.987	1.071	0.093	0.087	0.001	-2.302	2.283	.458E+14	-0.01	-0.09
33	0.987	1.045	0.101	0.096	0.001	-2.337	2.219	.481E+14	-0.01	-0.10
34	0.987	1.006	0.083	0.083	0.002	-2.401	2.396	.518E+14	0.01	-0.08
35	0.986	0.996	0.063	0.063	0.002	-2.403	2.954	.528E+14	0.04	-0.05
36	0.986	0.994	0.064	0.064	0.002	-2.401	-2.918	.530E+14	0.06	-0.03
37	0.985	0.995	0.070	0.070	0.002	-2.399	-2.681	.529E+14	0.07	-0.02
38	0.985	0.996	0.076	0.076	0.002	-2.396	-2.546	.527E+14	0.08	-0.01
39	0.984	0.999	0.081	0.081	0.001	-2.393	-2.468	.523E+14	0.08	-0.01
40	0.983	1.002	0.084	0.084	0.000	-2.391	-2.422	.519E+14	0.08	-0.00

H VALUES20.10. 7. 5. 4. 4. 4. 4. 4. 3. 3. 3. 3. 3. 3. 2. 2. 2. 2. 2.
1. 2. 2. 2. 3. 3. 3. 3. 3. 3. 3. 4. 4. 4. 4. 4. 5. 7.10.20.

K VALUES45.30.20.10. 5. 1. 1. 1. 1. 1. 2. 2. 2. 4. 4. 4. 5. 5. 5. 5.
7. 7. 7. 7. 7. 7. 7. 7. 7. 7.10.10.10.10.10.10.10.10.10.10.

SCALE = 100000. FREQ = 0.000196

Plate III-2

CALCULATED SURFACE VALUES COMPUTED FOR THE MODEL WITH 64 MINUTES PERIOD AND STOPPED ON TOTAL 110 NUMBER OF ITERATIONS

	AME	AMHY	AMHZ	HZHY	DPHASE	DPHAHY	DPHAHZ	APPRES	TREAL	TIMAG
2	0.998	0.988	0.156	0.158	0.015	-2.408	-1.996	.551E+14	0.14	0.06
3	0.996	1.018	0.238	0.234	0.011	-2.378	-1.852	.513E+14	0.20	0.12
4	0.995	1.069	0.266	0.245	0.007	-2.285	-1.826	.452E+14	0.22	0.11
5	0.995	1.121	0.240	0.214	0.005	-2.262	-1.855	.426E+14	0.20	0.08
6	0.994	1.144	0.225	0.197	0.003	-2.244	-1.875	.409E+14	0.18	0.07
7	0.994	1.163	0.218	0.187	0.001	-2.235	-1.886	.395E+14	0.18	0.06
8	0.993	1.188	0.213	0.179	-0.000	-2.216	-1.893	.378E+14	0.17	0.06
9	0.993	1.221	0.189	0.155	-0.002	-2.185	-1.934	.357E+14	0.15	0.04
10	0.992	1.239	0.158	0.127	-0.003	-2.177	-2.005	.346E+14	0.13	0.02
11	0.992	1.248	0.141	0.113	-0.004	-2.177	-2.057	.341E+14	0.11	0.01
12	0.992	1.265	0.131	0.104	-0.005	-2.165	-2.094	.332E+14	0.10	0.01
13	0.991	1.283	0.110	0.086	-0.005	-2.150	-2.202	.322E+14	0.09	-0.00
14	0.991	1.293	0.083	0.064	-0.006	-2.145	-2.449	.317E+14	0.06	-0.02
15	0.990	1.297	0.065	0.050	-0.006	-2.143	-2.886	.315E+14	0.04	-0.03
16	0.990	1.298	0.063	0.048	-0.006	-2.140	2.926	.314E+14	0.02	-0.05
17	0.990	1.291	0.071	0.055	-0.006	-2.146	2.602	.318E+14	0.00	-0.05
18	0.990	1.282	0.076	0.060	-0.006	-2.151	2.479	.322E+14	-0.00	-0.06
19	0.989	1.272	0.083	0.065	-0.005	-2.156	2.383	.327E+14	-0.01	-0.06
20	0.989	1.260	0.089	0.070	-0.005	-2.163	2.309	.333E+14	-0.02	-0.07
21	0.989	1.246	0.086	0.069	-0.005	-2.171	2.340	.340E+14	-0.01	-0.07
22	0.989	1.235	0.071	0.058	-0.005	-2.186	2.583	.346E+14	0.00	-0.06
23	0.989	1.222	0.068	0.055	-0.005	-2.192	2.686	.354E+14	0.01	-0.05
24	0.988	1.211	0.065	0.053	-0.005	-2.200	2.806	.360E+14	0.02	-0.05
25	0.988	1.201	0.063	0.052	-0.005	-2.210	2.933	.366E+14	0.02	-0.05
26	0.988	1.195	0.063	0.053	-0.005	-2.209	2.886	.369E+14	0.02	-0.05
27	0.987	1.189	0.068	0.057	-0.004	-2.210	2.671	.373E+14	0.01	-0.06
28	0.987	1.181	0.081	0.068	-0.004	-2.213	2.414	.377E+14	-0.01	-0.07
29	0.987	1.167	0.103	0.088	-0.004	-2.220	2.187	.386E+14	-0.03	-0.08
30	0.986	1.142	0.127	0.111	-0.003	-2.241	2.052	.403E+14	-0.05	-0.10
31	0.986	1.111	0.138	0.124	-0.002	-2.274	2.011	.426E+14	-0.05	-0.11
32	0.985	1.086	0.144	0.132	-0.002	-2.291	1.992	.445E+14	-0.06	-0.12
33	0.985	1.052	0.152	0.144	-0.001	-2.333	1.968	.474E+14	-0.06	-0.13
34	0.985	1.005	0.125	0.124	0.000	-2.407	2.068	.519E+14	-0.03	-0.12
35	0.984	0.991	0.082	0.082	0.001	-2.411	2.411	.533E+14	0.01	-0.08
36	0.984	0.987	0.065	0.066	0.001	-2.410	2.818	.536E+14	0.03	-0.06
37	0.983	0.987	0.062	0.063	0.001	-2.408	-3.089	.537E+14	0.05	-0.04
38	0.983	0.988	0.066	0.067	0.001	-2.406	-2.814	.535E+14	0.06	-0.03
39	0.982	0.991	0.072	0.073	0.001	-2.402	-2.630	.531E+14	0.07	-0.02
40	0.980	0.995	0.078	0.079	0.000	-2.398	-2.506	.525E+14	0.08	-0.01

H VALUES20.10. 7. 5. 4. 4. 4. 4. 4. 3. 3. 3. 3. 3. 3. 2. 2. 2. 2. 2.
1. 2. 2. 2. 3. 3. 3. 3. 3. 3. 3. 4. 4. 4. 4. 4. 5. 7.10.20.

K VALUES45.30.20.10. 5. 1. 1. 1. 1. 1. 2. 2. 2. 4. 4. 4. 5. 5. 5. 5.
7. 7. 7. 7. 7. 7. 7. 7. 7. 7.10.10.10.10.10.10.10.10.10.10.

SCALE = 100000. FREQ = 0.000260

Plate III-3

CALCULATED SURFACE VALUES COMPUTED FOR THE MODEL WITH 51 MINUTES PERIOD AND STOPPED ON TOTAL 157 NUMBER OF ITERATIONS

	AME	AMHY	AMHZ	HZHY	DPHASE	DPHAHY	DPHAHZ	APPRES	TREAL	TIMAG
2	0.997	0.980	0.198	0.202	0.015	-2.411	-1.908	.553E+14	0.18	0.10
3	0.995	1.018	0.294	0.289	0.009	-2.374	-1.805	.512E+14	0.24	0.16
4	0.995	1.102	0.327	0.296	0.004	-2.270	-1.788	.436E+14	0.26	0.14
5	0.994	1.141	0.296	0.259	0.001	-2.244	-1.811	.405E+14	0.24	0.11
6	0.993	1.170	0.276	0.236	-0.002	-2.226	-1.829	.386E+14	0.22	0.09
7	0.993	1.194	0.265	0.222	-0.004	-2.215	-1.840	.370E+14	0.21	0.08
8	0.992	1.224	0.257	0.210	-0.006	-2.195	-1.849	.351E+14	0.20	0.07
9	0.992	1.264	0.226	0.179	-0.008	-2.162	-1.884	.329E+14	0.17	0.05
10	0.991	1.237	0.187	0.145	-0.010	-2.153	-1.945	.317E+14	0.14	0.03
11	0.991	1.298	0.163	0.126	-0.011	-2.153	-1.997	.312E+14	0.12	0.02
12	0.990	1.317	0.148	0.113	-0.012	-2.142	-2.039	.302E+14	0.11	0.01
13	0.990	1.339	0.120	0.090	-0.013	-2.126	-2.150	.292E+14	0.09	-0.00
14	0.990	1.350	0.085	0.063	-0.013	-2.121	-2.413	.287E+14	0.06	-0.02
15	0.989	1.354	0.063	0.046	-0.014	-2.120	-2.937	.285E+14	0.03	-0.03
16	0.989	1.355	0.064	0.048	-0.014	-2.116	2.764	.285E+14	0.01	-0.05
17	0.989	1.346	0.080	0.059	-0.013	-2.123	2.393	.288E+14	-0.01	-0.06
18	0.988	1.336	0.091	0.068	-0.013	-2.128	2.257	.293E+14	-0.02	-0.06
19	0.988	1.324	0.103	0.078	-0.013	-2.133	2.159	.298E+14	-0.03	-0.07
20	0.988	1.309	0.114	0.087	-0.012	-2.141	2.089	.304E+14	-0.04	-0.08
21	0.987	1.292	0.114	0.088	-0.012	-2.148	2.088	.312E+14	-0.04	-0.08
22	0.987	1.279	0.099	0.077	-0.012	-2.164	2.190	.319E+14	-0.03	-0.07
23	0.987	1.263	0.094	0.074	-0.011	-2.172	2.232	.327E+14	-0.02	-0.07
24	0.987	1.249	0.089	0.071	-0.011	-2.180	2.282	.334E+14	-0.02	-0.07
25	0.987	1.235	0.084	0.068	-0.011	-2.191	2.344	.341E+14	-0.01	-0.07
26	0.985	1.227	0.086	0.070	-0.010	-2.190	2.313	.345E+14	-0.01	-0.07
27	0.986	1.218	0.099	0.081	-0.010	-2.192	2.195	.350E+14	-0.03	-0.08
28	0.985	1.207	0.120	0.099	-0.009	-2.196	2.067	.356E+14	-0.04	-0.09
29	0.985	1.189	0.150	0.126	-0.009	-2.204	1.954	.367E+14	-0.07	-0.11
30	0.985	1.159	0.179	0.154	-0.008	-2.227	1.884	.386E+14	-0.09	-0.13
31	0.984	1.122	0.191	0.170	-0.006	-2.262	1.863	.411E+14	-0.09	-0.14
32	0.984	1.092	0.196	0.180	-0.005	-2.281	1.856	.434E+14	-0.10	-0.15
33	0.983	1.052	0.204	0.194	-0.003	-2.328	1.845	.467E+14	-0.10	-0.17
34	0.983	0.997	0.170	0.171	-0.002	-2.412	1.910	.519E+14	-0.06	-0.16
35	0.982	0.981	0.113	0.115	-0.001	-2.417	2.115	.536E+14	-0.02	-0.11
36	0.982	0.976	0.082	0.084	0.000	-2.417	2.383	.541E+14	0.01	-0.08
37	0.981	0.974	0.066	0.068	0.000	-2.415	2.720	.542E+14	0.03	-0.06
38	0.980	0.975	0.061	0.063	0.001	-2.413	3.076	.541E+14	0.04	-0.04
39	0.979	0.978	0.064	0.065	0.001	-2.410	-2.901	.537E+14	0.06	-0.03
40	0.978	0.982	0.070	0.071	0.000	-2.405	-2.663	.530E+14	0.07	-0.02

H VALUES20.10. 7. 5. 4. 4. 4. 4. 4. 3. 3. 3. 3. 3. 3. 2. 2. 2. 2. 2.
1. 2. 2. 2. 3. 3. 3. 3. 3. 3. 3. 4. 4. 4. 4. 4. 5. 7.10.20.

K VALUES45.30.20.10. 5. 1. 1. 1. 1. 1. 2. 2. 2. 4. 4. 4. 5. 5. 5. 5.
7. 7. 7. 7. 7. 7. 7. 7. 7. 7.10.10.10.10.10.10.10.10.10.10.

SCALE = 100000. FREQ = 0.000327

Plate III-4

CALCULATED SURFACE VALUES COMPUTED FOR THE MODEL WITH 32 MINUTES PERIOD AND STOPPED ON 284 TOTAL NUMBER OF ITERATIONS

	AME	AMHY	AMHZ	HZHY	DPHASE	DPHAHY	DPHAHZ	APPRES	TREAL	TIMAG
2	0.996	0.951	0.309	0.325	0.015	-2.414	-1.805	.553E+14	0.27	0.19
3	0.994	1.006	0.428	0.425	0.004	-2.362	-1.756	.492E+14	0.35	0.24
4	0.993	1.120	0.464	0.415	-0.006	-2.239	-1.750	.396E+14	0.37	0.19
5	0.992	1.174	0.422	0.360	-0.012	-2.209	-1.769	.359E+14	0.33	0.15
6	0.991	1.214	0.393	0.324	-0.017	-2.188	-1.783	.336E+14	0.30	0.13
7	0.990	1.249	0.374	0.299	-0.021	-2.176	-1.794	.317E+14	0.28	0.11
8	0.990	1.291	0.358	0.277	-0.025	-2.154	-1.803	.296E+14	0.26	0.10
9	0.989	1.344	0.314	0.233	-0.029	-2.121	-1.829	.273E+14	0.22	0.07
10	0.988	1.376	0.259	0.188	-0.032	-2.112	-1.872	.260E+14	0.18	0.04
11	0.988	1.391	0.221	0.159	-0.034	-2.112	-1.912	.254E+14	0.16	0.03
12	0.987	1.416	0.195	0.138	-0.036	-2.101	-1.950	.245E+14	0.14	0.02
13	0.987	1.445	0.152	0.105	-0.037	-2.086	-2.040	.235E+14	0.10	0.00
14	0.986	1.460	0.099	0.067	-0.038	-2.082	-2.271	.230E+14	0.07	-0.01
15	0.985	1.465	0.060	0.041	-0.039	-2.080	-2.884	.228E+14	0.03	-0.03
16	0.985	1.465	0.065	0.044	-0.039	-2.077	2.553	.228E+14	-0.00	-0.04
17	0.985	1.453	0.097	0.067	-0.038	-2.084	2.111	.231E+14	-0.03	-0.06
18	0.985	1.440	0.122	0.085	-0.038	-2.088	1.973	.236E+14	-0.05	-0.07
19	0.984	1.423	0.146	0.103	-0.037	-2.094	1.887	.241E+14	-0.07	-0.08
20	0.984	1.403	0.169	0.121	-0.036	-2.101	1.831	.248E+14	-0.08	-0.09
21	0.984	1.350	0.179	0.130	-0.035	-2.109	1.814	.256E+14	-0.09	-0.09
22	0.983	1.362	0.173	0.127	-0.035	-2.125	1.829	.263E+14	-0.09	-0.09
23	0.983	1.339	0.171	0.128	-0.034	-2.133	1.834	.271E+14	-0.09	-0.09
24	0.983	1.319	0.170	0.129	-0.033	-2.142	1.839	.280E+14	-0.09	-0.10
25	0.983	1.299	0.166	0.127	-0.032	-2.154	1.849	.288E+14	-0.08	-0.10
26	0.982	1.285	0.172	0.134	-0.031	-2.153	1.837	.294E+14	-0.09	-0.10
27	0.982	1.270	0.193	0.152	-0.029	-2.157	1.802	.301E+14	-0.10	-0.11
28	0.981	1.252	0.224	0.179	-0.027	-2.161	1.762	.309E+14	-0.13	-0.13
29	0.981	1.226	0.264	0.215	-0.025	-2.170	1.725	.322E+14	-0.16	-0.15
30	0.980	1.185	0.301	0.254	-0.023	-2.196	1.700	.345E+14	-0.19	-0.17
31	0.980	1.134	0.316	0.279	-0.020	-2.236	1.694	.376E+14	-0.20	-0.20
32	0.979	1.094	0.322	0.294	-0.017	-2.259	1.694	.404E+14	-0.20	-0.21
33	0.979	1.040	0.330	0.317	-0.014	-2.314	1.694	.447E+14	-0.21	-0.24
34	0.978	0.969	0.284	0.293	-0.010	-2.419	1.725	.513E+14	-0.16	-0.25
35	0.977	0.947	0.206	0.217	-0.007	-2.427	1.806	.537E+14	-0.10	-0.19
36	0.977	0.938	0.157	0.167	-0.005	-2.428	1.901	.546E+14	-0.06	-0.15
37	0.976	0.935	0.121	0.130	-0.004	-2.427	2.024	.549E+14	-0.03	-0.13
38	0.975	0.934	0.094	0.101	-0.002	-2.426	2.193	.549E+14	-0.01	-0.10
39	0.974	0.936	0.074	0.079	-0.001	-2.423	2.438	.546E+14	0.01	-0.08
40	0.972	0.940	0.061	0.065	0.000	-2.418	2.810	.539E+14	0.03	-0.06

H VALUES20.10. 7. 5. 4. 4. 4. 4. 4. 3. 3. 3. 3. 3. 3. 2. 2. 2. 2. 2.
1. 2. 2. 2. 3. 3. 3. 3. 3. 3. 3. 4. 4. 4. 4. 4. 5. 7.10.20.

K VALUES45.30.20.10. 5. 1. 1. 1. 1. 1. 2. 2. 2. 4. 4. 4. 5. 5. 5. 5.
7. 7. 7. 7. 7. 7. 7. 7. 7. 7.10.10.10.10.10.10.10.10.10.10.

Plate III-5

CALCULATED SURFACE VALUES COMPUTED FOR THE MODEL WITH 24 MINUTES PERIOD AND STOPPED ON 381 TOTAL NUMBER OF ITERATIONS

	AME	AMHY	AMHZ	HZHY	DPHASE	DPHAHY	DPHAHZ	APPRES	TREAL	TIMAG
2	0.995	0.923	0.386	0.413	0.014	-2.415	-1.782	.552E+14	0.34	0.25
3	0.993	0.990	0.517	0.523	-0.002	-2.355	-1.749	.477E+14	0.43	0.30
4	0.991	1.123	0.556	0.495	-0.015	-2.220	-1.748	.369E+14	0.44	0.22
5	0.990	1.188	0.507	0.427	-0.024	-2.189	-1.767	.329E+14	0.39	0.17
6	0.989	1.235	0.471	0.381	-0.031	-2.167	-1.780	.304E+14	0.35	0.14
7	0.988	1.276	0.447	0.350	-0.037	-2.155	-1.791	.284E+14	0.33	0.12
8	0.987	1.326	0.427	0.322	-0.043	-2.135	-1.800	.263E+14	0.30	0.11
9	0.986	1.389	0.374	0.269	-0.049	-2.102	-1.821	.239E+14	0.26	0.07
10	0.985	1.426	0.310	0.217	-0.053	-2.094	-1.856	.226E+14	0.21	0.05
11	0.985	1.444	0.264	0.183	-0.056	-2.094	-1.889	.220E+14	0.18	0.04
12	0.984	1.474	0.231	0.157	-0.059	-2.084	-1.920	.211E+14	0.15	0.03
13	0.983	1.506	0.178	0.118	-0.061	-2.070	-1.992	.202E+14	0.12	0.01
14	0.983	1.524	0.113	0.074	-0.062	-2.066	-2.178	.197E+14	0.07	-0.01
15	0.982	1.530	0.060	0.039	-0.063	-2.065	-2.754	.195E+14	0.03	-0.03
16	0.982	1.530	0.061	0.040	-0.063	-2.061	2.478	.195E+14	-0.01	-0.04
17	0.981	1.517	0.104	0.069	-0.062	-2.068	1.981	.199E+14	-0.04	-0.05
18	0.981	1.501	0.137	0.091	-0.062	-2.072	1.846	.203E+14	-0.07	-0.06
19	0.981	1.482	0.170	0.114	-0.061	-2.077	1.769	.208E+14	-0.09	-0.07
20	0.980	1.458	0.200	0.137	-0.059	-2.084	1.721	.214E+14	-0.11	-0.08
21	0.980	1.431	0.216	0.151	-0.058	-2.092	1.703	.222E+14	-0.12	-0.09
22	0.980	1.410	0.218	0.154	-0.057	-2.107	1.706	.229E+14	-0.12	-0.10
23	0.980	1.384	0.219	0.158	-0.056	-2.115	1.706	.238E+14	-0.12	-0.10
24	0.979	1.359	0.221	0.162	-0.054	-2.124	1.707	.246E+14	-0.13	-0.10
25	0.979	1.336	0.219	0.164	-0.053	-2.135	1.711	.255E+14	-0.13	-0.11
26	0.978	1.318	0.228	0.173	-0.050	-2.134	1.703	.261E+14	-0.13	-0.11
27	0.978	1.300	0.254	0.196	-0.048	-2.138	1.682	.269E+14	-0.15	-0.12
28	0.977	1.277	0.291	0.227	-0.045	-2.143	1.659	.278E+14	-0.18	-0.14
29	0.977	1.246	0.337	0.271	-0.042	-2.151	1.637	.291E+14	-0.22	-0.16
30	0.976	1.197	0.381	0.318	-0.038	-2.177	1.623	.315E+14	-0.25	-0.19
31	0.975	1.138	0.398	0.350	-0.034	-2.219	1.621	.349E+14	-0.27	-0.22
32	0.975	1.090	0.405	0.372	-0.030	-2.243	1.623	.380E+14	-0.28	-0.25
33	0.975	1.026	0.414	0.404	-0.024	-2.303	1.626	.428E+14	-0.28	-0.29
34	0.974	0.945	0.363	0.384	-0.019	-2.420	1.643	.504E+14	-0.23	-0.31
35	0.973	0.918	0.274	0.298	-0.014	-2.430	1.700	.533E+14	-0.16	-0.25
36	0.973	0.907	0.217	0.239	-0.011	-2.432	1.756	.545E+14	-0.12	-0.21
37	0.972	0.902	0.174	0.193	-0.008	-2.432	1.823	.550E+14	-0.09	-0.17
38	0.971	0.901	0.140	0.155	-0.006	-2.432	1.910	.552E+14	-0.06	-0.14
39	0.970	0.901	0.110	0.122	-0.003	-2.429	2.033	.549E+14	-0.03	-0.12
40	0.968	0.905	0.083	0.092	0.000	-2.424	2.239	.543E+14	-0.00	-0.09

H VALUES20.10. 7. 5. 4. 4. 4. 4. 4. 3. 3. 3. 3. 3. 3. 2. 2. 2. 2. 2.
1. 2. 2. 2. 3. 3. 3. 3. 3. 3. 3. 4. 4. 4. 4. 4. 5. 7.10.20.

K VALUES45.30.20.10. 5. 1. 1. 1. 1. 1. 2. 2. 2. 4. 4. 4. 5. 5. 5. 5.
7. 7. 7. 7. 7. 7. 7. 7. 7. 7.10.10.10.10.10.10.10.10.10.10.

SCALE = 100000. FREQ = 0.000694

Plate III-6

CALCULATED SURFACE VALUES COMPUTED FOR THE MODEL WITH 16 MINUTES PERIOD AND STOPPED ON TOTAL 500 NUMBER OF ITERATIONS

	AME	AMHY	AMHZ	HZHY	DPHASE	DPHAHY	DPHAHZ	APPRES	TREAL	TIMAG
2	0.992	0.874	0.436	0.556	0.013	-2.421	-1.786	.552E+14	0.45	0.33
3	0.988	0.956	0.636	0.664	-0.013	-2.347	-1.766	.455E+14	0.56	0.36
4	0.986	1.121	0.630	0.606	-0.035	-2.198	-1.771	.331E+14	0.55	0.25
5	0.984	1.202	0.620	0.516	-0.049	-2.168	-1.791	.287E+14	0.48	0.19
6	0.983	1.261	0.577	0.457	-0.059	-2.147	-1.805	.260E+14	0.43	0.15
7	0.982	1.312	0.547	0.417	-0.069	-2.137	-1.816	.240E+14	0.40	0.13
8	0.980	1.373	0.521	0.379	-0.079	-2.118	-1.826	.213E+14	0.36	0.11
9	0.979	1.449	0.457	0.315	-0.088	-2.088	-1.844	.195E+14	0.31	0.08
10	0.978	1.495	0.380	0.254	-0.095	-2.082	-1.871	.183E+14	0.25	0.05
11	0.977	1.518	0.323	0.213	-0.099	-2.083	-1.897	.178E+14	0.21	0.04
12	0.977	1.554	0.281	0.181	-0.103	-2.075	-1.921	.169E+14	0.18	0.03
13	0.976	1.593	0.216	0.135	-0.107	-2.063	-1.973	.161E+14	0.13	0.01
14	0.975	1.614	0.134	0.083	-0.109	-2.060	-2.105	.156E+14	0.08	-0.00
15	0.975	1.622	0.062	0.038	-0.110	-2.059	-2.579	.155E+14	0.03	-0.02
16	0.974	1.623	0.055	0.034	-0.110	-2.056	2.338	.154E+14	-0.01	-0.03
17	0.974	1.606	0.113	0.070	-0.109	-2.062	1.792	.157E+14	-0.05	-0.05
18	0.973	1.588	0.157	0.099	-0.108	-2.065	1.675	.161E+14	-0.08	-0.06
19	0.973	1.564	0.200	0.128	-0.107	-2.070	1.613	.166E+14	-0.11	-0.07
20	0.973	1.536	0.241	0.157	-0.105	-2.076	1.576	.172E+14	-0.14	-0.08
21	0.972	1.503	0.264	0.176	-0.102	-2.082	1.563	.179E+14	-0.15	-0.08
22	0.972	1.478	0.274	0.186	-0.101	-2.096	1.563	.185E+14	-0.16	-0.09
23	0.972	1.446	0.279	0.193	-0.099	-2.102	1.563	.193E+14	-0.17	-0.10
24	0.972	1.416	0.286	0.202	-0.096	-2.110	1.563	.202E+14	-0.17	-0.10
25	0.971	1.387	0.287	0.207	-0.094	-2.120	1.565	.210E+14	-0.18	-0.11
26	0.971	1.365	0.300	0.220	-0.090	-2.119	1.562	.217E+14	-0.19	-0.11
27	0.970	1.341	0.333	0.248	-0.085	-2.122	1.552	.224E+14	-0.21	-0.13
28	0.970	1.313	0.377	0.287	-0.081	-2.125	1.541	.233E+14	-0.25	-0.14
29	0.969	1.275	0.433	0.340	-0.075	-2.133	1.531	.247E+14	-0.29	-0.17
30	0.969	1.215	0.486	0.400	-0.069	-2.158	1.525	.272E+14	-0.34	-0.21
31	0.968	1.142	0.508	0.444	-0.062	-2.200	1.527	.308E+14	-0.37	-0.25
32	0.968	1.083	0.517	0.477	-0.055	-2.224	1.534	.342E+14	-0.39	-0.28
33	0.967	1.005	0.528	0.526	-0.046	-2.288	1.540	.397E+14	-0.41	-0.33
34	0.967	0.905	0.469	0.518	-0.036	-2.423	1.557	.488E+14	-0.35	-0.39
35	0.965	0.872	0.366	0.420	-0.029	-2.435	1.588	.525E+14	-0.27	-0.32
36	0.965	0.858	0.300	0.350	-0.023	-2.438	1.621	.542E+14	-0.21	-0.28
37	0.965	0.851	0.250	0.294	-0.018	-2.440	1.658	.550E+14	-0.17	-0.24
38	0.964	0.848	0.208	0.245	-0.013	-2.440	1.703	.553E+14	-0.13	-0.21
39	0.962	0.847	0.171	0.202	-0.007	-2.438	1.762	.553E+14	-0.10	-0.18
40	0.961	0.849	0.134	0.158	0.000	-2.435	1.854	.548E+14	-0.06	-0.14

H VALUES20.10. 7. 5. 4. 4. 4. 4. 4. 3. 3. 3. 3. 3. 3. 2. 2. 2. 2. 2.
1. 2. 2. 2. 3. 3. 3. 3. 3. 3. 3. 4. 4. 4. 4. 4. 5. 7.10.20.

K VALUES45.30.20.10. 5. 1. 1. 1. 1. 1. 2. 2. 2. 4. 4. 4. 5. 5. 5. 5.
7. 7. 7. 7. 7. 7. 7. 7. 7. 7.10.10.10.10.10.10.10.10.10.10.

SCALE = 100000. FREQ = 0.001042

Plate III-7

APPENDIX I

LISTS OF CALCULATED TRANSFER FUNCTION OF STATIONS :

1. Western Junction
2. Scottsdale
3. Deloraine
4. Rosevale
5. Lilydale
6. Pipers River
7. West Frankford
8. Tayene
9. Nabowla
10. Forester
11. Beechford

Appendix I

CALCULATED TRANSFER FUNCTIONS

Station name : Western Junction
Events used : 14
Sampling interval : 2.0 minutes
Recording period : 9/2-1978 until 13/3-1978

Period		Real	Imaginary	Uncertainty
Period : 128.0 minutes	A	-0.31	+0.30	± 0.18
	B	+0.21	+0.08	± 0.18
Period : 64.0 minutes				
	A	-0.12	+0.33	± 0.17
	B	+0.24	-0.02	± 0.20
Period : 42.7 minutes				
	A	+0.03	+0.26	± 0.21
	B	+0.16	-0.07	± 0.13
Period : 32.0 minutes				
	A	+0.04	+0.27	± 0.19
	B	+0.12	-0.06	± 0.13
Period : 25.6 minutes				
	A	+0.11	+0.27	± 0.27
	B	+0.07	-0.08	± 0.21
Period : 21.3 minutes				
	A	+0.10	+0.08	± 0.18
	B	+0.06	+0.01	± 0.12
Period : 18.3 minutes				
	A	+0.09	+0.09	± 0.21
	B	+0.09	-0.02	± 0.15
Period : 16.0 minutes				
	A	+0.13	+0.10	± 0.19
	B	+0.09	-0.01	± 0.18
Period : 14.2 minutes				
	A	+0.04	+0.06	± 0.16
	B	+0.12	+0.01	± 0.14
Period : 12.8 minutes				
	A	+0.14	+0.03	± 0.17
	B	-0.01	+0.06	± 0.17

Station name : Scottsdale
Events used : 11
Sampling interval : 2.0 minutes
Recording period : 15/3-1978 until 13/5-1978

Period		Real	Imaginary	Uncertainty
Period : 128.0 minutes				
	A	-0.38	+0.22	± 0.31
	B	+0.17	-0.07	± 0.24
Period : 85.3 minutes				
	A	-0.26	+0.26	± 0.27
	B	+0.15	+0.10	± 0.35
Period : 64.0 minutes				
	A	-0.25	+0.26	± 0.20
	B	+0.15	-0.06	± 0.16
Period : 51.2 minutes				
	A	-0.33	+0.08	± 0.25
	B	+0.14	-0.11	± 0.17
Period : 42.7 minutes				
	A	-0.27	+0.16	± 0.28
	B	+0.04	-0.15	± 0.21
Period : 36.6 minutes				
	A	-0.04	+0.17	± 0.22
	B	-0.04	-0.20	± 0.17
Period : 32.0 minutes				
	A	-0.16	+0.22	± 0.19
	B	+0.07	-0.25	± 0.19
Period : 28.4 minutes				
	A	-0.18	+0.08	± 0.16
	B	-0.07	-0.20	± 0.20
Period : 26.6 minutes				
	A	-0.14	+0.10	± 0.15
	B	+0.10	+0.01	± 0.28
Period : 23.4 minutes				
	A	-0.19	+0.10	± 0.17
	B	-0.13	-0.17	± 0.11
Period : 21.3 minutes				
	A	+0.03	+0.02	± 0.16
	B	-0.11	-0.22	± 0.23

Period		Real	Imaginary	Uncertainty
Period : 19.7 minutes				
	A	-0.14	+0.09	± 0.14
	B	-0.05	-0.09	± 0.16
Period : 18.3 minutes				
	A	-0.15	+0.04	± 0.24
	B	-0.19	-0.05	± 0.34
Period : 17.1 minutes				
	A	-0.21	+0.01	± 0.18
	B	-0.03	+0.05	± 0.15
Period : 16.0 minutes				
	A	-0.15	+0.03	± 0.16
	B	-0.03	-0.06	± 0.16
Period : 15.1 minutes				
	A	-0.04	-0.03	± 0.12
	B	+0.04	-0.13	± 0.11
Period : 14.2 minutes				
	A	-0.18	-0.02	± 0.29
	B	-0.20	-0.06	± 0.42
Period : 13.5 minutes				
	A	-0.04	-0.03	± 0.16
	B	+0.04	+0.05	± 0.19
Period : 12.8 minutes				
	A	+0.06	-0.03	± 0.16
	B	-0.15	-0.03	± 0.16

Station name : Deloraine

Events used : 9

Sampling interval : 6.0 minutes

Recording period : 10/6-1978 until 16/9-1978

Period		Real	Imaginary	Uncertainty
Period : 96.0 minutes				
	A	-0.21	+0.39	± 0.26
	B	+0.17	-0.05	± 0.20
Period : 48.0 minutes				
	A	+0.16	+0.38	± 0.43
	B	+0.15	+0.09	± 0.30
Period : 32.0 minutes				
	A	+0.32	+0.44	± 0.26
	B	+0.12	-0.08	± 0.20
Period : 24.0 minutes				
	A	+0.15	+0.34	± 0.31
	B	+0.17	+0.06	± 0.32
Period : 19.2 minutes				
	A	+0.28	+0.28	± 0.32
	B	+0.13	+0.06	± 0.31
Period : 16.0 minutes				
	A	+0.48	+0.22	± 0.49
	B	+0.10	-0.04	± 0.37
Period : 13.7 minutes				
	A	+0.15	+0.04	± 0.23
	B	+0.25	+0.04	± 0.16
Period : 12.0 minutes				
	A	+0.40	+0.04	± 0.25
	B	+0.38	+0.00	± 0.31

Station name : Rosevale

Events used : 13

Sampling interval : 6.0 minutes

Recording period : 16/9-1978 until 20/10-1978

Period		Real	Imaginary	Uncertainty
Period : 96.0 minutes				
	A	-0.12	+0.49	± 0.28
	B	+0.23	-0.12	± 0.48
Period : 64.0 minutes				
	A	-0.04	+0.38	± 0.23
	B	+0.13	0.0o	± 0.23
Period : 48.0 minutes				
	A	+0.09	+0.23	± 0.21
	B	+0.03	+0.04	± 0.12
Period : 38.4 minutes				
	A	+0.04	+0.10	± 0.15
	B	-0.07	+0.12	± 0.16
Period : 32.0 minutes				
	A	+0.17	+0.18	± 0.26
	B	+0.06	-0.02	± 0.34
Period : 27.4 minutes				
	A	+0.12	+0.15	± 0.17
	B	+0.07	+0.01	± 0.17
Period : 24.0 minutes				
	A	+0.20	+0.13	± 0.25
	B	+0.06	+0.02	± 0.25
Period : 21.3 minutes				
	A	+0.04	+0.06	± 0.15
	B	-0.01	+0.17	± 0.15
Period : 19.2 minutes				
	A	+0.12	+0.03	± 0.13
	B	-0.02	+0.11	± 0.12
Period : 17.5 minutes				
	A	+0.07	-0.03	± 0.12
	B	-0.01	+0.22	± 0.13

		Real	Imaginary	Uncertainty
Period : 16.0 minutes				
	A	+0.15	-0.03	± 0.12
	B	+0.06	+0.08	± 0.20
Period : 14.8 minutes				
	A	+0.20	+0.06	± 0.15
	B	0.00	+0.14	± 0.25
Period : 13.7 minutes				
	A	+0.27	-0.02	± 0.19
	B	-0.03	-0.05	± 0.12
Period : 12.8 minutes				
	A	+0.12	+0.02	± 0.15
	B	-0.15	+0.09	± 0.19

Station name : Lilydale
Events used : 9
Sampling interval : 2.0 minutes
Recording period : 20/10-1978 until 8/12-1978

Period		Real	Imaginary	Uncertainty
Period : 128.0 minutes				
	A	-0.34	+0.17	± 0.33
	B	+0.13	-0.09	± 0.14
Period : 85.3 minutes				
	A	-0.17	+0.15	± 0.21
	B	+0.07	-0.14	± 0.19
Period : 64.0 minutes				
	A	-0.19	+0.15	± 0.33
	B	+0.02	-0.10	± 0.25
Period : 51.2 minutes				
	A	-0.15	+0.19	± 0.14
	B	+0.05	-0.13	± 0.13
Period : 42.7 minutes				
	A	-0.05	+0.18	± 0.16
	B	-0.03	-0.18	± 0.25
Period : 36.6 minutes				
	A	-0.07	+0.21	± 0.16
	B	-0.01	-0.19	± 0.14
Period : 32.0 minutes				
	A	-0.03	+0.19	± 0.21
	B	-0.08	-0.15	± 0.17
Period : 28.4 minutes				
	A	+0.02	+0.18	± 0.19
	B	-0.08	-0.16	± 0.19
Period : 25.6 minutes				
	A	-0.08	+0.11	± 0.16
	B	-0.04	-0.12	± 0.13
Period : 23.3 minutes				
	A	-0.05	+0.17	± 0.18
	B	-0.05	-0.16	± 0.14

		Real	Imaginary	Uncertainty
Period : 21.3 minutes				
	A	+0.02	+0.10	± 0.17
	B	-0.11	-0.12	± 0.20
Period : 19.7 minutes				
	A	-0.02	+0.09	± 0.10
	B	-0.05	-0.12	± 0.15
Period : 18.3 minutes				
	A	0.00	+0.04	± 0.15
	B	-0.10	-0.09	± 0.17
Period : 17.1 minutes				
	A	-0.04	+0.11	± 0.16
	B	-0.07	-0.09	± 0.11
Period : 16.0 minutes				
	A	+0.02	+0.11	± 0.12
	B	-0.02	-0.06	± 0.11
Period : 15.1 minutes				
	A	0.00	+0.04	± 0.08
	B	-0.08	-0.07	± 0.10
Period : 14.2 minutes				
	A	-0.03	+0.03	± 0.16
	B	-0.12	-0.03	± 0.13
Period : 13.7 minutes				
	A	0.00	+0.02	± 0.03
	B	-0.07	-0.02	± 0.08
Period : 12.8 minutes				
	A	-0.03	+0.09	± 0.02
	B	+0.03	-0.10	± 0.03

Station name : Pipers River -
Events used : 15
Sampling interval : 3.0 minutes
Recording period : 8/12-1978 until 16/2-1979

Period		Real	Imaginary	Uncertainty
Period : 96.0 minutes				
	A	-0.13	+0.37	± 0.18
	B	+0.09	-0.04	± 0.18
Period : 64.0 minutes				
	A	-0.08	+0.30	± 0.20
	B	+0.05	-0.07	± 0.13
Period : 48.0 minutes				
	A	-0.01	+0.26	± 0.18
	B	+0.01	-0.11	± 0.11
Period : 38.4 minutes				
	A	+0.11	+0.18	± 0.17
	B	-0.12	-0.13	± 0.19
Period : 32.0 minutes				
	A	+0.04	+0.23	± 0.09
	B	-0.02	-0.09	± 0.08
Period : 27.4 minutes				
	A	+0.10	+0.17	± 0.09
	B	-0.03	-0.09	± 0.13
Period : 24.0 minutes				
	A	+0.06	+0.13	± 0.08
	B	-0.08	-0.07	± 0.07
Period : 21.3 minutes				
	A	+0.06	+0.14	± 0.09
	B	-0.03	-0.04	± 0.11
Period : 19.2 minutes				
	A	+0.02	+0.08	± 0.07
	B	-0.07	-0.03	± 0.06
Period : 17.5 minutes				
	A	+0.03	+0.09	± 0.07
	B	+0.01	+0.03	± 0.07

Period		Real	Imaginary	Uncertainty
Period : 16.0 minutes	A	+0.13	+0.06	± 0.11
	B	-0.16	-0.11	± 0.15
Period : 14.8 minutes				
	A	+0.03	+0.04	± 0.07
	B	-0.09	-0.01	± 0.09
Period : 13.7 minutes				
	A	+0.02	+0.05	± 0.07
	B	-0.04	-0.03	± 0.06
Period : 12.8 minutes				
	A	+0.09	+0.04	± 0.09
	B	-0.11	-0.01	± 0.10

Station name : West Frankford
Events used : 15
Sampling interval : 3.0 minutes
Recording period : 16/2-1979 until 20/3-1979

Period		Real	Imaginary	Uncertainty
Period : 96.0 minutes				
	A	-0.13	+0.34	± 0.19
	B	+0.09	-0.06	± 0.15
Period : 64.0 minutes				
	A	+0.03	+0.26	± 0.16
	B	+0.15	-0.01	± 0.13
Period : 48.0 minutes				
	A	+0.06	+0.26	± 0.13
	B	+0.12	-0.05	± 0.07
Period : 38.4 minutes				
	A	+0.10	+0.23	± 0.15
	B	+0.06	-0.04	± 0.16
Period : 32.0 minutes				
	A	+0.16	+0.19	± 0.11
	B	+0.02	-0.03	± 0.12
Period : 27.4 minutes				
	A	+0.12	+0.17	± 0.15
	B	+0.05	-0.08	± 0.15
Period : 24.0 minutes				
	A	+0.22	+0.14	± 0.14
	B	+0.07	-0.05	± 0.17
Period : 21.3 minutes				
	A	+0.23	+0.16	± 0.14
	B	+0.05	-0.04	± 0.13
Period : 19.2 minutes				
	A	+0.25	+0.07	± 0.30
	B	+0.03	-0.03	± 0.11
Period : 17.5 minutes				
	A	+0.19	+0.06	± 0.17
	B	+0.04	-0.09	± 0.15

		Real	Imaginary	Uncertainty
Period : 16.0 minutes				
	A	+0.19	+0.01	± 0.11
	B	+0.01	-0.02	± 0.15
Period : 14.8 minutes				
	A	+0.21	+0.05	± 0.15
	B	0.00	-0.01	± 0.15
Period : 13.7 minutes				
	A	+0.18	+0.03	± 0.13
	B	+0.02	+0.01	± 0.12
Period : 12.8 minutes				
	A	+0.19	+0.03	± 0.13
	B	-0.03	0.00	± 0.15

Station name : Tayene
Events used : 15
Sampling interval : 3.0 minutes
Recording period : 20/3-1979 until 12/4-1979

Period		Real	Imaginary	Uncertainty
Period : 96.0 minutes				
	A	-0.30	+0.07	± 0.23
	B	+0.11	-0.21	± 0.35
Period : 64.0 minutes				
	A	-0.30	+0.14	± 0.19
	B	-0.01	-0.12	± 0.16
Period : 48.0 minutes				
	A	-0.07	-0.05	± 0.19
	B	-0.06	-0.28	± 0.28
Period : 38.4 minutes				
	A	-0.16	+0.11	± 0.33
	B	-0.15	-0.31	± 0.26
Period : 32.0 minutes				
	A	+0.12	+0.04	± 0.22
	B	-0.10	-0.17	± 0.20
Period : 27.4 minutes				
	A	-0.09	-0.12	± 0.33
	B	-0.29	-0.11	± 0.32
Period : 24.0 minutes				
	A	+0.12	+0.13	± 0.29
	B	-0.14	-0.29	± 0.30
Period : 21.3 minutes				
	A	+0.05	-0.02	± 0.21
	B	-0.18	-0.05	± 0.24
Period : 19.2 minutes				
	A	+0.20	-0.04	± 0.22
	B	-0.04	0.00	± 0.18
Period : 17.5 minutes				
	A	+0.22	+0.07	± 0.23
	B	-0.04	-0.18	± 0.21

Period			Real	Imaginary	Uncertainty
Period :	16.0 minutes				
		A	+0.11	0.00	± 0.19
		B	-0.11	-0.08	± 0.23
Period :	14.8 minutes				
		A	0.00	+0.11	± 0.27
		B	+0.16	-0.09	± 0.29
Period :	13.7 minutes				
		A	+0.04	+0.02	± 0.40
		B	+0.31	+0.02	± 0.32
Period :	12.8 minutes				
		A	+0.03	-0.02	± 0.21
		B	+0.23	+0.06	± 0.30

Station name : Nabowla
Events used : 12
Sampling interval : 2.0 minutes
Recording period : 12/4-1979 until 3/7-1979

Period		Real	Imaginary	Uncertainty
Period : 128.0 minutes				
	A	-0.37	+0.25	± 0.34
	B	+0.14	-0.10	± 0.26
Period : 85.3 minutes				
	A	-0.30	+0.23	± 0.37
	B	+0.01	-0.23	± 0.26
Period : 64.0 minutes				
	A	-0.36	+0.25	± 0.31
	B	-0.03	-0.23	± 0.24
Period : 51.2 minutes				
	A	-0.31	+0.31	± 0.33
	B	+0.03	-0.24	± 0.41
Period : 42.7 minutes				
	A	-0.37	+0.17	± 0.35
	B	+0.06	-0.13	± 0.25
Period : 36.6 minutes				
	A	-0.40	+0.22	± 0.37
	B	-0.05	-0.12	± 0.28
Period : 32.0 minutes				
	A	-0.27	+0.31	± 0.35
	B	+0.05	-0.25	± 0.29
Period : 28.4 minutes				
	A	-0.37	-0.02	± 0.33
	B	-0.18	-0.16	± 0.22
Period : 25.6 minutes				
	A	-0.20	+0.23	± 0.28
	B	-0.12	-0.14	± 0.20
Period : 23.3 minutes				
	A	-0.52	+0.15	± 0.41
	B	-0.06	-0.17	± 0.31

Period		Real	Imaginary	Uncertainty
Period : 21.3 minutes	A	-0.20	+0.23	± 0.21
	B	-0.11	-0.23	± 0.24
Period : 19.7 minutes				
	A	-0.32	+0.14	± 0.29
	B	-0.05	-0.28	± 0.25
Period : 18.3 minutes				
	A	-0.29	+0.27	± 0.36
	B	-0.01	-0.14	± 0.19
Period : 17.1 minutes				
	A	-0.54	-0.08	± 0.42
	B	-0.15	-0.14	± 0.24
Period : 16.0 minutes				
	A	-0.44	+0.22	± 0.48
	B	+0.01	-0.21	± 0.36
Period : 15.1 minutes				
	A	-0.56	+0.16	± 0.71
	B	+0.04	-0.07	± 0.41
Period : 14.2 minutes				
	A	-0.48	+0.07	± 0.34
	B	-0.08	-0.29	± 0.34
Period : 13.5 minutes				
	A	-0.43	+0.13	± 0.41
	B	-0.14	-0.19	± 0.29
Period : 12.8 minutes				
	A	-0.48	+0.13	± 0.39
	B	-0.17	-0.17	± 0.28

Station name : Forester
Events used : 13
Sampling interval : 2.0 minutes
Recording period : 8/8-1979 until 14/10-1979

Period		Real	Imaginary	Uncertainty
Period : 128.0 minutes				
	A	-0.10	+0.16	± 0.16
	B	+0.26	+0.10	± 0.23
Period : 85.3 minutes				
	A	-0.14	+0.53	± 0.53
	B	+0.16	+0.09	± 0.38
Period : 64.0 minutes				
	A	-0.24	+0.23	± 0.24
	B	-0.04	-0.07	± 0.25
Period : 51.2 minutes				
	A	-0.20	+0.33	± 0.31
	B	+0.23	0.00	± 0.29
Period : 42.7 minutes				
	A	-0.07	+0.29	± 0.23
	B	+0.11	-0.09	± 0.19
Period : 36.6 minutes				
	A	-0.04	+0.33	± 0.68
	B	+0.06	-0.13	± 0.66
Period : 32.0 minutes				
	A	-0.02	+0.33	± 0.39
	B	+0.04	-0.16	± 0.44
Period : 28.4 minutes				
	A	+0.12	+0.23	± 0.15
	B	-0.01	-0.21	± 0.20
Period : 25.6 minutes				
	A	-0.02	+0.18	± 0.17
	B	-0.08	-0.07	± 0.20
Period : 23.3 minutes				
	A	+0.05	+0.28	± 0.20
	B	-0.06	-0.16	± 0.21

		Real	imaginary	Uncertainty
Period : 21.3 minutes	A	+0.03	+0.16	± 0.15
	B	-0.16	-0.12	± 0.20
Period : 19.7 minutes				
	A	+0.06	+0.20	± 0.19
	B	-0.17	-0.16	± 0.25
Period : 18.3 minutes				
	A	+0.14	+0.08	± 0.18
	B	-0.21	-0.19	± 0.26
Period : 17.1 minutes				
	A	+0.11	+0.06	± 0.28
	B	-0.18	-0.23	± 0.43
Period : 16.0 minutes				
	A	+0.02	+0.13	± 0.12
	B	-0.11	-0.26	± 0.13
Period : 15.1 minutes				
	A	+0.06	+0.18	± 0.08
	B	-0.07	-0.32	± 0.19
Period : 14.2 minutes				
	A	+0.07	+0.16	± 0.17
	B	-0.06	-0.17	± 0.26
Period : 13.5 minutes				
	A	+0.02	+0.09	± 0.12
	B	-0.27	+0.02	± 0.35
Period : 12.8 minutes				
	A	+0.08	+0.14	± 0.15
	B	-0.29	-0.01	± 0.26

Station name : Beechford

Events used : 9

Sampling interval : 2.0 minutes

Recording period : 3/7-1979 until 8/8-1979

Period		Real	Imaginary	Uncertainty
Period : 128.0 minutes				
	A	-0.29	+0.19	± 0.26
	B	+0.11	-0.06	± 0.11
Period : 85.3 minutes				
	A	-0.18	+0.28	± 0.19
	B	-0.01	-0.18	± 0.16
Period : 64.0 minutes				
	A	-0.10	+0.36	± 0.19
	B	-0.04	-0.25	± 0.20
Period : 51.2 minutes				
	A	-0.04	+0.51	± 0.44
	B	+0.01	-0.18	± 0.23
Period : 42.7 minutes				
	A	-0.05	+0.19	± 0.28
	B	-0.19	-0.12	± 0.23
Period : 36.6 minutes				
	A	-0.03	+0.12	± 0.20
	B	-0.15	-0.13	± 0.15
Period : 32.0 minutes				
	A	+0.05	+0.20	± 0.26
	B	-0.14	-0.18	± 0.21
Period : 28.4 minutes				
	A	+0.09	+0.17	± 0.28
	B	-0.20	-0.20	± 0.25
Period : 25.6 minutes				
	A	+0.08	+0.21	± 0.22
	B	-0.21	-0.23	± 0.20
Period : 23.3 minutes				
	A	+0.02	+0.19	± 0.19
	B	-0.16	-0.19	± 0.16

Period		Real	Imaginary	Uncertainty
Period : 21.3 minutes	A	-0.02	-0.02	± 0.28
	B	-0.25	+0.09	± 0.19
Period : 19.7 minutes				
	A	+0.15	+0.06	± 0.18
	B	-0.26	0.00	± 0.16
Period : 18.3 minutes				
	A	+0.22	-0.03	± 0.20
	B	-0.25	-0.15	± 0.18
Period : 17.1 minutes				
	A	+0.04	+0.16	± 0.26
	B	-0.13	+0.06	± 0.25
Period : 16.0 minutes				
	A	+0.02	+0.09	± 0.13
	B	-0.11	+0.13	± 0.20
Period : 15.1 minutes				
	A	+0.06	-0.03	± 0.19
	B	-0.24	+0.05	± 0.26
Period : 14.2 minutes				
	A	+0.07	-0.09	± 0.26
	B	-0.38	+0.09	± 0.38
Period : 13.5 minutes				
	A	+0.26	+0.06	± 0.29
	B	-0.34	-0.07	± 0.30
Period : 12.8 minutes				
	A	+0.06	+0.06	± 0.15
	B	-0.24	+0.03	± 0.20

APPENDIX II

LISTS OF CALCULATED VALUES OF AZIMUTHS (Ø) AND LENGTHS (L) OF THE INDUCTION VECTORS OR 'PARKINSON VECTORS'

Appendix II

CALCULATED VALUES OF AZIMUTHS (Ø) AND LENGTHS (L) OF THE INDUCTION VECTORS

The values Ø, θ and L are derived from the equations :

$$\theta = \tan^{-1}\sqrt{A^2 + B^2}$$

$$\emptyset = \tan^{-1}\frac{B}{A}$$

$$L = \sin\theta$$

The abbreviation for each station are ; DLR - Deloraine, RSV - Rosevale, LLD - Lilydale, NBL - Nabowla, SCD - Scottsdale, FRT - Forester, WFR - West Frankford, PPR - Pipers River, WJC - Western Junction, BFR - Beechford and TAY - Tayene.

Note : Since the magnetic declination or variation at Launceston area is about 12.5° to 13.0° East, for the Epoch 1970.0 (Journal ASEG, pp. 139, vol. 10, no. 1, March 1979) all the Ø values have to be added by 13° to the east.

Real (13 minutes period)

	DLR	RSV	LLD	NBL	SCD	FRT	WFR	PPR	WJC	BFR	TAY
Direction	NE	NW	SW	SW	NW	NW	NW	NW	NW	NW	NE
Ø	51.1	10.6	73.3	19.5	68.2	66.0	09.0	50.7	04.1	76.0	82.6
θ	21.7	09.3	06.0	27.0	09.2	11.4	10.9	08.1	08.0	13.9	13.1
L	0.37	0.16	0.10	0.45	0.16	0.19	0.19	0.14	0.14	0.24	0.23

Imaginary (13 minutes period)

	DLR	RSV	LLD	NBL	SCD	FRT	WFR	PPR	WJC	BFR	TAY
Direction	NE	NE	NW	NW	SW	NW	NW	NW	NE	NE	SE
Ø	36.9	77.5	48.0	52.6	45.0	04.1	00.2	14.0	63.4	26.6	71.6
θ	2.9	5.3	7.7	12.1	2.4	8.0	1.7	2.4	3.8	3.8	3.6
L	0.05	0.09	0.13	0.21	0.04	0.14	0.03	0.04	0.07	0.07	0.06

Real (16.0 minutes period)

	DLR	RSV	LLD	NBL	SCD	FRT	WFR	PPR	WJC	BFR	TAY
Direction	NE	NE	NW	SE	SW	NW	NE	NW	NE	NW	NW
Ø	19.7	07.6	45.0	01.3	11.3	69.8	03.0	53.1	34.7	80.5	45.0
θ	16.6	08.6	01.6	23.8	08.7	11.5	10.8	05.7	09.0	13.7	08.8
L	0.28	0.15	0.03	0.40	0.15	0.20	0.19	0.10	0.16	0.24	0.15

Imaginary (16.0 minutes period)

	DLR	RSV	LLD	NBL	SCD	FRT	WFR	PPR	WJC	BFR	TAY
Direction	NW	SE	NW	NW	NW	NW	NW	NW	NW	NE	NW
Ø	10.3	69.4	28.6	43.7	63.4	63.4	63.4	61.4	05.7	55.3	89.9
θ	12.6	04.9	07.1	16.9	03.8	16.2	01.3	07.1	05.7	09.0	04.6
L	0.22	0.09	0.12	0.29	0.07	0.28	0.02	0.12	0.10	0.16	0.08

Real (24 minutes period)

	DLR	RSV	LLD	NBL	SCD	FRT	WFR	PPR	WJC	BFR	TAY
Direction	NE	NE	SW	SW	SW	SW	NE	NW	NE	NW	NW
Ø	48.6	16.7	26.6	31.0	34.4	76.0	17.7	53.1	32.5	82.9	49.4
θ	12.8	11.8	05.1	13.1	13.0	04.7	13.0	05.7	07.4	09.2	10.5
L	0.22	0.20	0.09	0.23	0.22	0.08	0.22	0.10	0.13	0.16	0.18

Imaginary (24 minutes period)

Direction	NE	NE	NW	NW	NW	NW	NW	NW	NW	NW	NW
Ø	10.0	08.8	47.5	31.3	59.5	23.6	19.7	28.3	16.5	45.0	65.9
θ	19.1	07.5	09.3	15.1	11.2	09.9	08.5	08.4	15.7	15.0	17.6
L	0.33	0.13	0.16	0.26	0.19	0.17	0.15	0.15	0.27	0.26	0.30

Real (32 minutes period)

Direction	NE	NE	SW	SE	SW	SE	NE	NW	NE	NW	NW
Ø	20.6	19.4	69.4	10.5	23.6	45.0	07.1	26.6	71.6	70.4	39.8
θ	18.8	10.2	04.9	15.4	09.9	03.2	09.2	02.6	07.2	08.5	08.9
L	0.32	0.18	0.09	0.26	0.17	0.06	0.16	0.04	0.13	0.15	0.15

Imaginary (32 minutes period)

Direction	NW	NW	NW	NW	NW	NW	NW	NW	NW	NW	NW
Ø	10.3	06.3	38.3	38.9	48.7	25.9	09.0	21.4	12.5	42.0	76.8
θ	24.1	10.3	13.6	21.7	18.4	20.1	10.9	13.9	15.5	15.1	09.9
L	0.41	0.18	0.24	0.37	0.32	0.34	0.19	0.24	0.27	0.26	0.17

Real (48 - 51 minutes period)

Direction	NE	NE	SE	SE	SE	SE	NE	SE		SE	SW
Ø	53.1	40.6	18.4	05.5	35.0	49.0	69.0	33.7		14.0	21.0
θ	11.3	05.3	09.0	17.3	13.7	17.0	07.9	02.1		02.4	07.9
L	0.20	0.09	0.16	0.30	0.24	0.29	0.14	0.04		0.04	0.14

Imaginary (48 - 51 minutes period)

Direction	NE	NE	NW	NW	NW	NE	NW	NW		NW	NW
Ø	13.7	06.3	34.4	37.8	54.0	00.0	08.8	20.3		19.4	87.6
θ	20.9	15.2	13.0	21.4	07.8	18.3	14.7	16.1		28.4	13.5
L	0.36	0.26	0.22	0.36	0.13	0.31	0.25	0.28		0.48	0.23

Real (64 minutes period)

	DLR	RSV	LLD	NBL	SCD	FRT	WFR	PPR	WJC	BFR	TAY
Direction	SE	SE	SE	SW	SE	SE	NE	SE	SE	SW	SW
ø	86.8	72.9	06.0	04.8	31.0	35.3	78.7	32.0	63.4	21.8	01.9
θ	10.2	07.8	10.8	19.9	16.3	16.4	08.7	05.4	15.0	06.2	16.7
L	0.18	0.13	0.19	0.34	0.28	0.28	0.15	0.09	0.26	0.11	0.29

Imaginary (64 minutes period)

	DLR	RSV	LLD	NBL	SCD	FRT	WFR	PPR	WJC	BFR	TAY
Direction	NE	NE	NW	NW	NW	NW	NW	NW	NW	NW	NW
ø	05.9	0.15	33.7	42.6	13.0	16.9	02.2	13.1	03.5	34.8	40.6
θ	21.4	20.8	10.2	18.8	14.9	13.5	14.6	17.1	18.3	23.7	10.5
L	0.36	0.36	0.18	0.32	0.26	0.23	0.25	0.29	0.31	0.40	0.18

Real (85 - 96 minutes period)

	DLR	RSV	LLD	NBL	SCD	FRT	WFR	PPR	WJC	BFR	TAY
Direction	SE	SE	SE	SE	SE	SE	SE	SE	SE	SE	SE
ø	50.2	61.2	22.4	01.9	30.0	48.8	48.0	32.5	45.0	03.2	14.9
θ	13.2	12.9	10.4	16.7	16.7	12.0	07.7	07.4	17.3	10.2	17.2
L	0.23	0.22	0.18	0.29	0.29	0.21	0.13	0.13	0.30	0.18	0.30

Imaginary (85 - 96 minutes period)

	DLR	RSV	LLD	NBL	SCD	FRT	WFR	PPR	WJC	BFR	TAY
Direction	NW	NW	NW	NW	NE	NE	NW	NW	NE	NW	NW
ø	04.7	09.7	43.0	45.0	21.0	09.6	09.4	07.9	07.4	32.7	64.7
θ	19.9	26.0	11.6	18.0	15.6	28.3	16.9	20.0	17.4	18.4	11.9
L	0.34	0.43	0.20	0.31	0.27	0.47	0.29	0.34	0.30	0.32	0.21

APPENDIX III

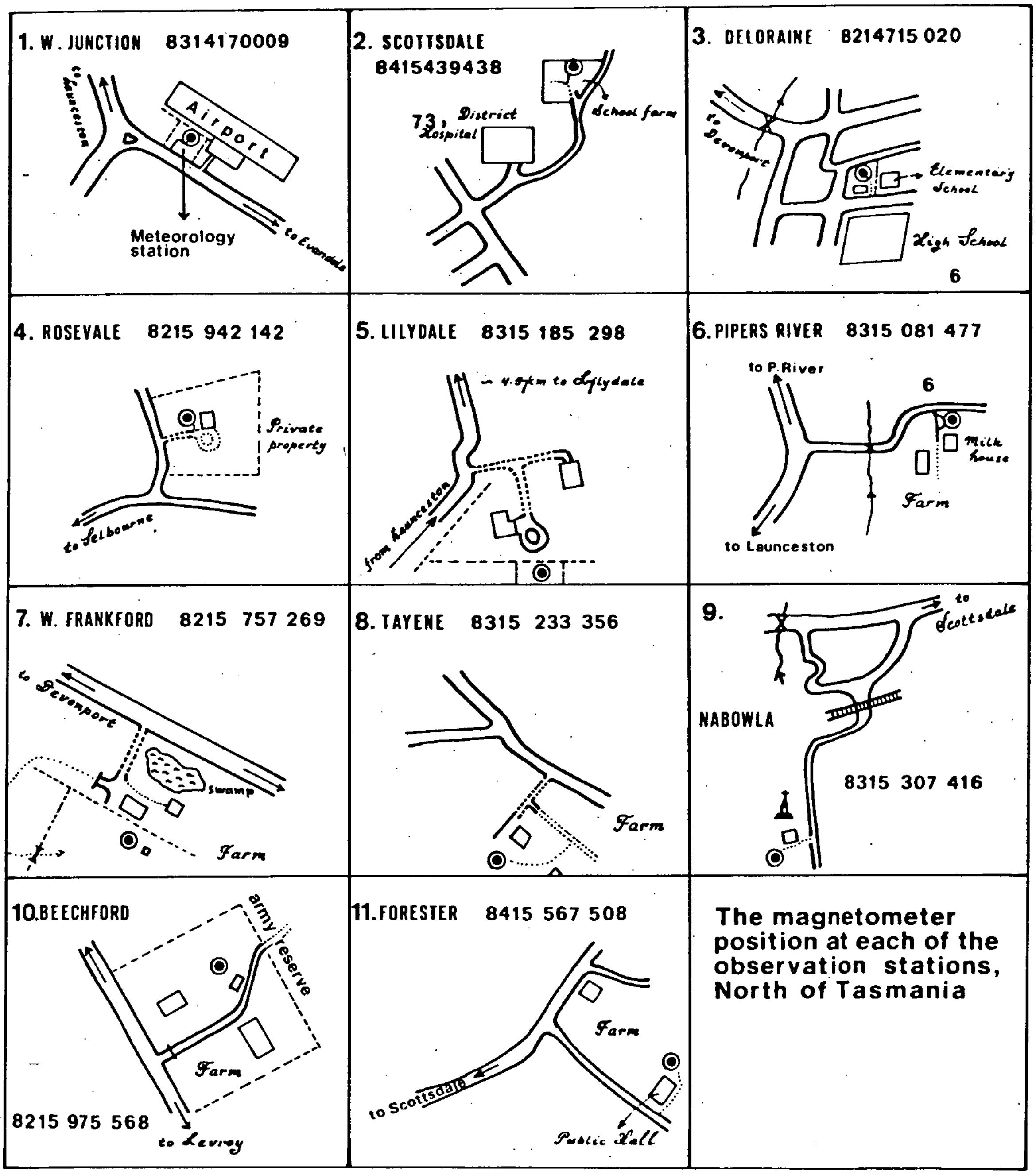

The magnetometer position at each of the observation stations, North of Tasmania